PRECISE ATOMIC MASS DIFFERENCE DETERMINATIONS FOR Tl AND Pb

BY

MOHAMED HUSSIEN SIDKY

A Thesis
Submitted to the Faculty of Graduate Studies
in Partial Fulfillment of the Requirements
for the Degree of

DOCTOR OF PHILOSOPHY

Department of Physics
University of Manitoba
Winnipeg, Manitoba

February , 1990

ISBN 0-315-63303-4

PRECISE ATOMIC MASS DIFFERENCE DETERMINATIONS FOR Tl and Pb

BY

MOHAMED HUSSIEN SIDKY

A thesis submitted to the Faculty of Graduate Studies of
the University of Manitoba in partial fulfillment of the requirements
of the degree of

DOCTOR OF PHILOSOPHY

ACKNOWLEDGEMENTS

I like to thank my supervisor, Dr. K. S. Sharma for his guidance during my research work. I am grateful to Mr. C. A. Lander for his assistance. I also wish to thank the members of the University of Manitoba Atomic Mass Determinations group for their help in the experimental work.

ABSTRACT

Atomic mass differences are usually determined by a variation of a technique known as "peak matching". Two techniques have been developed and applied to the Manitoba II spectrometer : visual null peak matching and computer-assisted peak matching. For the computer matching technique, peaks may be located by using either a centroid or a least squares method. In this work, an improved procedure is established for the least squares method. With this new procedure the accuracy and the precision of a calculated mass difference is significantly improved.

The Manitoba II mass spectrometer has been used to measure the spacings of 4 doublets in the mass spectra of $TlCl_x$ and $PbCl_y$. The average precision of the new mass differences (least squares method computer runs) surpasses that of our earlier work (centroid method computer runs and visual runs) by a factor of about 1.3. This program of measurements was aimed at determining the ^{205}Pb-^{205}Tl atomic mass difference, which is used to determine the threshold energy of the neutrino capture reaction : $\nu + {}^{205}\mathrm{Tl} \rightarrow {}^{205}\mathrm{Pb} + e^-$. It has been suggested that this reaction may provide a good mechanism on which a solar neutrino detector may be based (Freedman, 1976). A new value for the ^{205}Pb-^{205}Tl mass difference is calculated by combining our new data with other precise data obtained from (n,γ) reactions and β decays. Our value (51.87 ± 0.84 keV) agrees with accepted values and substantially improves the precision of this mass difference.

TABLE OF CONTENTS

LIST OF TABLES

LIST OF FIGURES

CHAPTER (1)

INTRODUCTION

1-1 The concept of mass

Mass is a property of an object which somehow describes the quantity of matter contained in it and which is conserved when matter changes its form. It is a measure of the inertial and gravitational properties of matter. Inertial mass and gravitational mass have been shown to be the same to 4 parts in 10^{11} (Keiser, 1981).

Newton showed that gravitational mass could be expressed in terms of the attraction experienced as a result of the presence of another object according to the universal law of gravitation :

$$F = \frac{GM_1M_2}{R^2} \qquad (1\text{-}1)$$

where F is the attractive force between two bodies with masses M_1 and M_2 separated by a distance R and G is the universal gravitation constant. It has been found that G is constant in time to within 1 part in 10^{11} / year (Reasonberg, 1976).

Inertial mass is defined through Newton's second law :

$$F = ma \qquad (1\text{-}2)$$

where "a" is the acceleration of the body induced by the force, F, and "m" is the mass of the body.

The Newtonian laws of motion are valid only in inertial frames of reference. Mach criticized Newton's concept of motion with respect to absolute space as being unobservable. He replaced it by motion relative to the fixed stars, which at his time represented the bulk of the observed matter in the universe. Mach claimed that the inertial mass of a body depended upon some interaction with the remaining mass in the universe (Clotfelter, 1970).

Einstein abolished the role of preferred inertial frames of reference through his principle of equivalence. His general theory of relativity is considered to express Mach's principle. In Einstein's special theory of relativity, each observer generates his own coordinate system such that there is no absolute frame of reference. The theory showed that a particle has a relativistic inertial mass, m, which varies with the velocity, v, according to the relation :

$$m = \frac{m_0}{\sqrt{1-\left(\frac{v}{c}\right)^2}} \qquad (1\text{-}3)$$

where; m_0 is the mass of a particle at rest and c is the speed of light.

The theory concludes that mass (m) and energy (E) are two aspects of the same fundamental quantity. Mass can be converted into energy and vice versa. This equivalence is stated in the famous relationship :

$$E = mc^2 \qquad (1\text{-}4)$$

1-2 Standards of mass and energy

The international unit of mass is the kilogram, kg, which was originally defined as the mass of a cubic decimeter of water. The present standard kilogram was constructed in 1889 from a platinum-iridium alloy (90/10) and is in the form of a solid cylinder with height equal to its diameter. This primary standard is preserved by the International Bureau of Weights and Measures at Sévres, France. Copies of the prototype are distributed throughout the world.

In 1860, an international conference on atomic masses officially adopted the Dalton-Avogadro scheme for relative atomic masses. A natural unit for this scheme was the mass of hydrogen, the lightest atom (this was Dalton's choice). By 1923 the basis was changed when Aston (Aston, 1923) had already observed small divergences from the whole number rule for a score of elements. Aston chose ^{16}O to be the standard of atomic mass which, in contrast to ^{1}H, forms stable and tractable compounds with most elements. However, after the discovery of isotopy, two different atomic masses were defined : one was based on ^{16}O, which served as the physicists' standard of mass, and the other was based on the natural mixture of ^{16}O, ^{17}O and ^{18}O, which was the basis for chemical atomic masses. The two mass scales are related by a constant; however, natural variations in the abundance of oxygen isotopes contribute a variation in such a conversion factor ranging from 1.000268 to 1.000278 (Nier, 1950). To unify the two scales and improve the precision in the definition of the chemical scale, A.O.Nier and A.Olander (Kohman, 1958) independently suggested that a unified scale be based on $^{12}C = 12$ u. This required a relatively small change in the chemical scale (~ 43 ppm) and removed the ambiguity in it. Accordingly, in a coordinated action, both the International Union of Pure and Applied Chemistry and the International

Union of Pure and Applied Physics adopted in that year the "unified" scale of atomic mass, with symbol u (Wichers, 1962). The atomic mass unit u is 1/12 of the mass of a neutral atom of ^{12}C. Atomic masses of other nuclides may be compared to ^{12}C with precisions occasionally as high as 1 part in 10^9 (Smith, 1975).

The "u" is related to the kilogram by the following equation :

$$1u = \frac{1}{N_A} \quad kg \tag{1-5}$$

Where N_A is the Avogadro's constant which is the number of atoms in exactly 12 kg of ^{12}C. Avogadro's constant has been determined by Deslattes to be $(6.022\,060 \pm 0.000\,009)10^{23}$ (Deslattes, 1974). The energy unit in the atomic scale is the electron volt (eV) which is defined as the kinetic energy gained when an electron passes through a potential difference of 1 volt. The mass-to-energy conversion factor is obtained from the fundamental constants N_A, e and c. Thus :

$$1u = \frac{c^2}{eN_A} \quad eV \tag{1-6}$$

Cohen obtained the best values of these constants from a least squares adjustment (Cohen, 1976). The analysis of Cohen recommends the conversion factor :

$$1u = (1.660\,566\,0 \pm 0.000\,008\,6)10^{-27} \quad kg \tag{1-7a}$$

,more recently, Cohen and Wapstra (Cohen, 1983) show that :

$$1u = 931501.2 \pm 0.3 \quad keV \tag{1-7b}$$

which represents a precision of 0.3 ppm. This value has been used in the 1983 Atomic Mass Evaluation (Wapstra, 1985).

1-3 The importance of atomic mass determinations

The mass of an atom M(A,Z) is less than the combined masses of its constituent, free particles. That is :

$$M(A,Z) = Z(m_p + m_e) + (A - Z)m_n - (B.E.)_{nucleus} - (B.E.)_{electron} \qquad (1\text{-}8)$$

where Z is the number of protons; m_p, m_e and m_n are the masses of the proton, electron and neutron, respectively; $(B.E.)_{nucleus}$ and $(B.E.)_{electron}$ represent the total binding energies of the nuclear particles and of the atomic electrons, respectively. $(B.E.)_{electron}$ may be calculated for the light atoms ($2 \le Z \le 8$) on the basis of the Fermi-Thomas model to be (Foldy, 1951):

$$(B.E.)_{electron} = 15.73Z^{7/3} \qquad eV \qquad (1\text{-}9)$$

For the heavy atoms the dependence of the $(B.E.)_{electron}$ on Z becomes approximately $Z^{12/5}$. The value of $(B.E.)_{electron}$ just approaches 1 MeV for the heaviest elements while $(B.E.)_{nucleus}$ is on the order of 8 MeV per nucleon (Evans, 1955) corresponding to about 2 GeV for the heaviest nuclides. Inasmuch as $(B.E.)_{electron}$ is small relative to $(B.E.)_{nucleus}$, the variation of average nuclear stability with nuclear size may be expressed in terms of the binding energy per nucleon, $B.E./nucleon = \frac{(B.E.)_{nucleus}}{A}$:

$$B.E./nucleon = \frac{Z(m_p + m_e) + (A - Z)m_n - M(A,Z)}{A} \qquad (1\text{-}10)$$

This quantity increases quickly from 1.1 MeV for ^{2}H to ~ 6.5 MeV at A=10 and increases thereafter to a maximum value of 8.793 MeV for ^{56}Fe; from this value it declines to 7.6 MeV in uranium. In some cases, $(B.E.)_{electron}$ cannot be neglected with respect to $(B.E.)_{nucleus}$. As an example, in Fig. 6-1, the binding energy of a K-level electron determines the direction of the $^{205}Tl^{81+}$ decay channel (β decay), which is opposite to that of $^{205}Tl^0$ (e capture).

In an approach to describe *B.E./nucleon*, Aston defined the packing fraction *f(A,Z)* in terms of the atomic mass *M(A,Z)* and the mass number A :

$$f(A,Z) = \frac{M(A,Z) - A}{A} \qquad (1\text{-}11)$$

The greatest stability is associated with those atoms whose packing fractions are the smallest. Combining (1-10) and (1-11) :

$$B.E./nucleon = \frac{Z(m_p + m_e) + (A - Z)m_n}{A} - [1 + f(A,Z)] \qquad (1\text{-}12)$$

Thus, the maximum in the B.E./nucleon curve occurs at roughly the same A as does the minimum in the packing fraction curve. Accordingly, greatest stability is associated with those atoms whose packing fractions are the smallest.

Although Aston obtained masses for some of the isotopes of chromium, krypton and xenon (Aston, 1942), most of the pioneer work involving the masses of heavier atoms was done by Dempster during the period 1936-1938. This led to his well-known version of the packing fraction curve (Dempster, 1938) which superseded Aston's earlier version.

An important result of Dempster's packing fraction work was his discovery that the slope of the packing fraction curve in the region $90 < A < 104$ was twice its value in the region $180 < A < 208$. This could be construed as evidence either for a modest improvement in nuclear stability near A=180 or for a rather violent deterioration in it near A=90 (Dempster, 1938; Feenberg, 1947). This question was subsequently investigated and the latter interpretation found to be correct (Duckworth, 1950). An explanation of this sudden and rather unexpected change in slope at A~90 was conveniently provided by the concept of nuclear shells, which was first proposed by Maria Mayer in the "Shell Model" (Mayer, 1950). The

main feature of this model is the prediction that certain values of N or Z lead to great stability of the nucleus; this has been confirmed experimentally for the so-called "magic numbers" 2,8,20,28,50,82,126, which represent shell closures.

Evidence of the enhanced stability associated with closed nuclear shells may be seen in the fine detail of the variation of B.E./nucleon. It may be seen more clearly in a comparison, among isotopes of a given element, of the systematic changes in the energy required to remove the last pair of neutrons, S_{2n}. Abrupt and dramatic decreases in this energy are seen as the "magic numbers" (N = 28,50,82,126) are exceeded. In a similar way, it can be demonstrated that the same magic numbers of protons are also configurations of enhanced stability. In the region near the magic number 82, the values of S_{2n} for N~90 that would be expected on the basis of the behaviour for N<88 lie much below the measured values (Meredith, 1972). This feature was noted earlier by others (Barber, 1964 a,b; Duckworth, 1964; Macdougall, 1966) who drew attention to a major discontinuity in slope at N=88. This behaviour has been attributed to the onset of nuclear deformation that occurs in this region.

Atomic mass determinations as well as the energies available for α and β decay studies are of great interest in nuclear physics. The masses of stable nuclides provide a data base from which the best values for the semi-empirical atomic mass formula constants may be derived. This formula may be used for determination of atomic masses of unstable nuclides, which have obvious consequences in many nuclear processes of astrophysical interest, e.g., in the r-process of nucleosynthesis. Comparison between the predictions of the atomic mass formula and experimental masses is of interest for nuclear structure studies.

1-4 Methods of atomic mass determination

1-4-1 Alpha decay

Alpha decay is represented by :

$$ {}^{A}_{Z}X \rightarrow {}^{A-4}_{Z-2}Y + \alpha + Q \qquad (1\text{-}13) $$

where ${}^{A}X$, ${}^{A-4}Y$ are parent and daughter nuclei respectively, and Q is the energy released. The mass difference between ${}^{A}_{Z}X$ and ${}^{A-4}_{Z-2}Y$ may be determined by measuring the kinetic energy of the α particle and accounting for its rest energy and the recoil energy of ${}^{A-4}_{Z-2}Y$. This technique has provided most of the mass information for nuclei heavier than Bi since these are all unstable to some extent with respect to α emission. Usually, measurements of the highest precision are performed using a magnetic analyzer which must first be calibrated by an α of known energy. Such energy standards have been determined with standard errors as low as 0.05 keV (Rytz, 1972), although typical uncertainties lie in the range 1 to 6 keV (Hagberg, 1979). For atomic mass differences, these measurements must be corrected for the total binding energies of the atomic electrons.

1-4-2 Beta decay

The beta decay of a nucleus ${}^{A}_{Z}X$ may occur in three different ways :

A. Electron emission :

$$ {}^{A}_{Z}X \rightarrow {}^{A}_{Z+1}Y + e^{-} + \bar{\nu} + Q_{\beta^-} \qquad (1\text{-}14) $$

B. Positron emission :

$$ {}^{A}_{Z}X \rightarrow {}^{A}_{Z-1}Y + e^{+} + \nu + Q_{\beta^+} \qquad (1\text{-}15) $$

C. Electron capture :

$$ {}^{A}_{Z}X + e^{-} \rightarrow {}^{A}_{Z-1}Y + \nu + Q_{e.c} \qquad (1\text{-}16) $$

Because the total available energy Q is shared between the beta particles, the neutrino ν and recoil of the daughter nucleus Y, the beta particles are emitted with a continuous energy spectrum up to a maximum, or end point, value which determines the mass difference. If the mass difference between the atoms of the nuclides ${}^{A}_{Z}X$ and ${}^{A}_{Z-1}Y$ is in the range 0 to $2m_e c^2$ only electron capture will take place ($0 \leq Q_{e.c} \leq 2m_e c^2$). Electron capture does not usually provide useful mass difference results because the energy of the neutrino cannot be measured directly.

The typical precision of beta decay energy data is in the range 1 to 13 keV (Decker, 1981). However, in specific cases the beta decay energy was measured to a high precision of 13 eV using a toroidal beta spectrometer (Lubimov, 1980) and 7 eV using a Si(Li) detector (Simpson, 1985).

1-4-3 Nuclear reactions

A nuclear reaction may be expressed in the general form :

$$a + X \rightarrow Y + b + Q \qquad (1\text{-}17)$$

where a is the bombarding particle, b is the emitted particle, Q is the net energy released, and X, Y are the initial and final nuclei in their ground states, respectively. The Q-value may be obtained by measuring the kinetic energies of a, b and Y. Thus, from equation (1-17) one may derive the mass difference X-Y. The particles a and b may be charged particles, such as proton (p), deutron (d), tritium (t) and α, or neutrons or photons. The most accurate results of charged-particle reactions are found by deflecting the particles in magnetic or electric fields of known strength. Some nuclear reactions, like (p,t), (p,d) and (d,t) reactions, have precisions in the range of 1 to 10 keV (Berrier-Ronsin, 1978).

In particular, the (n,γ) reactions involving the capture of thermal neutrons provide the most precise mass differences between even-A and odd-A isotopes, with typical precisions of 0.5 keV or less (Table 5-2). γ-ray energies below 1 MeV may be determined with a curved-crystal spectrometer, while at higher energies Ge(Li) detectors are used.

1-4-4 Mass spectroscopy

Mass spectrometers are grouped into two main classes :

(I) Dynamic mass spectrometers :

In these instruments the time (frequency) properties of ionic motion in the electro-magnetic fields are of fundamental significance. In this group of machines the mass analysis depends on :

(1) the velocity and the time of flight of the ion (Time of flight instruments),

(2) the cyclotron frequency of the ion (Cyclotron resonance instruments), or

(3) the stability of the ion path within radio frequency electric fields (Quadrupole field instruments).

(II) Deflection-type instruments :

In such instruments the mass analysis is accomplished by static electromagnetic fields. Ions of a specific charge-to-mass ratio are separated in the deflection-type instruments by combinations of electric and magnetic fields.

Deflection-type and cyclotron resonance instruments have been used for precise atomic mass determination. The mass spectroscopic values are usually obtained by studying a pair of mass spectral peaks produced by two species of ions whose charge-to-mass ratios are approximately equal. Such a pair is called a doublet.

Mass spectroscopic data are of two types :

a) Absolute mass data

Mass differences like :

$$\Delta M = {}^{A}M^{+} - {}^{A}X^{+} \qquad (1\text{-}18)$$

are used to determine the absolute mass of the element X which has the same mass number A as a hydrocarbon molecule of well known mass M. The atomic masses of H, D, ^{13}C, ^{14}N, ^{35}Cl and ^{37}Cl were determined to precisions of 5, 10, 10, 11, 29 and 56 nu, respectively (Smith, 1971; Smith, 1975) by measuring the spacings of the doublets :

$C_9 H_{20}$ - $C_{10} H_8$, $C_5 D_{12}$ - $C_6 D_6$, CH - ^{13}C, CD - ^{14}N, $C_5 H_{10}$ - $^{35}Cl_2$, $C_2 D_8$ - $^{37}Cl H_3$ and using C as the standard of atomic masses (C = ^{12}C = 12u). These nuclides may be used as secondary standards for atomic mass determinations (Table 5-3). The precision of the absolute mass determination is typically 1 part in 10^8, the typical values of the uncertainties are in the range 1 to 5 keV (Hall, 1984).

b) Mass difference data

$$\Delta M = ({}^{A+2}X\ {}^{35}Cl)^{+} - ({}^{A}Y\ {}^{37}Cl)^{+} \qquad (1\text{-}19)$$

By measuring the doublet spacing ΔM and combining the result with the well known mass difference ^{37}Cl - ^{35}Cl, the mass difference between the elements ^{A+2}X and ^{A}Y may be obtained. The precision of this type of data can be as high as 2 parts in 10^9, which represents an uncertainty of about 0.5 keV, as demonstrated in this work (Table 5-1).

Most of the mass spectroscopic atomic mass determinations have been made by means of deflection instruments; however, the most precise measurements (precision as low as 5 eV) were obtained by L.G.Smith using his last version of the rf mass spectrometer at Princeton (Smith, 1971).

1-5 Atomic mass evaluations

Each measured mass difference can be expressed in the form of a linear equation involving two or more atomic masses as parameters. The number of possible equations generally exceeds the number of parameters and so the solution is overdetermined. Therefore, the method of least squares is appropriate to the calculation of the best values for the atomic masses (Mattauch, 1960; Bearden, 1957; Taylor, 1970). This method allows important consistency checks to be made on the deduced masses and clearly identifies areas where mistakes have been made in the earlier determinations (sec. 5-2, 5-3).

Such a major evaluation of all the atomic mass data has been undertaken with the encouragement of the International Union of Pure and Applied Physics SUNAMCO Commission. Compilations of such data have been made by Wapstra & Bose (Wapstra, 1977) and Wapstra & Audi (Wapstra, 1985).

References for chapter (1)

Aston, F. W. (1923). Philosophical Magazine, 39, 449.

Aston, F. W. (1942). Mass Spectra and Isotopes, London, Edward Arnold and Company.

Barber, R. C., Duckworth, H. E., Hogg, B. G., Macdougall, J. D., McLatchie, W. & van Rookhuyzen, P. (1964a). Phys. Rev. Lett., 12, 597.

Barber, R. C., Bishop, R. L., Cambey, L. A., Duckworth, H. E., Macdougall, J. D., McLatchie, W., Ormrod, J. H. & van Rookhuyzen, P. (1964b). Proc. Second Int. Conf. Nuclidic Masses, edited by W. H. Johnson, (Springer Verlag, Vienna), p.393.

Bearden, J. A. & Thompson, J. S. (1957). Nuovo Cimento Suppl., 5, 326.

Berrier-Ronsin, G., Vergnes, M., Rotbard, G., Vernotte, J., Kalifa, J., Seltz, R. & Sharma, H. L. (1978). Phys. Rev. C, 17, 529.

Clotfelter, B. E. (1970). Reference Systems and Inertia, Iowa State University Press, Ames., 60.

Cohen, E. R. & Taylor, B. N. (1976) At. Nuc. Data Tables 18, 587.

Cohen, E. R. & Wapstra, A. H. (1983). Nucl. Instr. Meth. 211, 153.

Decker, R., Wunsch, K. D., Wollnik, H., Jung, G., Munzel, J., Siegert, G. & Koglin, E. (1981). Zeitschrift für Physik A, 301, 165.

Dempster, A. J. (1938). Phys. Rev., 53, 64, 869.

Deslattes, R. D. (1974). Phys. Rev. Lett., 33, 463.

Duckworth, H. E., Woodcock, K. S. & Preston, R. S. (1950). Phys. Rev., 79, 198.

Duckworth, H. E.,Barber, R. C., Hogg, B. G., Macdougall, J. D., McLatchie, W. & van Rookhuyzen, P. (1964). Congr. Int. Phys. Nucl. Vol. II, edited by P. Gugenberger (Centre National de la Recherche Scientifique, Paris), p.557.

Evans, R. D. (1955). The Atomic Nucleus. New York : McGraw-Hill, chapter 28.

Feenberg, E. (1947). Review of Modern Physics, 19, 239.

Foldy, L. L. (1951). Phys. Rev., 88, 397.

Hagberg, E., Hansen, P. G., Hornshoj, P., Johnson, B., Mattson, S., Tidemand-Petersson, P. (1979). Nucl. Phys. A, 318, 29.

Hall, B. J., Ellis, R. J., Dyck, G. R., Lander, C. A., Beach, R., Sharma, K. S., Barber, R. C. & Duckworth, H. E. (1984). Phys. Lett. B, 138, 4, 260.

Keiser, G. M. & Faller, J. E. (1981). Proceedings of the Second Marcel Grossman Meeting on Recent Developments in General Relativity ed. Ruffini, R. (Amsterdam, North Holland).

Kohman, T. P., Mattauch, J. H. E. & Wapstra, A. H. (1958). Science, 127, 1431.

Lubimov, V. A., Novikov, E. G., Nozik, V. Z., Tretyakov, E. F. & Kosik, V. S. (1980). Phys. Lett. B, 94, 266.

Macdougall, J. D., McLatchie, W., Whineray, S. & Duckworth, H. E. (1966). Z. Naturforsch, 21a, 63.

Mattauch, J. H. E. (1960). Proc. Int. Conf. Nuclidic Masses edited by H .E. Duckworth (University of Toronto Press, Toronto)

Mayer, M. G. (1950). Phys. Rev. 78, 17.

Meredith, J. O. & Barber, R. C. (1972). Can. J. Phys, 50, 1195.

Nier, A. O. (1950). Phys. Rev., 77, 789.

Reasonberg, R. D. & Shapiro, I. I. (1976). Atomic Masses and Fundamental Constants, 5, ed. by J. H. Sanders and A. H. Wapstra (Plenum Publishing Corp., London), p.643.

Rytz, A., Grennberg, B. & Gorman, D. J. (1972). Atomic Masses and Fundamental Constants, 4, ed. by J. H. Sanders and A. H. Wapstra (Plenum Publishing Corp., London), p.1.

Simpson, J. J., Dixon, W. R. & Storey, R. S. (1985). Phys. Rev. C, 31, 1891.

Smith, L. G. (1971). Phys. Rev. C, 4, 22.

Smith, L. G. & Wapstra, A. H. (1975). Phys. Rev. C, 11, 1392.

Taylor, B. N., Parker, W. H. & Langenberg, D. N. (1970). The Fundamental Constants and Quantum Electrodynamics (Academic Press, New York), 327.

Wapstra, A. H. & Bose, K. (1977). Atomic Data and Nuclear Data Tables, 1977 Atomic Mass Evaluation, ed. Katherine Way. New York and London, Academic Press, 20.

Wapstra, A. H. & Audi, G. (1985). The 1983 Atomic Mass Evaluation, Nucl. Phys. A, 432, 1.

Wichers, E. (1962). Nature, 194, 621.

CHAPTER (2)

MASS SPECTROSCOPY

2-1 The development of mass spectroscopy

Mass spectroscopy made its start in the early 1900's when J.J.Thomson employed his first parabola apparatus. He made use of the discovery by Goldstein in 1886 that positive rays are obtained in an electrical discharge and the subsequent discovery by Wien in 1898 that these rays could be deflected by a magnetic field. Thomson observed that, in addition to the intense line for neon at atomic weight 20, there was a much fainter line that accompanied it at mass 22 (Thomson, 1912). This was the first indication that isotopes exist among the stable elements.

Thomson's apparatus was improved upon by Aston. He devised an instrument in 1919 (Aston, 1919), which he termed the mass spectrograph. In such an instrument, ions with the same values of (m/e) are focused at one point regardless of their velocity spread. This property is known as "velocity focusing". With this instrument, Aston achieved a resolution γ (γ = W/M, where M is the atomic mass of the nuclide considered and W is the full width of the peak in mass units) of about 1 part in 130, which represented an improvement by a factor of 10 over Thomson's apparatus. Aston determined the isotopic composition of neon, chlorine, mercury, nitrogen and the noble gases. The second version of his mass spectrograph was completed in 1925, possessing a resolution of 1 part in 600 and its accuracy of mass determination approached 1 part in 10,000 (Aston, 1927).

At about the same time a different type of mass spectrograph had been constructed by Dempster (Dempster, 1918). Here, ions were accelerated after their formation and deflected through 180° in a uniform magnetic field. Such a field possesses direction focusing; that is, a beam of ions diverging from a point at the entrance boundary of the magnetic field is focused after completing the semicircle. The resolution of this instrument was 1 part in 100.

In the early 1930's the stage was set for modern mass spectroscopy. Vacuum techniques were steadily improving, the vacuum tube electrometer replaced the quadrant electrometer and electroscope for measuring small currents, and the magnetically collimated electron beam for producing ions was introduced.

During the 1930's and 1940's, there was strong interest in determining atomic masses precisely. The instruments described above, having a single focusing (velocity or direction focusing) property, would not suffice. Several studies of the focusing properties of electric and magnetic fields culminated in 1934 in the definitive work of Herzog and Mattauch (Herzog & Mattauch, 1934; Herzog 1934) in which general focusing equations were derived for radial electric and/or homogeneous magnetic fields. This made possible the design of high-resolution, double-focusing, mass spectrographs which accommodated ions beams possessing both angle and velocity spread. These instruments were used for the precise determination of atomic masses. In one of these, the Mattauch-Herzog mass spectrograph, ions pass through a 31.8° cylindrical condenser followed by a 90° magnet. In the first instrument, the resolution achieved was 1 part in 5600. This double focusing arrangement has served as the basis for several other mass comparison instruments. Both Mattauch and Ewald constructed instruments in which a resolution of ~1 part in 100,000 was obtained (Mattauch, 1954; Everling et al, 1957). This type of instrument was particularly appropriate for experiments where velocity focusing is desired and where the simultaneous collection

of more than one mass is required. A later version, approximately eight times as large as the original, was constructed at Harvard University (Collins, 1957; Bainbridge, 1960). A resolution of up to 1/250,000 full width at half maximum was attained with electrical detection. Another commonly used double-focusing geometry, the Nier-Johnson, employs a 90° electrical analyzer followed by a 60° magnetic analyzer (Nier, 1951; Johnson, 1953). Using a collector slit with an electrical detector placed at the position of double focus, the full width at half maximum (FWHM) of the peaks corresponded to a resolution of 1/14,000. A second, enlarged version of this instrument was built at the University of Minnesota (Quisenberry, 1956). A resolution of 1/75,000 has been obtained. Atomic mass differences have been determined with this instrument to a precision of up to $2/10^9$ of the mass at which the doublet occurs (Kayser, 1976).

In the 1950's, some instruments were constructed by Duckworth at McMaster University (Duckworth, 1957) and by Ogata in Japan (Ogata, 1957) and resolutions in excess of 1/100,000 were achieved. Nier & Roberts (Nier, 1951) and Johnson & Nier (Johnson, 1953) described a double-focusing combination possessing, at a given point, direction focusing to second order together with velocity focusing to first order. Similarly, several other instruments which attain the partial second-order double focusing were constructed by Hintenberger and Mattauch at Mainz (Everling et al, 1957), Nier at Minnesota (Nier, 1957), Bainbridge at Harvard (Collins, 1957) and by Stevens at Argonne National Laboratory (Stevens, 1960). Direction focusing and velocity focusing have been obtained to second order in instruments which were built by Matsuda at Osaka (Matsuda, 1966) and by Barber at the University of Manitoba (Barber, 1971) (see sec. 2-2-4).

In addition to the deflection-type mass spectrometers, cyclotron resonance instruments (sec. 1-4-4) have also been used for atomic mass determination. In these latter mass spec-

trometers the ions describe circular paths in a homogeneous magnetic field. The mass of an ion is determined by measuring the cyclotron frequency, sometimes in terms of a high harmonic with rf fields, such as in the rf mass synchrometer developed by L.G.Smith (Smith, 1951 a, b). With a later version of this instrument, utilizing higher frequencies and fields, he achieved a resolution, full width at half maximum in the range $2.5 - 5.0 \times 10^{-6}$. In another type, ions are formed in a Penning trap placed in a high uniform magnetic field. Ion cyclotron motion is excited by an electric field between two plates which are connected to an oscillator. The oscillator frequency is adjusted such that the power absorption at the resonance frequency is observed. This type of instruments is called an ion cyclotron resonance (ICR) mass spectrometer. A high resolution of $1/10^8$ has been achieved and a mass difference was measured to a high precision of 2 eV (Lippmaa, 1985) with this type of instruments.

2-2 Positive ion optics

In deflection-type mass spectrometers, the ion orbit is determined by the Lorentz force equation :

$$\vec{F} = q(\vec{E} + \vec{v} \times \vec{B}) \qquad (2\text{-}1)$$

where q and $\vec{v}$ are the charge and velocity of the ion which moves under the influence of electromagnetic fields $\vec{E}$ and $\vec{B}$. The magnetic and electric fields possess ion-focusing properties. These properties may be appreciated by examining the results of a general first-order analysis presented by Herzog (Herzog, 1934).

2-2-1 Direction focusing in uniform magnetic fields

When an ion traverses a magnetic field $\vec{B}$, of constant magnitude and direction, at right angles, the ion is constrained to follow a circular path of radius a_m :

$$a_m = \frac{mv}{qB} \tag{2-2}$$

Thus, a uniform magnetic field discriminates between ions according to their momentum-to-charge ratio.

In Fig. 2-1, suppose that a group of ions of mass M_0 and velocity v_0 with a half angular spread $\alpha(\alpha \ll 1)$ emerge from an object point O located at a distance l_m' from the entrance boundary of the magnetic field. The ions following the optic axis or central path enter the magnetic field normally, proceed along a circular path of radius a_m through an angle ϕ_m and emerge normal to the exit boundary. The ion beam which diverges from the object point O converges to the image point I located a distance l_m'' from the exit boundary, such that the object O, the center of curvature C and the image I lie on a straight line (Barber's rule) (Barber, 1933).

Herzog likened this arrangement to the optical combination of a prism plus a cylindrical lens, and showed that its focal length is given by :

$$f_m = \frac{a_m}{\sin \phi_m} \tag{2-3}$$

Also, the object and image distances, l_m' and l_m'', are related by :

$$(l_m' - g_m)(l_m'' - g_m) = f_m^2 \tag{2-4}$$

where:

$$g_m = f_m \cos\phi_m \tag{2-5}$$

is the distance from the boundary of the field to the principal focus.

Herzog (Herzog, 1934) investigated the effect on the displacement of the image b_m'' resulting from a displacement of the object b_m', a change of the ionic mass to $M = M_0(1+\gamma)$ from M_0 and of the ionic velocity to $v = v_0(1+\beta)$ from v_0, where both γ and β are small quantities

$$b_m'' = a_m(\beta+\gamma)\left[1+\frac{f_m}{(l_m'-g_m)}\right] - b_m'\frac{f_m}{(l_m'-g_m)} \tag{2-6}$$

For the original group (M_0, v_0), where $\gamma = \beta = 0$, the magnification is :

$$\frac{b_m''}{b_m'} = -\frac{f_m}{(l_m'-g_m)} \tag{2-7}$$

which has the value unity for symmetrical arrangements $(l_m' = l_m'')$.

For the special case of an object slit of width $S_o = 2b_m'$ with a monoenergetic ion beam $(\gamma+2\beta = 0$ to first order) and symmetrical arrangements, the mass resolution is given by :

$$\gamma = \frac{S_o}{a_m} \tag{2-8}$$

When electrical detection is used an image slit of width S_i is placed at point I and the resolution is reduced to :

$$\gamma = \frac{(S_o+S_i)}{a_m} \tag{2-9}$$

The dispersion D is found from eqn. (2-6) by computing the displacement of the image corresponding to a 1% mass change. For a monoenergetic ion beam and symmetrical arrangements, the dispersion is :

$$D = \frac{a_m}{100} \tag{2-10}$$

for a 1% mass difference, measured in the plane normal to the central beam.

2-2-2 Direction focusing in radial electrostatic fields

The radial electrostatic field is the field which exists between the plates of a cylindrical condenser. This field may be established by applying a potential difference, V, between a pair of concentric cylindrical electrodes of radii $a_e - k$ and $a_e + k$ (Fig. 2-2), such that the separation between the electrodes is 2k.

For ions travelling through the optic axis :

$$a_e = (mv^2/2q)4k/V \tag{2-11}$$

Thus, a radial electric field acts as a kinetic energy analyzer, dispersing ions according to their energy-to-charge ratio.

Herzog developed the general focusing equations for radial electrostatic fields, which take the same form as those given for a homogeneous magnetic fields. The object and image distances l_e' and l_e'' are related through :

$$(l_e' - g_e)(l_e'' - g_e) = f_e^2 \tag{2-12}$$

where :

$$f_e = \frac{a_e}{\sqrt{2}\sin\sqrt{2}\phi_e} \tag{2-13}$$

and :

$$g_e = f_e \cos\sqrt{2}\phi_e \tag{2-14}$$

$$b_e'' = a_e\left(\beta + \frac{\gamma}{2}\right)\left[1 + \frac{f_e}{(l_e' - g_e)}\right] - b_e' \frac{f_e}{(l_e' - g_e)} \tag{2-15}$$

In the case of a monoenergetic ion beam, for which $\beta = -\frac{\gamma}{2}$, all ions, regardless of their mass, are focused at the same point. Thus, the radial electrostatic analyzer is an energy selector, and has been frequently used as such to determine the energies of charged particles involved in nuclear reactions.

2-2-3 Double focusing

The term involving β in eqns. (2-6) and (2-15) gives the velocity dispersion associated with the electric and magnetic fields. It can be envisaged that a compound system including both an electrostatic and a magnetic field could be designed such that the velocity dispersion produced in one will be counter balanced by that produced in the other while leaving a non-zero mass dispersion. Thus, the final image position will be independent of both velocity and direction spread. This combination is said to be double focusing.

The most commonly employed double-focusing arrangement is one in which the image formed by a radial electrostatic field serves as the object for a following magnetic field. Combining eqns. (2-6) and (2-15) yields a relationship between the final image displacement b_m'', and the initial object displacement b_e' :

$$b_m'' = a_m(\beta+\gamma)\left[1+\frac{f_m}{(l_m'-g_m)}\right]-\frac{f_m}{(l_m'-g_m)}\left\{a_e\left(\beta+\frac{\gamma}{2}\right)\left[1+\frac{f_e}{(l_e'-g_e)}\right]-b_e'\frac{f_e}{(l_e'-g_e)}\right\} \qquad (2\text{-}16)$$

Velocity focusing will occur when the coefficient of β vanishes in eqn. (2-16). This occurs when :

$$a_m\left[\frac{(l_m'-g_m)}{f_m}+1\right]=a_e\left[1+\frac{f_e}{(l_e'-g_e)}\right] \qquad (2\text{-}17)$$

Equation (2-17) represents the condition for first-order double focusing.

2-2-4 Second–order double focusing

Hintenberger and König (Hintenberger, 1957) extended Herzog's theory to include second-order terms in α and β. In their calculations they assumed that the electric fields are radial, the magnetic fields are uniform, and that all the field boundaries are abrupt. The displacement, Y_B, of the ion path from the optic axis is given by :

$$Y_B = a_m(B_1\alpha + B_2\beta + B_{11}\alpha^2 + B_{12}\alpha\beta + B_{22}\beta^2) + \textit{higher order terms} \qquad (2\text{-}18)$$

The coefficients B_1, B_2, B_{11}, B_{12} and B_{22} are functions of eight geometrical instrument parameters : $\phi_m, \varepsilon', \varepsilon'', \phi_e, \frac{a_e}{a_m}, \frac{l_e'}{a_m}, \frac{l_m''}{a_m}$ and $\frac{\Delta}{a_m}$ (Δ is the distance between the electric and magnetic fields while ε' and ε'' represent the angles of inclination of the entrance and exit boundaries, respectively, of the magnetic field with respect to a direction perpendicular to the optic axis). Hintenberger and König selected values for three of the parameters and obtained unique solutions for the remaining five by solving the five simultaneous equations

$$B_1 = B_2 = B_{11} = B_{12} = B_{22} = 0 \qquad (2\text{-}19)$$

Eqn. (2-19) represents the condition for a complete second-order double focus. Hintenberger and König presented a number of geometrical arrangements which provide a complete second-order focus. One of these arrangements is the basis for a mass spectrometer which has been constructed at the University of Manitoba (Barber, 1971). The Manitoba instrument (referred to as "Manitoba II") is the instrument used for all the new mass determinations reported in this thesis.

The effects of the fringe fields for homogeneous magnetic fields and cylindrical electrostatic fields have been studied to second order (Wollnik, 1965, 1967b; Enge, 1964, 1967). The general case of the fringe field of an homogeneous magnetic field has been described to third order (Matsuda, 1970a, b). Similarly, the general case of the fringe field

of a toroidal electrostatic analyzer has been described to third order by Matsuda (Matsuda, 1971). Higher order focusing properties, including fringe effects, have been examined by Fujita & Matsuda (Fujita, 1975) and by Matsuda & Wollnik (Matsuda, 1972).

Matsuo, Matsuda, Fujita & Wollnik (Matsuo, 1975) have developed a computer program for third order ion optics called "TRIO" for the calculation of ion trajectories through any combination of drift spaces, cylindrical or toroidal electric sector fields, homogeneous or inhomogeneous magnetic sector fields, and magnetic or electrostatic quadrupole lenses. The effect of the fringe fields is included and the calculation is carried out to third order for the radial direction and to second order for the axial direction.

2-3 Mass spectroscopic atomic mass determinations

The mass width, W, of a mass spectral peak is given by :

$$W = \gamma M \qquad (2\text{-}20)$$

where γ is the resolution and M is the ionic mass. If the position of a peak can be located to some fraction f of its width W, the resulting uncertainty δM will be :

$$\delta M = fW = f\gamma M \qquad (2\text{-}21)$$

For mass spectrographs, in which photographic detection is used, f is typically 1/50 of a line width; here the resolution is limited by the grain size of the photographic plate ($\sim 10^{-4} cm$). This limit became a practical one in the work of Mattauch and his collaborators (Everling, 1957) who secured, with careful adjustment, a resolution of 1 part in 10,000. For mass spectrometers, the introduction of electrical detection leads to :

(1) A deterioration in the resolution by a factor of 2 (i.e. γ increases by a factor of 2) when the collector slit has the same width as the image, and

(2) a reduction of the factor f to about 1/1000.

Thus, a significant overall improvement in precision is achieved. For mass spectrometers, the mass difference is usually determined by some variation of the peak matching technique.

2-3-1 Peak matching

The technique of peak matching originated with Smith (Smith, 1953, 1956) and was first applied to deflection instruments by the group at the University of Minnesota (Giese, 1954; Quisenberry, 1956).

This technique depends on a general theorem by Swann (Swann, 1931) and Bleakney (Bleakney, 1936). Suppose that an ion of mass M, initially at rest, traverses a particular path through the mass spectrometer. Then an ion of mass M', also initially at rest at the same point, will traverse exactly the same path through the instrument provided that all magnetic fields remain constant and all electric fields, E, are changed in magnitude to E', such that :

$$ME = M'E' \tag{2-22}$$

Accordingly, if a potential V_e is applied to the electrodes of the electrostatic analyzer shown in Figure 2-2, it must be changed to V_e', so that :

$$MV_e = M'V_e' \tag{2-23}$$

This equation may be rewritten in the convenient form :

$$\frac{\Delta M}{M'} = \frac{\Delta V_e}{V_e} \qquad (2\text{-}24)$$

where $\Delta M = M' - M$ and $\Delta V_e = V_e - V_e'$.

Thus, at the matched condition, the ratio of $\frac{\Delta V_e}{V_e}$ is measured and the mass difference ΔM is calculated. Two techniques have been applied to the Manitoba II spectrometer for the precise determination of the matched condition (sec. 4-1, 4-2).

2-3-2 Systematic errors

Systematic errors may occur when a small unswitched voltage gives rise to an electric field in the instrument. This would displace the trajectories of M and M' by amounts which differ in proportion to ΔM. Such errors have been investigated in detail for Manitoba II by Southon (Southon, 1973, 1977). It is believed that the dominant mechanism for producing these potentials is the collection of charges on insulating films that are formed on the electrostatic analyzer plates. The phenomenon of surface charges accumulating on relatively clean metal plates has been investigated by Petit-Clerc and Carette (Petit-Clerc, 1968, 1970) who found that it was possible for potentials of up to 0.5 V to develop and persist for several hours when the plates were subjected to electron or ion bombardment.

Systematic errors may also arise when the two members of the doublet are formed in the ion source with different energy distributions. Such a situation may occur if dissociation energies differ or if the two species are ionized at different locations in the ion source. Even though the beams might coincide at the beginning and end, in general, they follow different paths, experiencing different fields, etc.

The magnitude of the systematic error, E, is determined by measuring the spacing between two widely spaced mass spectral peaks whose separation is well known :

$$E = \frac{(\Delta M - \Delta M_{meas})}{\Delta M} \qquad (2\text{-}25)$$

where ΔM_{meas} is the measured mass difference and ΔM is the well known value of the mass difference. Then, if $\Delta M'$ is the mass difference determined for a narrow doublet, the corrected value, ΔM, is given by :

$$\Delta M = \Delta M'(1 + E) \qquad (2\text{-}26)$$

For Manitoba II, E is typically 150 ppm.

References for chapter (2)

Aston, F. W. (1919). Philosophical Magazine, 38, 709.

Aston, F. W. (1927). Proceedings of the Royal Society A, 115, 487.

Bainbridge, K. T., Moreland, P. E. (1960). Proc. Int. Conf. Nuclidic Masses edited by H .E. Duckworth p. 460, (University of Toronto Press, Toronto).

Barber, N. F. (1933). Proceedings of the Leeds Philosophical and Literary Society 2, 427.

Barber, R. C., Bishop, R. L. , Duckworth, H. E., Meredith, J. O., Southon , F. C. G., van Rookhuyzen, P. & Williams, P. (1971). Rev. of Sci. Instr., 42, 1.

Bleakney, W. (1936). American Physics Teacher, 4, 12.

Collins, T. L. & Bainbridge, K. T. (1957). Nuclear Masses and Their Determination, ed. by H. Hintenberger, p. 253. (Pergman Press, New York, London, Paris).

Dempster, A. J. (1918). Phys. Rev., 11, 316.

Duckworth, H. E., Kerr, J. T. & Bainbridge, G. R. (1957). Nuclear Masses and Their Determination, ed. by H. Hintenberger, p. 218. (Pergman Press, London).

Enge, H. A. (1964). Rev. of Sci. Instr., 32, 859.

Enge, H. A. (1967). Focusing of Charged Particles, vol. 2, ed. A. Septier, p. 203. (Academic Press, New York and London).

Everling, F., Hintenberger, H., König, L. A., Mattauch, J., Muller-Warmuth, W. & Wende, H. (1957). Nuclear Masses and Their Determination, ed. by H. Hintenberger, p. 221. (Pergamon Press, London).

Everling, F. (1957). Nuclear Masses and Their Determination, ed. by H. Hintenberger, p. 253. (Pergman Press, New York, London, Paris).

Fujita, Y. & Matsuda, H. (1975). Nucl. Instr. Meth., 123, 495.

Giese, C. F. & Collins, T. L. (1954). Phys. Rev., 96, 823.

Herzog, R. & Mattauch, J. H. E. (1934). Annalen der Physik, Leipzig, 19, 345.

Herzog, R. (1934). Zeitschrift für Physik, 89, 447.

Hintenberger, H. & König, L. A. (1957). Z.Naturforschg, 12a, 773.

Johnson, E. G. & Nier, A. O. (1953). Phys. Rev., 91, 10.

Kayser, D. C., Halvorson, J. & Johnson, W. H. Jr. (1976). Atomic Mases and Fundamental Constants, 5, ed. by J. H. Sanders and A. H. Wapstra, p.178. (Plenum Press, New York, London).

Lippmaa, E., Pikver, R., Suurmaa, E., Past, J., Koppel, I. & Tammik, A. (1985). Phys. Rev. Lett., 54, 285.

Matsuda, H., Fukumoto, S. & Kuroda, Y. (1966). Z.Naturforschg, 21a, 25.

Matsuda, H. & Wollnik, H. (1970a). Nucl. Instr. Meth., 77, 40.

Matsuda, H. & Wollnik, H. (1970b). Nucl. Instr. Meth., 77, 283.

Matsuda, H. (1971). Nucl. Instr. Meth., 91, 637.

Matsuda, H. & Wollnik, H. (1972). Nucl. Instr. Meth., 103, 117.

Matsuo, T., Matsuda, H., Fujita, Y. & Wollnik, H. (1975). Mass Spectroscopy (Japan), 24, 19.

Mattauch, J. H. E. & Bieri, R. (1954). Zeitschrift für Naturforschung, 9a, 303.

Nier, A. O. & Roberts, T. R. (1951). Phys. Rev., 81, 507.

Nier, A. O., Quisenberry, K. S. & Scolman, T. T. (1957). Nuclear Masses and Their Determination, ed. by H. Hintenberger, p.49. (Pergamon Press, London).

Ogata, K. & Matsuda, H. (1957). Nuclear Masses and Their Determination, ed. by H. Hintenberger, p.202. (Pergamon Press, London).

Petit-Clerc, Y. & Carette, J. D. (1968). Vacuum, 18, 7.

Petit-Clerc, Y. & Carette, J. D. (1970). Abst. of 38 th ACFAS Congress, Quebec, Canada.

Quisenberry, K. S., Scolman, T. T. & Nier, A. O. (1956). Phys. Rev., 102, 1071.

Smith, L. G. (1951a). Phys. Rev., 81, 295.

Smith, L. G. (1951b). Rev. of Sci. Instr., 22, 115.

Smith, L. G. & Damm, C. C. (1953). Phys. Rev., 90, 324.

Smith, L. G. & Damm, C. C. (1956). Rev. of Sci. Instr., 27, 638.

Southon, F. C. G. (1973). PhD. Thesis, University of Manitoba.

Southon, F. C. G., Meredith, J. O., Barber, R. C. & Duckworth, H. E. (1977). Can. J. Phys., 55, 383.

Stevens, C. M., Terandy, J., Lobell, G., Wolfe, J., Beyer, N. & Lewis, R. (1960). Proc. Int. Conf. Nuclidic Masses edited by H .E. Duckworth p. 403, (University of Toronto Press, Toronto).

Swann, W. F. G. (1931). Journal of Franklin Institute, 212, 439.

Thomson, J. J. (1912). Philosophical Magazine, VI, 24, 209, 668.

Wollnik, H. & Ewald, H. (1965). Nucl. Instr. Meth., 36, 93.

Wollnik, H. (1967). Nucl. Instr. Meth., 52, 250.

FIGURE 2-1

Uniform sector magnetic analyzer

FIGURE 2-2

Radial sector electric analyzer

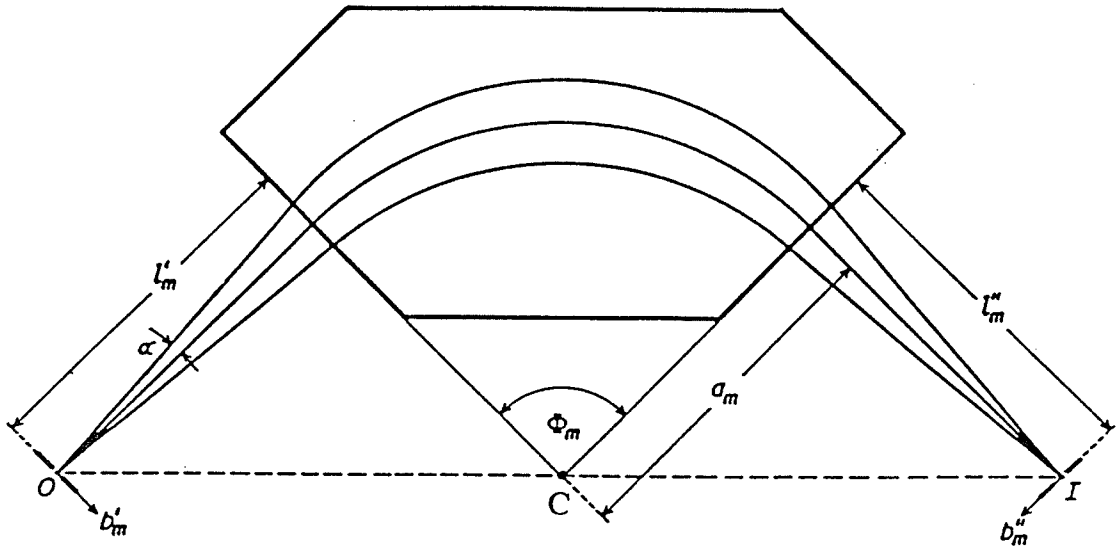
l'_m
α
Φ_m
a_m
l''_m
O
C
I
b'_m
b''_m

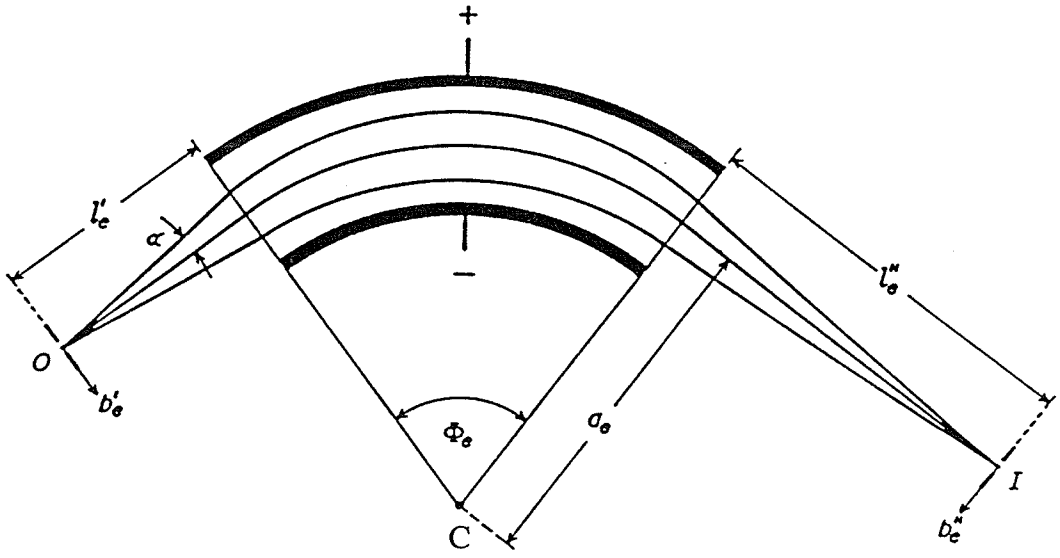
+
−
l'_e
α
Φ_e
a_e
l''_e
O
C
I
b'_e
b''_e

CHAPTER (3)

THE MANITOBA II MASS SPECTROMETER

3-1 Instrument geometry

The geometry of the Manitoba II mass spectrometer (Fig. 3-1) is one of many instrument configurations proposed by Hintenberger and König (Hintenberger, 1959) which produce complete second-order double focusing with small (negligible) third-order effects. The advantages in choosing this particular geometry, are :

(1) An intermediate direction focus is obtained between the electrostatic and magnetic analyzers. This focus allows the use of an energy defining slit S_β to control the range of ion energies transmitted, and also aids in the focusing and operation of the instrument.

(2) A compact design in which the individual ion path lengths l_e', l_e'', l_m' and l_m'' are relatively short. This compactness minimizes problems associated with mechanical vibrations and stray magnetic fields.

(3) The total ion path (4.59 m) is short compared to the mean radius of curvature in the electrostatic analyzer ($a_e = 1m$). The short path length reduces effects resulting from the scattering of ions by residual gases in the vacuum, while the large radii of curvature, a_e and a_m, provide good energy and momentum dispersion.

(4) An overall magnification of 0.5, which allows less stringent requirements on the object slit quality. The object slit S_o experiences more intense ion bombardment than the collector slit S_c and, consequently, deteriorates more rapidly.

(5) The magnetic field boundaries are straight rather than curved and thereby simplifies, considerably, the construction, assembly and the alignment of the magnet.

The scale of the instrument was determined by choosing the mean radius of curvature of the electrostatic analyzer a_e to be equal to 1m. The dispersion of the instrument is 5.3 mm for a 1% mass difference. For a resolution of 1/200,000 at the base of the peaks and with the width of S_c equal to the image width, S_o is 2.7 μm wide.

3-2 Ion source geometry

The ion source shown in Fig. 3-2 is an electron bombardment type. It is a variation of the Finkelstein source (von Ardenne, 1962). This type of source has been described by Bishop (Bishop, 1969) and Barber (Barber, 1971). Ions are produced by electron bombardment in the vicinity of a small hole in the oven (B) which contains the sample vapour. The sample is contained in a copper tube located outside the ion source body and may be heated by passing a current through a nichrome ribbon wrapped around the tube. The sample vapour enters the oven through a gas inlet tube (A) which is electrically isolated from the source casing.

The electrons are emitted from a rhenium filament (C) which is held at a potential of approximately -150 V with respect to the oven. The source case is held approximately -400 V with respect to the oven and, thus, acts both as an electron repeller and a positive ion extractor. The electromagnet is excited by a coil (D), so that there is a magnetic field of about 1 kG in the central region of the oven, directed parallel to the axis of the source. Thus, the emitted electrons are constrained to follow helical paths along the axis of the source, passing through the hole in the back of the oven and then oscillating back and forth.

The ion accelerating potential, V_a, of about 20 kV is applied directly to the oven and, thus, defines the energy of the ions produced. This potential is provided by a commercial power supply (Universal Voltronics Corp., Model BRE 30-2, 30 kV, 2 mA) which has a short-term stability of about 0.5 V. The accelerating voltage is switched according to eqn. (2-23) by adding to it a voltage, ΔV_a, derived from a Kepco model ABC 425, 425 V programmable power supply. The total ion current extracted from the source is usually 1 to 5 μA.

The ions are extracted from the plasma through the front aperture of the oven by a grounded electrode located just outside the source. The ion beam emerging from the source can be steered horizontally or vertically by separate pairs of electrostatic deflection plates. Subsequently, the ions are focused on the principal, or object, slit by an electrostatic quadrupole lens pair. The potentials applied to the quadrupoles and deflection plates are derived from a pair of Kepco ABC power supplies. These potentials are also switched according to eqn. (2-23). The steering and focusing system is described in detail by Southon (Southon, 1973).

The principal slit is variable in width and in orientation about the optic axis. The position of the object slit relative to the electrostatic analyzer may be adjusted by means of lathe slides. A rotary table is available to adjust the angle of entry of the ion beam into the electrostatic analyzer.

The ion source region is evacuated by two 100 l/s diffusion pumps. The pressure in this region is approximately 1×10^{-6} Torr.

3-3 Electrostatic analyzer region

The electrostatic analyzer is a cylindrical condenser of mean radius of curvature $a_e = 1m$ and sector angle $\phi_e = 94.65°$. The analyzer plates, which are made of gold-plated Armco iron, are separated by a gap of 2 cm. The electric field is terminated at the physical boundaries of the plates by grounded blocks positioned according to Herzog's theory (Herzog, 1935). A variable slit, S_α, located at the analyzer entrance is usually set to limit the half-angular divergence, α, of the accepted ion beam to $\sim \pm 2 \times 10^{-3}$ radians. Another variable slit, S_β, placed at the intermediate direction focus is used to limit the velocity dispersion, β, to $\sim \pm 8 \times 10^{-4}$. The position of the object slit , S_o, relative to the electrostatic analyzer can be adjusted by a rotary table mounted on the I-beam support which is bolted to the analyzer base. Lathe slides are placed directly beneath the intermediate direction focus to adjust the position of the electrostatic analyzer relative to the magnetic analyzer. The electrostatic analyzer is enclosed in a vacuum vessel having 12.5 mm thick stainless steel walls and metal gaskets. The entire chamber is evacuated by means of a Leybold Turbotronik 150 l/s turbomolecular pump which is backed by a mechanical roughing pump.

The potential supply for the electrostatic analyzer is shown in Fig. 3-3. The potential difference, V, across the plates is about 780 V and is provided by eight 97.2 V mercury batteries. Two power supplies are available to supply the switched voltage, ΔV, one of which is used for wide calibration doublets and the other for narrow doublets. Both ΔV supplies are described in detail by Southon (Southon, 1973). A mechanical chopper is used to switch ΔV on and off according to Bleakney's theorem (eqn. 2-23). A precision potentiometer described by Bishop and Barber (Bishop, 1970) is used to measure both V and ΔV in units called "micro Bishop" (1 μBishop ≈ 4 μV). The power supply for this potentiometer is

referenced to a 97.2 V mercury battery which is identical to the others. All nine mercury batteries, together with the potentiometer and associated power supply, are located in the same temperature-controlled box.

3-4 Magnetic analyzer region

The magnetic analyzer has a sector angle, ϕ_m, of 90° and mean radius of $a_m = 62.74cm$. The pole pieces are single blocks of Armco iron. Below and above the pole pieces, a small shimming gap has been introduced to improve the homogeneity of the field. Recent improvements to the magnetic analyzer include :

(1) The old, low-current, high-voltage coils have been replaced by a twelve new coils, each consisting of sixty turns. These coils are arranged in pairs on three C-shaped yokes. The three pairs are connected in parallel electrically.

(2) Use of a new magnet power supply, (BRUKER type B-MN15/200) has been added which is a low-voltage (15 V), high-current (200 A) power supply with a power consumption of about 4.9 kW. The short-term stability of the magnet current supply is better than 3 ppm over one minute. Remote control of the power supply is available through a personal computer. The control unit is equipped with a standard IEEE-488 interface.

(3) A closed-loop cooling system is shown in Fig. 3-4 in which a mechanical pump circulates water through the magnet coils and the magnet power supply to the heat exchanger. The cooling water required for this supply has a temperature range of 15 to 30° c. The water consumption at 3 bar is 12 l/min. The circulated water has an electrical resistance, R_w connected in parallel with the resistance of the coils, $R_c(\approx 1\Omega)$. Water impurities change the value of R_w and, thus, the magnet current stability is

governed by two factors : the short-term stability of the power supply (3 ppm) and R_w. Deionized water with $R_w \approx 18 M\Omega/cm$ has been used to limit short term instabilities in the current to a few ppm.

3-5 Ion collection region

The image, or collector, slit, S_c, is similar in construction to the object, or principal, slit, S_o. The position of the collector slit may be adjusted by using two screw drives.

The ion beam is swept across the collector slit by a sawtooth magnetic field generated by a pair of Helmholtz coils located between the magnet and the collector slit. These coils are driven by the output current of a bipolar operational power supply (Kepco model 36-5M) which is used as a voltage-to-current converter. The input signal to this power supply is a linear-ramp voltage signal which passes symmetrically through ground potential. This signal is constructed by adding a constant bias voltage to the sweep voltage of the display oscilloscope. The resultant magnetic field, which has zero value at the center of the sweep, provides the following advantages :

(1) If the observed peak is centered on the oscilloscope screen, its position will be independent of the sweep amplitude.

(2) The magnetic field need not be adjusted to keep the mass peak at the center of the oscilloscope screen when the sweep direction is reversed.

The ions passing through the collector slit are detected by a Galileo model 4830 channel electron multiplier (CEM) which is connected to an Amptek model A-101 preamplifier.

This model provides a positive 5 V output pulse (width of 220 ns, 6 ns rise time and 20 ns fall time). The A-101 preamplifier is senstive to an input negative charge pulse of at least 1.6×10^{-10} coulomb. This threshold is equivalent to 10^6 electrons.

3-6 Focusing procedure

This section describes the procedure and tests for both direction and velocity focus, which were defined previously in section 2-1.

Initially, the distances l_e' and l_m' are set at their theoretical values (Fig. 3-1). With the electrostatic analyzer thus set up, the angle of entry of the ion beam into the magnetic field, ε', is varied in order to bring, in turn, the direction and velocity foci to the collector.

Velocity focus is checked by changing the ion accelerating potential, V_a, by about 10 V on alternate sweeps of the oscilloscope. The lack of a velocity focus is characterized by a peak being displaced with respect to its unperturbed position on alternate sweeps.

The direction focus is then moved to this position by adjusting l_e'. The direction focus is characterized by a very marked increase in the sharpness of the peaks.

3-7 Control circuitry

The control circuitry is shown in Fig. 3-5. The master trigger signal is derived from a mechanical chopper which switches the voltage ΔV_e applied to the electrostatic analyzer and supplies the start signal for the sweep of the display oscilloscope and the signal averager. The sawtooth voltage from the oscilloscope is amplified in order to drive the Helmholtz coils which modulate the beam position across the collector slit. The differentiated sawtooth triggers a flip-flop circuit which :

(1) switches the detector information through gain A or gain B,

(2) switches the voltage ΔV_a added to the ion acceleration potential V_a, and

(3) switches the voltages applied to the steering and quadrupole lens system.

Two timing signals A and B are also generated by the chopper. The relationship between these timing signals and the changes in the potentials applied to Manitoba II are shown in Fig. 3-6 a, b. As shown in these figures, a trigger pulse is generated approximately 500 μs after A or B changes. Thus, a period of greater than 500 μs is allowed for the applied voltages to settle before the spectrum is recorded.

Detailed descriptions of this control system including the modifications necessary for computer-assisted peak matching may be found in Meredith (Meredith, 1971) and Sharma (Sharma, 1979).

References for chapter (3)

Barber, R. C., Bishop, R. L. , Duckworth, H. E., Meredith, J. O., Southon , F. C. G., Van Rookhuyzen, P. & Williams, P. (1971). Rev. of Sci. Instr., 42, 1.

Bishop, R. L. (1969). PhD. Thesis, Winnipeg : University of Manitoba.

Bishop, R. L. & Barber, R. C. (1970). Rev. of Sci. Instr., 42, 327.

Herzog, R. (1935). Zeitschrift für Physik, 87, 596.

Hintenberger, H. & König, L. A. (1959). Adv. in Mass Spectrometry, ed. by Waldron, J. D., p.16 (Pergamon Press, London).

Meredith, J. O. (1971). PhD. Thesis, Winnipeg : University of Manitoba.

Sharma, K. S. (1979). PhD. Thesis, Winnipeg : University of Manitoba.

Southon, F. C. G. (1973). PhD. Thesis, Winnipeg : University of Manitoba.

von Ardenne, M. (1962). Tabellen Zur Angewandten Physik, Band I (Veb Deutscher Verlag der Wissenschaften, Berlin).

FIGURE 3-1

Manitoba II mass spectrometer

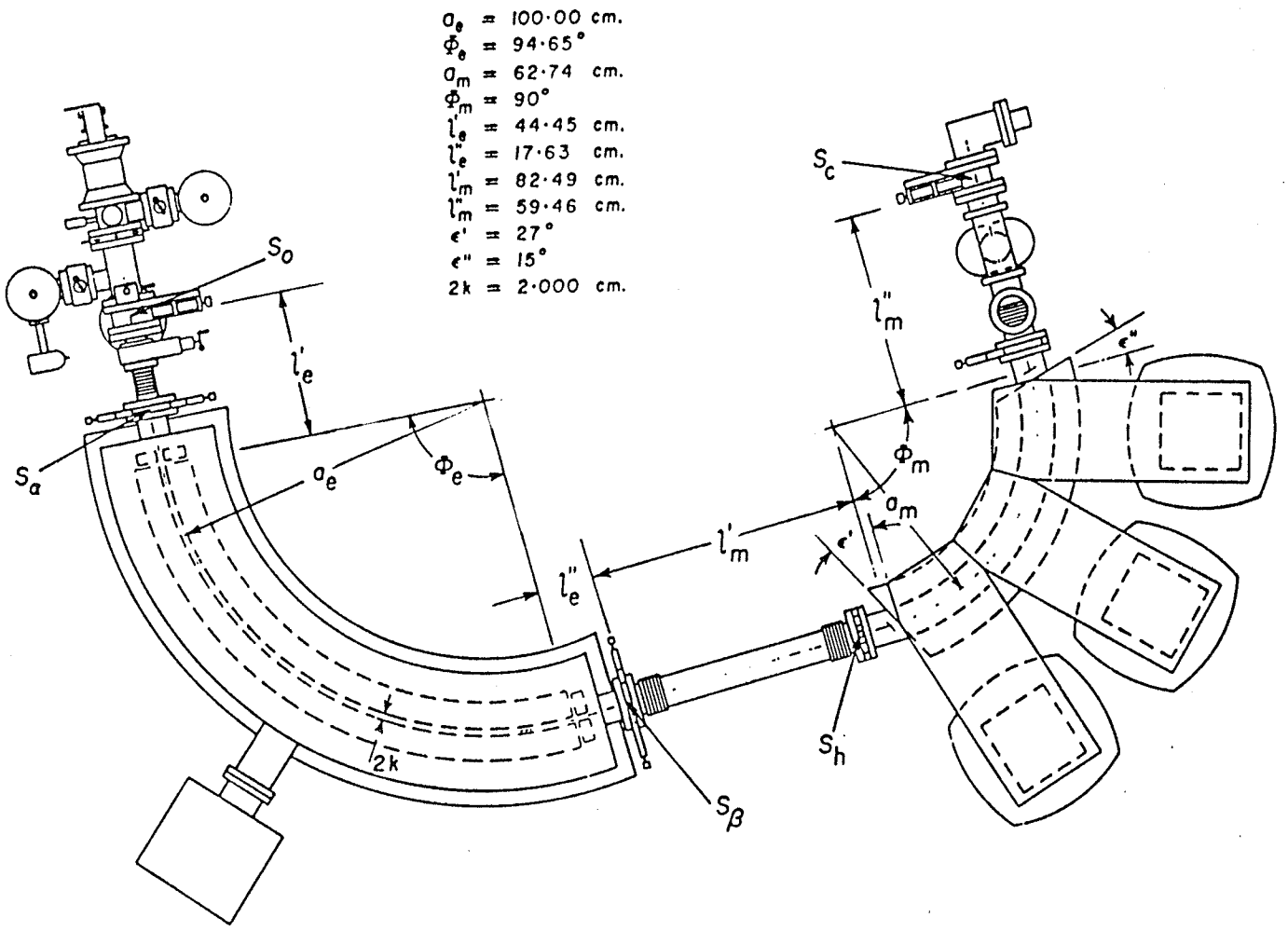
a_e = 100·00 cm.
Φ_e = 94·65°
a_m = 62·74 cm.
Φ_m = 90°
l'_e = 44·45 cm.
l''_e = 17·63 cm.
l'_m = 82·49 cm.
l''_m = 59·46 cm.
ϵ' = 27°
ϵ'' = 15°
2k = 2·000 cm.
S_o
S_a
S_c
S_h
S_β
l'_e
l''_e
l'_m
l''_m
a_e
a_m
Φ_e
Φ_m
ϵ'
ϵ''
2k

FIGURE 3-2

Ion source

/// 300 series stainless steel (non-magnetic)

... Iron

A Sample vapour inlet

B Oven (stainless steel)

C Re filament

D Cu windings for electromagnet

E 5 cm

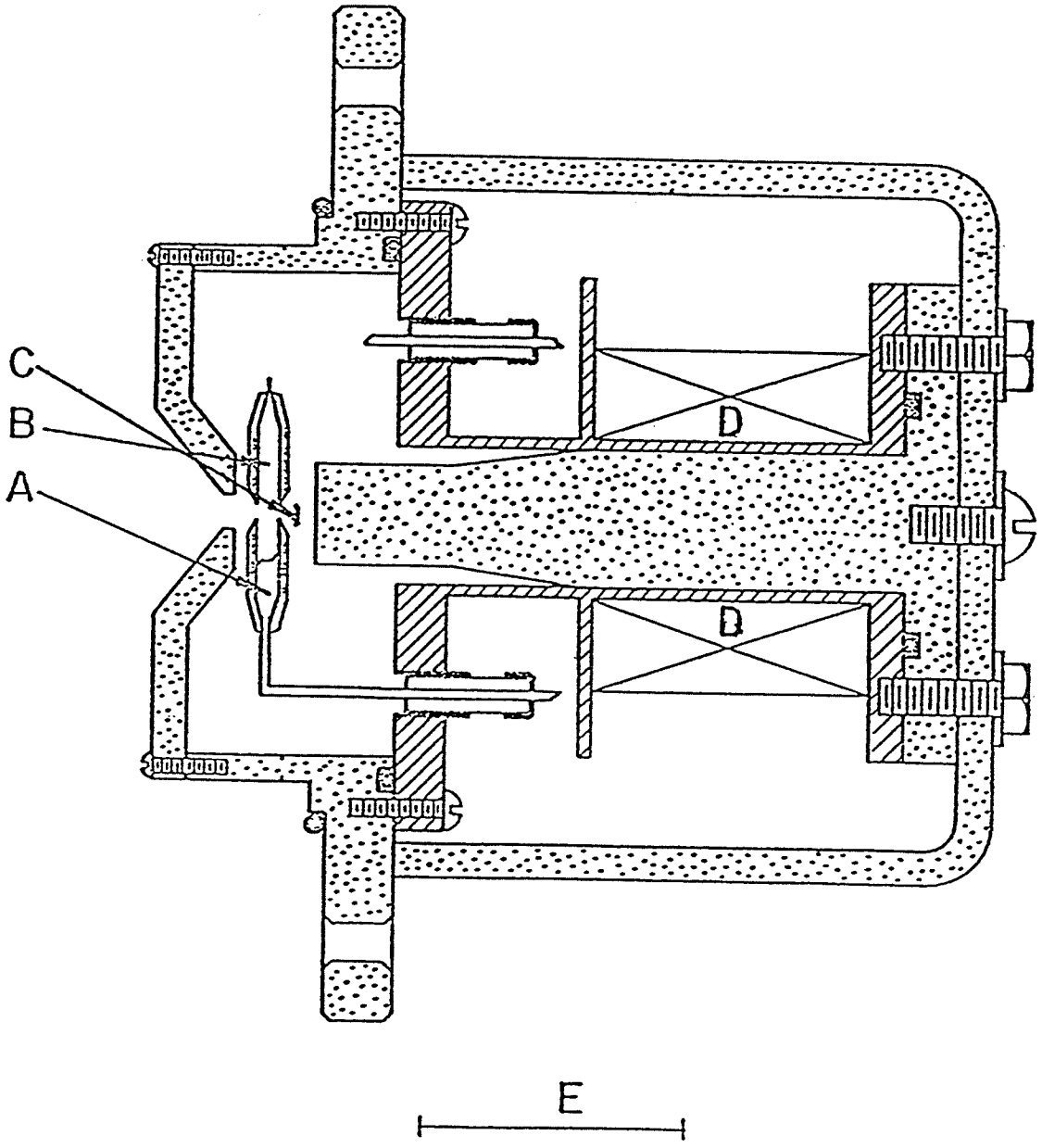
C
B
A
D
D
E

FIGURE 3-3

Potential supply for electrostatic analyzer

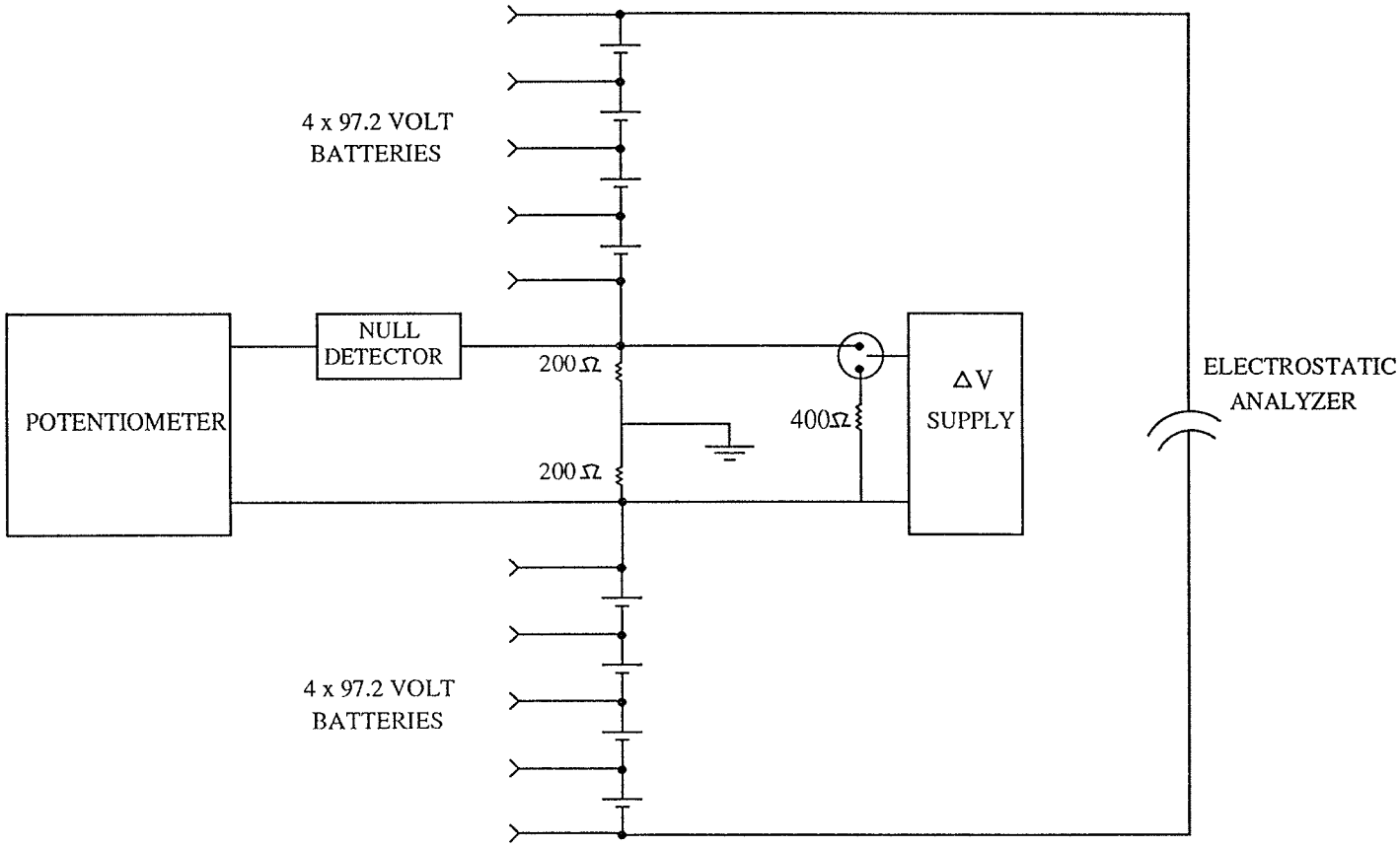
4 x 97.2 VOLT
BATTERIES
NULL
DETECTOR
POTENTIOMETER
200 Ω
200 Ω
400Ω
ΔV
SUPPLY
ELECTROSTATIC
ANALYZER
4 x 97.2 VOLT
BATTERIES

FIGURE 3-4

Cooling system for magnetic analyzer

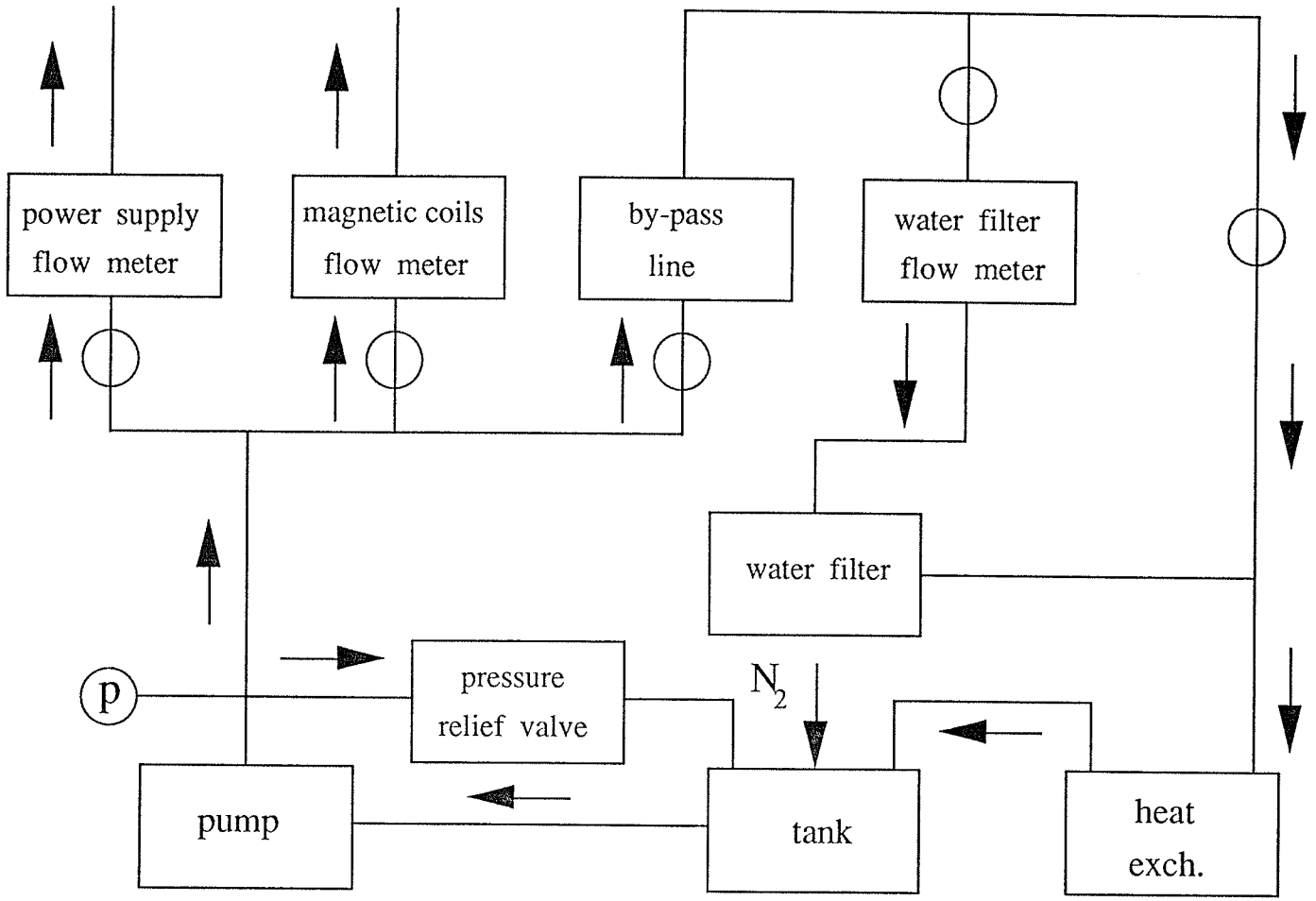
power supply
flow meter
magnetic coils
flow meter
by-pass
line
water filter
flow meter
water filter
p
pressure
relief valve
N_2
pump
tank
heat
exch.

FIGURE 3-5

Schematic diagram for the control circuitry

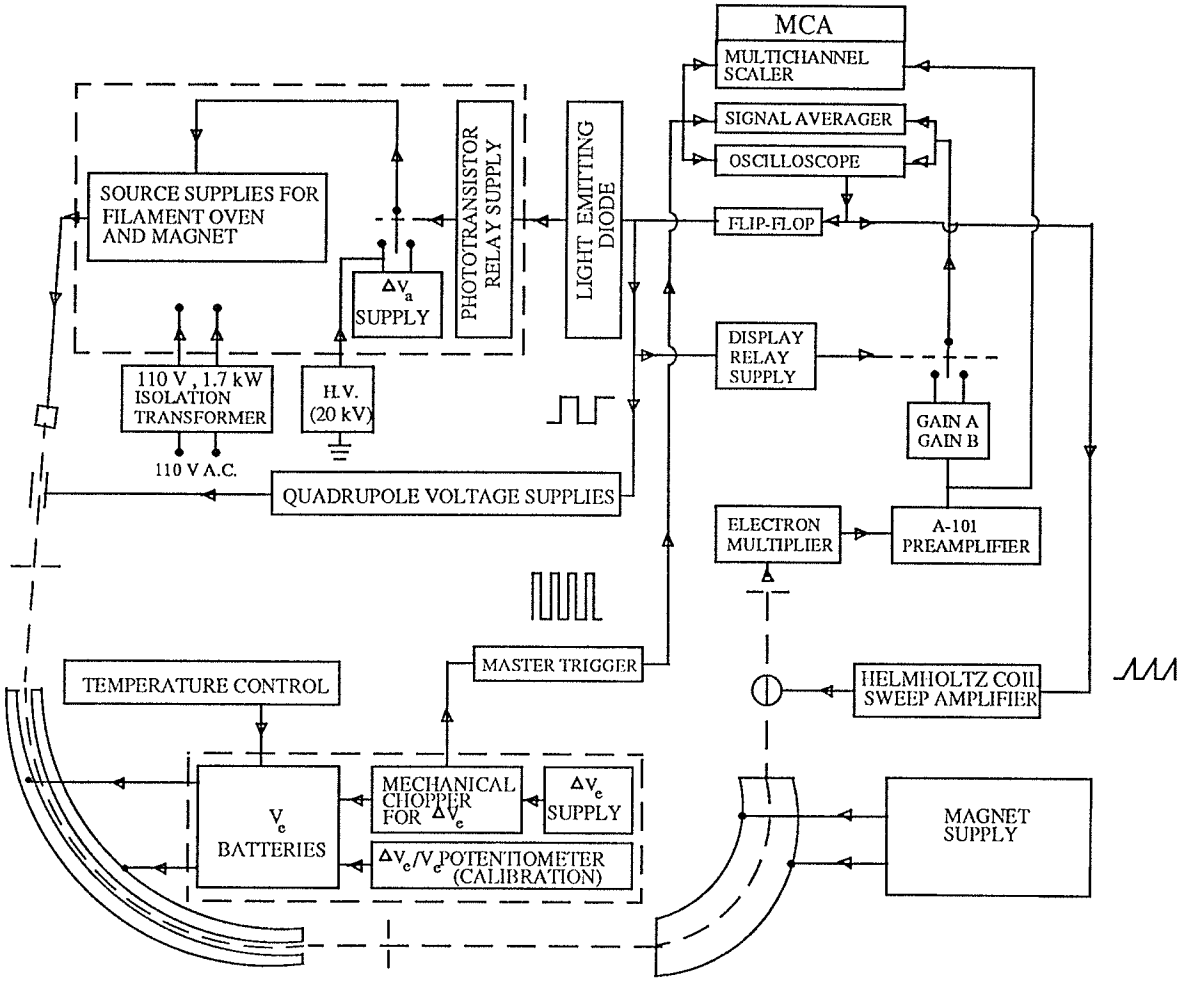
MCA
MULTICHANNEL SCALER
SIGNAL AVERAGER
OSCILLOSCOPE
FLIP-FLOP
SOURCE SUPPLIES FOR FILAMENT OVEN AND MAGNET
PHOTOTRANSISTOR RELAY SUPPLY
LIGHT EMITTING DIODE
ΔV_a SUPPLY
110 V, 1.7 kW ISOLATION TRANSFORMER
H.V. (20 kV)
110 V A.C.
DISPLAY RELAY SUPPLY
GAIN A
GAIN B
QUADRUPOLE VOLTAGE SUPPLIES
ELECTRON MULTIPLIER
A-101 PREAMPLIFIER
MASTER TRIGGER
TEMPERATURE CONTROL
HELMHOLTZ COIL SWEEP AMPLIFIER
V_e BATTERIES
MECHANICAL CHOPPER FOR ΔV_e
ΔV_e SUPPLY
$\Delta V_e/V_e$ POTENTIOMETER (CALIBRATION)
MAGNET SUPPLY

FIGURE 3-6a

Timing signals for visual null peak matching method

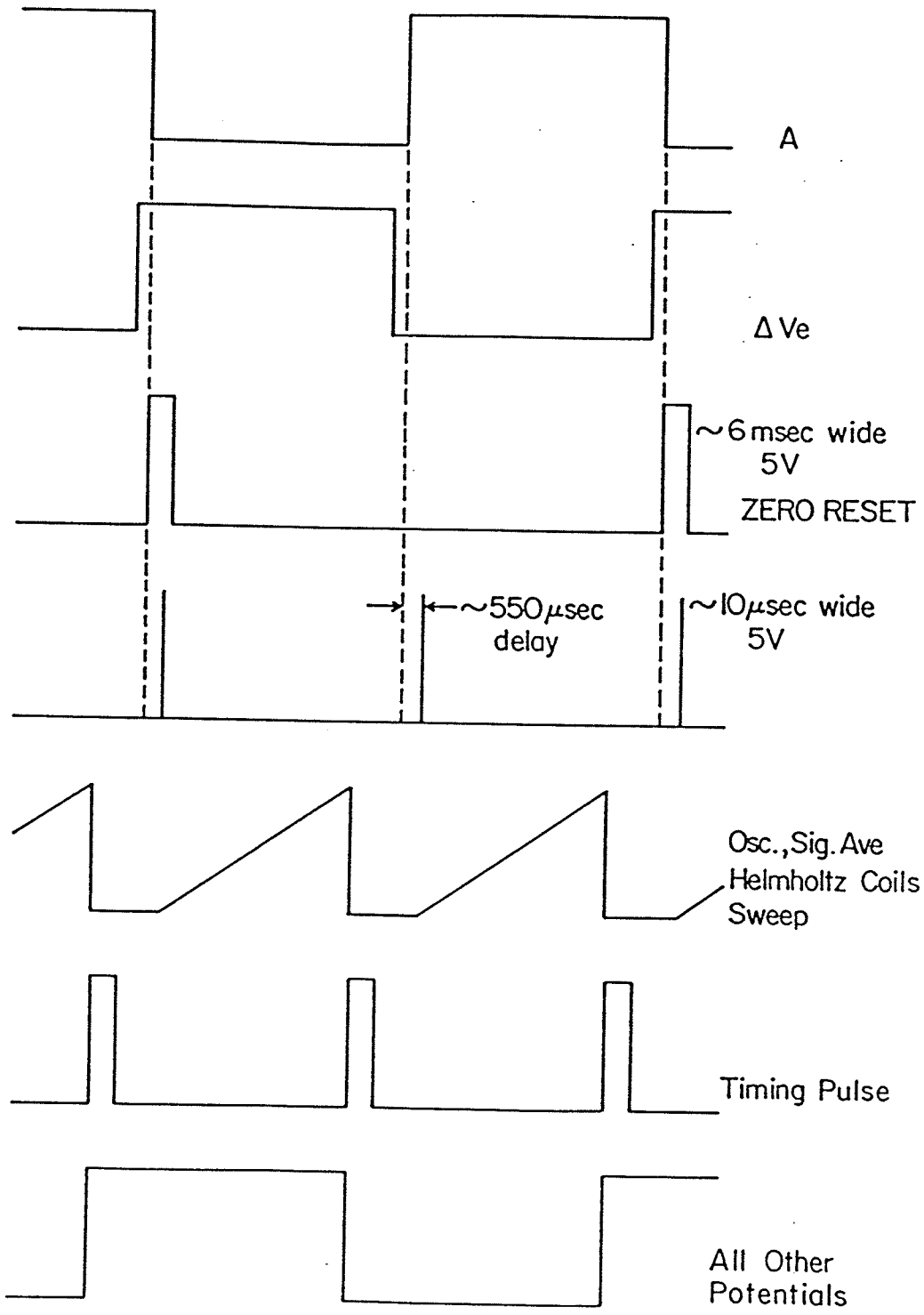
A
ΔVe
~6 msec wide
5V
ZERO RESET
~550 μsec
delay
~10 μsec wide
5V
Osc., Sig. Ave
Helmholtz Coils
Sweep
Timing Pulse
All Other
Potentials

FIGURE 3-6b

Timing signals for computer-assisted peak matching method

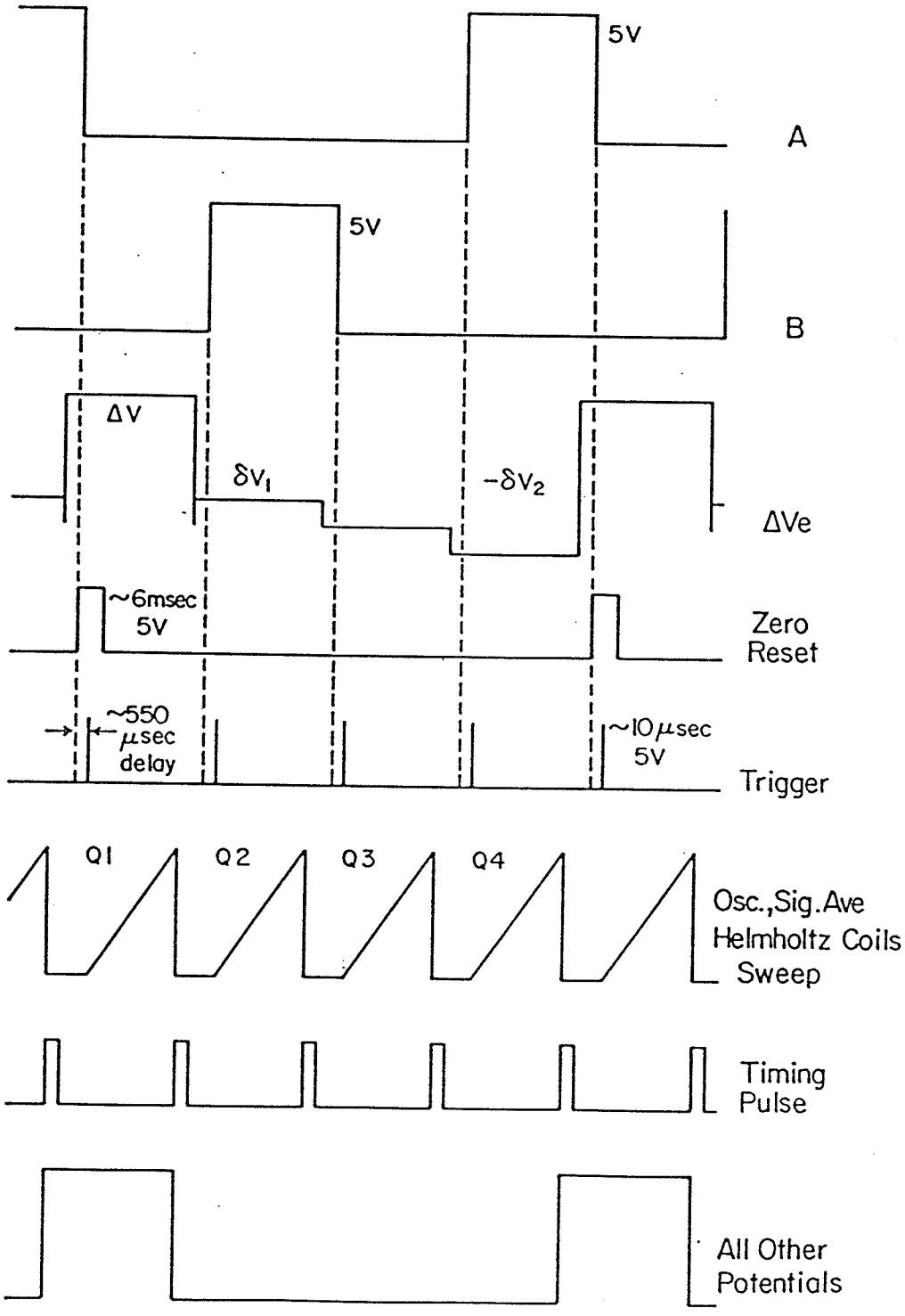
5V
A
5V
B
ΔV
δV1
-δV2
ΔVe
~6msec
5V
Zero
Reset
~550
μsec
delay
~10μsec
5V
Trigger
Q1
Q2
Q3
Q4
Osc.,Sig.Ave
Helmholtz Coils
Sweep
Timing
Pulse
All Other
Potentials

CHAPTER (4)

PEAK MATCHING

4-1 Visual null peak matching

The visual null peak matching technique was first introduced by Benson and Johnson (Benson, 1966) and was quickly adopted by others (Macdougall, 1966; Stevens, 1967; Barber, 1967). It may still be used on Manitoba II (Dyck, 1990) for the precise determination of atomic mass differences.

In the current version of this technique, the ion beam corresponding to mass M is swept across the collector slit with the potentials applied to the instrument at values V_i. For the next sweep, all potentials are changed to values V_i' and the next mass peak M' is detected. Approximate value for the change in the electrostatic analyzer potential, $\Delta V_e = V_e - V_e'$, is calculated from the available information of the masses corresponding to the doublet members (eqn. 2-24). Similarly, a rough value for the change in accelerating potential , $\Delta V_a = V_a - V_a'$, is obtained from : $\Delta M/M' = \Delta V_a/V_a$. The determination of the matched condition is carried out with the aid of a Nicolet model 535 multichannel analyzer (MCA), operating in the signal averaging mode. The primary advantage of signal averaging is that the signal-to-noise ratio improves as $\sqrt{N}$ where N is the number of sweeps accumulated. The sweeps of the MCA are synchronized to the sweeps of the Helmholtz coils (Fig. 3-6a). The detected ion current is digitized point by point and accumulated in the signal averager's memory. On alternate sweeps, the signal corresponding to the other member of the doublet is subtracted from the memory. The two signals may be matched in amplitude by routing them through separate adjustable gain controls (gain A and gain B in Fig. 3-5). The contents of the signal averager memory, representing the accumulated difference between the two

normalized peaks, is continuously displayed on an oscilloscope. If the two peaks do not coincide in position an asymmetric S-shaped error signal will grow with time (Fig. 4-1a). ΔV_e is then adjusted to find the matched condition where the two normalized peak signals cancel each other, leaving a symmetric noise signal (Fig. 4-1b). Each time ΔV_e is adjusted the previously accumulated data are discarded as the memory is erased. Only ΔV_e is adjusted since, for a double-focusing mass spectrometer, the peak position is insensitive to the other potentials applied to the instrument. The ratio $\Delta V_e/V_e$ is then measured with a precision potentiometer (Bishop, 1970) and used in eqn. 2-24 to determine the mass difference.

In order to minimize the effects of biases that may occur in any one particular configuration of the instrument, an unweighted average of the eight matches, corresponding to each of the possible configurations, is taken as the result of one "visual run". The eight possible configurations correspond to the permutations of :

(1) The lighter or the heavier member of a doublet may be displaced by "adding" or "subtracting" ΔV_e from the reference analyzer potential V_e.

(2) The ion beam may be swept across the collector slit in either the "forward" or "reverse" direction (when a forward sweep is used the mass scale increases from right to left on the oscilloscope screen).

(3) A mass peak may be routed through a display channel of either "gain A" or "gain B" as shown in Fig. 3-5.

Visual peak matching is performed on-line, i.e. the results of the mass determinations may be obtained with a minimum delay. The operator may detect problems such as peak movement during an observation. The primary drawback of visual matching is that most of the collected data is discarded in the course of adjusting the potentials. In addition to this, the method is not easily applicable to mass peaks of low intensity.

4-2 Computer-assisted peak matching

Computer matching was developed by Stevens and Moreland (Stevens, 1967) in an attempt to escape the possible effects of biases introduced by the operator and to use the collected data efficiently. This technique was first applied to Manitoba II by Meredith (Meredith, 1971, 1972).

4-2-1 The quadrant system

In the current version of this technique, the memory of the MCA is divided into four quadrants of 1024 channels each. A separate spectrum is accumulated in each quadrant. Thus, each complete sweep of the MCA corresponds to four sweeps of the Helmholtz coils and the display oscilloscope (Fig. 3-6b). The MCA is operated as a multichannel scaler. In this mode, each ion pulse from the electron multiplier is recorded as one event directly in the memory. This counting mode removes the stringent requirements on baseline variation and greatly improves the overall sensitivity for weak peaks (Sharma, 1977).

During the first sweep, the potentials applied to the instrument are changed according to eqn. 2-24 so that the spectrum is displaced by approximately one doublet width and the resulting spectrum is recorded in quadrant 1. On the second sweep, the potential V_e is changed by a small amount δV_1 (about $V_e/5 \times 10^5$) while all other potentials are at their normal values V_i and the resulting spectrum is stored in quadrant 2. On the next sweep, the spectrum recorded in quadrant 3 corresponds to that accumulated when all the potentials applied to the instrument are at their normal values V_i. During the last sweep, the potential V_e is changed by a small amount $\delta V_2 \approx -\delta V_1$ and all other potentials remain the same as in quadrant 3 and the resulting spectrum is stored in quadrant 4. This cycle is repeated many times until suf-

ficient data are accumulated (usually about 3000 sweeps). The accumulated memory contents are illustrated in Fig. 4-2 where the quadrants are shown one above the other. The voltage ratios $\frac{\Delta V_e}{V_e}$, $\frac{\delta V_1}{V_e}$ and $\frac{\delta V_2}{V_e}$ are measured with the precision potentiometer. The voltages δV_1 and δV_2 are referred to as the "split voltages". These voltages are provided by electronic circuitry which has been described in detail by Meredith (Meredith, 1971) and Southon (Southon, 1973).

In the computer-assisted method, as in the visual null method, there are eight possible configurations (matches) arising from the following choices :

(1) "Adding" or "subtracting" ΔV_e from the reference analyzer potential V_e.

(2) The ion beam can be swept in either the "forward" (high mass to low mass) or "reverse" direction.

(3) The voltages δV_1 and δV_2 may be applied to quadrants 2 and 4 in a decreasing staircase (normal) or an increasing staircase (backward).

A complete set of all eight possible matches constitutes one "computer run" :

match 1 : Normal, Add, Forward (NAF)

match 2 : Normal, Subtract, Forward (NSF)

match 3 : Normal, Subtract, Reverse (NSR)

match 4 : Normal, Add, Reverse (NAR)

match 5 : Backward, Add, Reverse (BAR)

match 6 : Backward, Subtract, Reverse (BSR)

match 7 : Backward, Subtract, Forward (BSF)

match 8 : Backward, Add, Forward (BAF)

The data are then stored on diskettes, using a personal computer, for subsequent analysis on a VAX750 computer.

4-2-2 Data analysis

The collected data are analysed using a computer program (APPENDIX A) which has been developed by the University of Manitoba Atomic Mass Determinations Group. In addition to the usual tasks of initialization and input of raw data, this program consists of the following steps (Fig. 4-3) :

(1) Correction applied to the observed peak counts

Because of the finite resolving time of the detector and its associated electronics, some of the ions arriving at the detector may not be registered in the memory of the signal averager. The counting losses occur primarily in the A-101 preamplifier (sec. 3-5). The preamplifier is in effect locked for a fixed time following the arrival of a pulse. The observed peak counts n_o are corrected point by point to be n_c to give a better representation of the true peak shape. The correction is applied according to the following equation (Campbell, 1956) :

$$n_c = \frac{n_o}{(1 - n_o \rho / t)} \qquad (4\text{-}1)$$

where n_o counts are observed in time t, and ρ is the dead time of the preamplifier. The value of ρ for the A-101 preamplifier was determined to be 0.22 μs. The total observation time per channel is given by the product of the number of the sweeps recorded and the dwell time per point of the signal averager. The correction applied at the peak maximum is about 5.5% at a count rate of 250 kHz.

(2) Baseline analysis

A constant baseline is calculated on the basis of regions AB and CD (Fig. 4-2) which are identified by visual inspection (Meredith, 1972). This baseline is subtracted from the peak counts between B and C before the peak analysis and , for resolved peaks, is caused by scattered ions and by noise generated in the detector. For partially resolved peaks like the doublet C (Tables 5-1a and 5-1b), the use of a constant baseline is not justified (Kozier, 1977). In this case the baseline is determined by fitting a quadratic function to the counts in regions AB and CD.

(3) Peak analysis

The peaks collected in quadrants 1, 2, 3 and 4 are analysed as follows : the height of a peak is obtained by fitting a smooth parabola to the top of the peak (Meredith, 1972). Initial peak limits are chosen at a certain ratio of the peak height. For each peak limit, a search procedure of eight consecutive points is used such that the first of these points is taken as the final location of the peak limit. In this work, we found that peak limits level lower than about 20% of the peak height makes the search difficult for those limits, (i.e.) changing the peak limits level alters the position of the centroid significantly. Thus, in this work the peak limits level is chosen at 20% of the peak height (Fig. 4-2). The peak positions are determined by :

(i) The centroid method

The centroid method was developed for Manitoba II by Meredith (Meredith, 1971, 1972). Only a brief description is presented here. Each peak occupies channels x_i, i = 1,2,3,.....,I in the memory of the signal averager. The peak height $n_j(x_i)$ at the i^{th} channel in quadrant j is equal to the number of ions (counts) accumulated in that channel. The average position, or centroid, of the distribution in quadrant j, is given by :

$$\overline{X}_j = \frac{\sum_{i=1}^{I} x_i n_j(x_i)}{\sum_{i=1}^{I} n_j(x_i)} \qquad (4\text{-}2)$$

where: j = 1, 2, 3, 4 and x_1, x_I are the limits of the peak in quadrant j.

The centroid uncertainty $\delta\overline{X}_j$ is given by :

$$\delta\overline{X}_j = \sqrt{\frac{\sum_{i=1}^{I} (x_i - \overline{X}_j)^2 n_j(x_i)}{N_j(N_j - 1)}} \qquad (4\text{-}3)$$

where N_j is the total number of peak counts in quadrant j. The separation between the peaks in quadrants j and 1 is given by :

$$(D_j)_{CEN} = \overline{X}_j - \overline{X}_1 \qquad (4\text{-}4)$$

with uncertainty :

$$(\delta D_j)_{CEN} = \sqrt{(\delta\overline{X}_j)^2 + (\delta\overline{X}_1)^2} \qquad (4\text{-}5)$$

where j = 2, 3, 4

(ii) The least squares method

The least squares method was developed for Manitoba II by Kozier (Kozier, 1977). A brief description is presented here. This method searches for the separation, $(D_j)_{LSQ}$, between the peaks in quadrants j and 1 such that the weighted sum of the squares of the differences between the counts of these two peaks, $\chi_j^2(r_j, d_j)$, is minimized. The function to be minimized has the form :

$$\chi_j^2(r_j, d_j) = \sum_{i=1}^{I} \left[\frac{r_j n_1(x_i) - n_j(x_i + d_j)}{\sigma_i} \right]^2 \qquad (4\text{-}6)$$

where;

$n_1(x_i)$ is the peak count at the position x_i which corresponds to channel i in quadrant 1.

$n_j(x_i + d_j)$ is the peak count in quadrant j which is displaced by a distance d_j from x_i.

r_j is the intensity ratio of the two peaks in quadrants j and 1.

σ_i is the uncertainty of the quantity $r_j n_1(x_i) - n_j(x_i + d_j)$ which is determined according to Poisson statistics to be $\sqrt{r_j^2 n_1(x_i) + n_j(x_i + d_j)}$.

χ_j^2 represents the fitting of a peak in quadrant j to match the height and the position of a peak in quadrant 1. The "goodness of fit" may be expressed by defining the reduced χ_j^2, $(\chi_j^2)_\nu$ (Bevington, 1969) :

$$(\chi_j^2)_\nu = \chi_j^2/\nu \qquad (4\text{-}7)$$

where ν is the number of degrees of freedom

$$\nu = x_I - x_1 - 1 \qquad (4\text{-}8)$$

$(\chi_j^2)_\nu$ should be close to unity when the peak in quadrant j is well fitted to that in quadrant 1. This means that the parameters r_j and d_j are determined assuming that the difference in shape between the two peaks is due to the random noise expected from Poisson statistics.

χ_j^2 may be expanded to first order (Bevington, 1969) near the minimum $(\chi_j^2)_{\min}$:

$$\chi_j^2 \cong (\chi_j^2)_{\min} + \frac{\partial(\chi_j^2)_{\min}}{\partial r_j}\delta r_j + \frac{\partial(\chi_j^2)_{\min}}{\partial d_j}\delta d_j \tag{4-9}$$

$(\chi_j^2)_{\min}$ should satisfy the following condition :

$$\left(\frac{\partial \chi_j^2}{\partial r_j}\right) = \left(\frac{\partial \chi_j^2}{\partial d_j}\right) = 0 \tag{4-10}$$

Differentiating eqn. (4-9) :

$$\frac{\partial \chi_j^2}{\partial r_j} \cong \frac{\partial(\chi_j^2)_{\min}}{\partial r_j} + \frac{\partial^2(\chi_j^2)_{\min}}{\partial r_j^2}\delta r_j + \frac{\partial^2(\chi_j^2)_{\min}}{\partial r_j \partial d_j}\delta d_j = 0 \tag{4-11}$$

$$\frac{\partial \chi_j^2}{\partial d_j} \cong \frac{\partial(\chi_j^2)_{\min}}{\partial d_j} + \frac{\partial^2(\chi_j^2)_{\min}}{\partial d_j \partial r_j}\delta r_j + \frac{\partial^2(\chi_j^2)_{\min}}{\partial d_j^2}\delta d_j = 0 \tag{4-12}$$

These equations can be arranged in a matrix form :

$$\overleftrightarrow{A}\vec{x} \cong \vec{b} \tag{4-13}$$

where;

$$\overleftrightarrow{A} = \begin{vmatrix} \dfrac{\partial^2(\chi_j^2)_{\min}}{\partial r_j^2} & \dfrac{\partial^2(\chi_j^2)_{\min}}{\partial r_j \partial d_j} \\ \dfrac{\partial^2(\chi_j^2)_{\min}}{\partial d_j \partial r_j} & \dfrac{\partial^2(\chi_j^2)_{\min}}{\partial d_j^2} \end{vmatrix}$$

$$\vec{x} = \begin{Bmatrix} \delta r_j \\ \delta d_j \end{Bmatrix}$$

$$\vec{b} = -\begin{Bmatrix} \dfrac{\partial (\chi_j^2)_{\min}}{\partial r_j} \\ \dfrac{\partial (\chi_j^2)_{\min}}{\partial d_j} \end{Bmatrix}$$

The intensity ratio $(R_j)_{LSQ}$ and the peak separation $(D_j)_{LSQ}$ determined by the least squares technique are obtained using the following iterative procedure :

(1) the initial guesses $(R_j)_{CEN}$ and $(D_j)_{CEN}$ are obtained from the centroid method. $(R_j)_{CEN}$ from the ratio of areas and $(D_j)_{CEN}$ from the difference in centroids (eqn. 4-4) for the two peaks in quadrants j and 1;

(2) $(R_j)_{CEN}$ and $(D_j)_{CEN}$ are used to calculate χ_j^2 and its partial derivatives;

(3) the increments δr_j and δd_j are obtained from the solution of eqn. (4-13);

(4) the values $(R_j)_{CEN}$ and $(D_j)_{CEN}$ are updated by the increments δr_j and δd_j;

(5) steps 2, 3 and 4 are repeated until $(R_j)_{CEN}$, $(D_j)_{CEN}$ and χ_j^2 converge to $(R_j)_{LSQ}$, $(D_j)_{LSQ}$ and $(\chi_j^2)_{\min}$.

The uncertainties for the final values $(R_j)_{LSQ}$ and $(D_j)_{LSQ}$ are obtained from the inverse matrix of $\overleftrightarrow{A}$ (Bevington, 1969) :

$$(\delta R_j)_{LSQ} = \sqrt{A_{11}^{-1}} \qquad (4\text{-}14)$$

$$(\delta D_j)_{LSQ} = \sqrt{A_{22}^{-1}} \qquad (4\text{-}15)$$

The partial derivatives of χ_j^2 with respect to the intensity ratio between the peaks in quadrants j and 1, r_j are calculated from eqn. (4-6). The quantity χ_j^2 and its derivatives with respect to the displacement of the peak in quadrant j relative to that in quadrant 1, d_j, can be evaluated only at discrete values of d_j. Fig. 4-4 shows an example of two peaks in quadrants 1 and 3 obtained from the mass spectral peaks of the doublet H_3 - DH. In this example, $(\chi_3^2)_v$ is calculated (eqns. 4-6 and 4-7) at integer values of d_3 corresponding to increments of one channel and the results are plotted in part IV of this figure. In this figure, when $|d_3| > W/2$ (regions 1 and 3) a value of (χ_3^2) represents the sum of the squares of the differences between the peak counts in quadrant 1 (part I) and the background counts of the peak in quadrant 3 (part II). Thus, the plotting of $(\chi_3^2)_v$ values in regions 1 and 3 yields a flat distribution as shown in part IV of Fig. 4-4. In this figure, when $|d_3| < W/2$ (region 2) only a fraction f of the peak in quadrant 3 (shaded area in part III) is included in the calculation of $(\chi_3^2)_v$ (eqns. 4-6 and 4-7), such that, as d_3 decreases, this fraction increases and the $(\chi_3^2)_v$ value decreases.

For the first few iterations, $\partial\chi_j^2/\partial d_j$ and $\partial^2\chi_j^2/\partial d_j^2$ are calculated roughly from a coarse grid with 3 values of d_j each separated by four channels such that the χ_j^2 of the middle one is lower than the others. To determine the final value of a peak separation $(D_j)_{LSQ}$, the partial derivatives of χ_j^2 with respect to d_j are obtained by fitting a parabola to the χ_j^2 values within the N channels. The fitted parabola :

$$\chi_j^2(d_j) = C_1 + C_2 d_j + C_3 d_j^2 \qquad (4\text{-}16)$$

represents the shape of the χ_j^2 function near the minimum (part IV of Fig. 4-4) assuming that r is fixed at r_{min}. In order to minimize χ_j^2 within this range of N channels :

(i) the curvature $(\partial^2\chi_j^2/\partial d_j^2 = 2C_3)$ of the parabola fitted to χ_j^2 values near the minimum should be positive (indicating a definite minimum);

(ii) the parabola's vertex d_{min} should fall within this range of channels.

From eqn. 4-16, $\chi_j^2(d_j)$ is minimized when :

$$d_j = d_{min} = -C_2/2C_3 \qquad (4\text{-}17)$$

In Fig. 4-5, $(\chi_3^2)_v$ function is minimized within a range of 11 channels.

(4) Determination of the matched condition

Once the displacements of the peaks in quadrants 2, 3 and 4 relative to the peak in quadrant 1 are determined, the peak separations thus obtained may be correlated with the split voltages of these quadrants. Over this small voltage range the peak separation has been shown to be linearly dependent on the split voltage applied (Meredith, 1972). Thus, the 3 pairs of split voltages and separations may be fitted to a straight line (Fig. 4-6). The intercept of this line, δV_0 (matched condition), gives the correction to be applied to the switched voltage in quadrant 1 to derive the desired ΔV_e, which is used to calculate ΔM (eqn. 2-24).

The data analysis procedure is carried out for each one of the eight matches (sec. 4-2-1) which constitute one "computer run". The mass differences of a match i are determined by the centroid and least squares methods to be $(\Delta M_i)_{CEN}$ and $(\Delta M_i)_{LSQ}$ respectively. The mass difference of a computer run (average value of the results of the eight matches) obtained from the least squares method $(\overline{\Delta M}_{LSQ} \pm \delta M_{LSQ})$ is expected to be consistent with that of the centroid method $(\overline{\Delta M}_{CEN} \pm \delta M_{CEN})$:

$$\overline{\Delta M}_{LSQ} = \sum_{i=1}^{8} (\Delta M_i)_{LSQ}/8 \qquad (4\text{-}18a)$$

$$\delta M_{LSQ} = \sqrt{\sum_{i=1}^{8} ((\Delta M_i)_{LSQ} - \overline{\Delta M}_{LSQ})^2/8(8-1)} \qquad (4\text{-}18b)$$

$$\overline{\Delta M}_{CEN} = \sum_{i=1}^{8} (\Delta M_i)_{CEN}/8 \qquad (4\text{-}19a)$$

$$\delta M_{CEN} = \sqrt{\sum_{i=1}^{8} ((\Delta M_i)_{CEN} - \overline{\Delta M}_{CEN})^2/8(8-1)} \qquad (4\text{-}19b)$$

4-3 Improvement in computer matching technique

The previous version of the least squares technique (as developed by Kozier, 1977) was first applied by Kozier to analyse the data collected from the mass spectral peaks of seven mercury chloride doublets (Kozier, 1977). However, at that time this method was not recommended for general use with real peaks due to the existence of a systematic bias in the results determined by Kozier (Kozier, 1977). In Sharma's work, computer runs were gathered for five chloride doublets among selected isotopes of Hf, Ta, W and erratic results were obtained from the least squares technique (Sharma, 1979).

In this work, we found, at times, that $\overline{\Delta M}_{LSQ}$ was far from $\overline{\Delta M}_{CEN}$ and δM_{LSQ} was much larger than δM_{CEN}. The reasons for this problem were identified and are presented below.

In the example presented in Table 4-1, the values of $\overline{\Delta M}_{LSQ}$ (4-18a) and δM_{LSQ} (4-18b) determined by the old procedure of the least squares method are higher than $\overline{\Delta M}_{CEN}$ (4-19a) and δM_{CEN} (4-19b) by about 30 μu and 20 μu. This can be explained by comparing $(\Delta M_i)_{LSQ}$ with $(\Delta M_i)_{CEN}$ for each one of the eight matches. These comparisons indicate that the mass

difference of match 6 [$(\Delta M_6)_{LSQ} = 2910.27\ \mu u$] determined by the old procedure of the least squares method is larger than $(\Delta M_i)_{LSQ}$ and $(\Delta M_i)_{CEN}$ of the other matches by about 200 μu and contributes by :

(1) $200/8 = 25\ \mu u$ (according to equations 4-18a and 4-19a) to the difference (29.62 μu) between $\overline{\Delta M}_{LSQ} = 2728.38\ \mu u$ and $\overline{\Delta M}_{CEN} = 2698.76\ \mu u$.

(2) $\sqrt{(2910.27 - 2728.38)^2/8(8-1)} \approx 23\ \mu u$ (according to equation 4-18b) to the value of $\delta M_{LSQ} = 26.55\ \mu u$.

The analysis of this particular match (match 6 in Table 4-1) is shown in Fig. 4-7. As discussed in the previous sections, the determination of a peak separation by the least squares method is based on fitting a parabola (eqn. 4-16) to χ_j^2 values within a range of N channels. In the example shown in Fig. 4-7, $N = 11$ channels is used. Within this range, the 11 values of $(\chi_2^2)_\nu$ and $(\chi_3^2)_\nu$ are fitted to a positive curvature parabola like Fig. 4-5. However, the 11 values of $(\chi_4^2)_\nu$ are fitted to a negative curvature parabola A as shown in part I of Fig. 4-7. This is because the values of $(\chi_4^2)_\nu$ in this region are the result of squaring the small difference between two large numbers. Over the range of 11 points the data are simply too noisy to reliably indicate the shape of the $(\chi_4^2)_\nu$ function in this region. Since it is clearly not possible to find a minimum for $(\chi_4^2)_\nu$ function with a parabola like this, early version of the software reversed the sign of C_3 (eqn. 4-16) thus forcing the parabola to have the desired shape. The effects of this prescription may be disastrous. The resulting new parabola, B, clearly does not fit the raw data. Moreover, while the vertex of parabola A passes through the 11 points, the vertex of parabola B is far from the raw data. So, neither parabola A nor B satisfy the conditions required to minimize $(\chi_4^2)_\nu$ listed in sec. 4-2-2. In part I of Fig. 4-7, the peak separation determined by the least squares method $(D_4)_{LSQ}$ is the vertex of parabola B. On the other hand, the peak separation obtained from the centroid method $(D_4)_{CEN}$ is approxi-

mately equal to the vertex of parabola A. Therefore, according to eqn. (4-17), $(D_4)_{LSQ}$ has an opposite sign to $(D_4)_{CEN}$ and their magnitudes, for this specific example, are approximately equal (i.e) :

$$|(D_4)_{LSQ} - (D_4)_{CEN}| \approx 2|(D_4)_{CEN}| \qquad \text{(Table 4-2, example a)}$$

Fig. 4-7 shows that $(D_4)_{LSQ} \pm (\delta D_4)_{LSQ}$ disagrees with $(D_4)_{CEN} \pm (\delta D_4)_{CEN}$. The erroneous value of $(D_4)_{LSQ} \pm (\delta D_4)_{LSQ}$ (Table 4-2, example a) affects the fitting of the points : $[(D_2)_{LSQ} \pm (\delta D_2)_{LSQ}, \delta V_1]$, $[(D_3)_{LSQ} \pm (\delta D_3)_{LSQ}, 0]$, $[(D_4)_{LSQ} \pm (\delta D_4)_{LSQ}, \delta V_2]$ to a straight line LSQ. These points are equally weighted as shown in part II of Fig. 4-7. Since it is clearly not possible to fit those points to a straight line, the line LSQ is forced to exclude them. On the other hand, the points : $[(D_2)_{CEN} \pm (\delta D_2)_{CEN}, \delta V_1]$, $[(D_3)_{CEN} \pm (\delta D_3)_{CEN}, 0]$, $[(D_4)_{CEN} \pm (\delta D_4)_{CEN}, \delta V_2]$ are fitted to a straight line CEN. As a result, the intercept (matched condition) $(\delta V_0)_{LSQ}$ of the line LSQ is much larger than $(\delta V_0)_{CEN}$ of CEN by about 284 μBishop. Therefore, the mass difference of this particular match $(\Delta M_6)_{LSQ}$ determined by the old procedure of the least squares method is greater than $(\Delta M_6)_{CEN}$ by about 200 μu as shown in Table 4-1.

In another example (Fig. 4-8) $N = 11$ is used. The 11 values of $(\chi_2^2)_\nu$ and $(\chi_3^2)_\nu$ are fitted to a positive curvature parabola like Fig. 4-5. On the other hand, the 11 values of $(\chi_4^2)_\nu$ are fitted to a flat parabola F which has a negative curvature as shown in part I of Fig. 4-8. As suggested earlier, to minimize $(\chi_4^2)_\nu$, the curvature of parabola F is reversed, thus another parabola G is produced. Unlike the example shown in Fig. 4-7, the vertex of parabola F lies outside the range of the raw data (N = 11 channels). As a result, $(D_4)_{LSQ}$ (vertex of parabola G) is far from $(D_4)_{CEN}$:

$$|(D_4)_{LSQ} - (D_4)_{CEN}| \approx 6|(D_4)_{CEN}| \qquad \text{(Table 4-2, example b)}$$

The curvature $\partial^2(\chi_4^2)_v/\partial d_j^2$ of parabola F is so small that the uncertainty $(\delta D_4)_{LSQ}$ is greatly increased (eqn. 4-15) :

$$(\delta D_4)_{LSQ} \approx 17(\delta D_4)_{CEN} \qquad \text{(Table 4-2, example b)}$$

It is interesting to study the effect of $(D_4)_{LSQ} \pm (\delta D_4)_{LSQ}$ on the determination of the matched condition $(\delta V_0)_{LSQ}$. The points :
$[(D_2)_{LSQ} \pm (\delta D_2)_{LSQ}, \delta V_1], [(D_3)_{LSQ} \pm (\delta D_3)_{LSQ}, 0], [(D_4)_{LSQ} \pm (\delta D_4)_{LSQ}, \delta V_2]$ are plotted as shown in part II of Fig. 4-8. The point $[(D_4)_{LSQ} \pm (\delta D_4)_{LSQ}, \delta V_2]$ has a higher uncertainty than the others. Therefore, the line LSQ excludes that point and passes through the other points. In this case, although the least squares method calculates one peak separation incorrectly, $(\delta V_0)_{LSQ}$ agrees with $(\delta V_0)_{CEN}$ as shown in Fig. 4-8.

In summary, the old version of the least squares technique (Kozier, 1977) has the following shortcomings :

N = 11 channels was always used.It is possible to express this width as a ratio of the peak width W. When $N/W \ll 1.0$, like the examples shown in Fig. 4-7 (N/W = 2.7%) and Fig. 4-8 (N/W = 2.5%), the search for the minimum value of χ_j^2 is confined to a narrow range of channels. In the vicinity of the minimum the χ_j^2 function is made up of the squares of the differences of large numbers that are close together in value. The statistical noise of the spectrum in this region causes a random variation of the χ_j^2 values so that the χ_j^2 function could not be minimized reliably as shown in Figures 4-7 and 4-8. In these cases, the following procedure (lines 1047, 1048, 1049 and 1050 of the computer program listed in APPENDIX A) was adopted : when the raw data are

fitted to a negative curvature parabola, the sign of the curvature should be reversed. This procedure gave a poor accuracy and large uncertainty of a peak separation which may affect the accuracy and the precision of the calculated mass difference by the least squares method. However, it allowed the program to continue the analysis without fatal run time errors.

In this work a new procedure is established for the least squares technique :

The search for the minimum value of χ_j^2 is carried out within a range of channels N which is carefully selected on a case by case basis rather than using the arbitrary constant value of 11 channels. Now, for a peak width W it is possible to select a value for N. The study of the distribution of the χ_j^2 function (part IV of Fig. 4-4) within different ranges of channels N indicates that : when N/W > 1.0, the search for the minimum value of χ_j^2 includes regions 1, 2 and 3 as shown in part IV of Fig. 4-4. The flat portions of the distribution (regions 1 and 3) do not provide any information about the location of minimum value of χ_j^2. Thus, the range of channels N has to be smaller than the peak width W (N/W < 1). It can also be dangerous to overly restrict the values of N/W. When the range of channels N is narrow relative to the peak width W like the examples shown in Figures 4-7 and 4-8, our experience suggests that the search for the minimum value of χ_j^2 will not be successful as explained earlier in this section. In this case, N has to be increased at increments of two channels (symmetric distribution of χ_j^2 values) until a certain value N_0 in which χ_j^2 function is minimized. Within the range $N_0 \leq N < W$, each value of N represents a one set of χ_j^2 values which are fitted to a parabola with a minimum value $(\chi_j^2)_{min}$. For a computer run, the minimum value of χ^2 function of quadrant j belong to match i is determined to be $(\chi^2_{quad.\,j,match\,i})_{min}$. In this case, there are three values of $(\chi^2_{quad.\,j,match\,i})_{min}$ calculated for each one of the eight matches

or a total of twenty four values of $(\chi^2_{quad.\,j,match\,i})_{\min}$ correspond to a one value of N ($N_0 \le N <$ W). Within this range of channels, the optimum value N_m is selected at the lowest value of $\overline{\chi^2}_{\min} \pm \delta\overline{\chi^2}_{\min}$:

$$\overline{\chi^2}_{\min} = \sum_{i=1}^{8} (\chi^2_{match\,i})_{\min}/8 \qquad (4\text{-}20)$$

$$\delta\overline{\chi^2}_{\min} = \sqrt{\sum_{i=1}^{8} \left((\chi^2_{match\,i})_{\min} - \overline{\chi^2}_{\min} \right)^2 / 8(8-1)} \qquad (4\text{-}21)$$

$$(\chi^2_{match\,i})_{\min} = \sum_{j=2}^{4} (\chi^2_{quad.\,j,match\,i})_{\min}/3 \qquad (4\text{-}22)$$

where;

$\overline{\chi^2}_{\min}$ represents the minimum value of χ^2 function of a computer run and is calculated as the average value (4-20) of $(\chi^2_{match\,i})_{\min}$ values of the eight matches of this run.

$\delta\overline{\chi^2}_{\min}$ is the uncertainty associated with $\overline{\chi^2}_{\min}$.

$(\chi^2_{match\,i})_{\min}$ represents the minimum value of χ^2 function of a match i and is calculated as the mean value (4-22) of $(\chi^2_{quad.\,j,match\,i})_{\min}$ values of quadrants : 2, 3, 4 belong to this match.

This new procedure is used to overcome the problems illustrated in this section. χ^2 function is minimized within a range of channels N such that $13 \le N < 405$ and $13 \le N <$ 437 for the examples shown in Figures 4-7 and 4-8 respectively. According to this procedure, the optimum values were selected for those examples to be $N_m = 13$ and $N_m = 15$ channels in which the lowest values of $\overline{\chi^2}_{\min} \pm \delta\overline{\chi^2}_{\min}$ are determined to be 2.283 ± 0.280 and 1.238 ± 0.018 respectively. Fig. 4-9 presents a comparison between the old (parabola B) and new (parabola C) procedures used to minimize the $(\chi^2_4)_\nu$ function in the case of fitting 11 values of $(\chi^2_4)_\nu$ to a negative curvature parabola A (obtained from Fig. 4-7). Parabola C satisfies the conditions required to minimize the $(\chi^2_4)_\nu$ function (sec. 4-2-2), while neither parabola A nor

B succeeds in doing that. In Fig. 4-9, the values of $(D_4)_{LSQ}$ based on the old (vertex of parabola B) and the new (vertex of parabola C) procedures are compared with $(D_4)_{CEN}$ (location of the centroid value of the raw data). This comparison indicates that the new procedure improves the reliability of $(D_4)_{LSQ}$ (Table 4-2, example a). Using the new procedure for each one of the eight matches in Table 4-1, the raw data of $(\chi^2_2)_v$, $(\chi^2_3)_v$ and $(\chi^2_4)_v$ are fitted to a positive curvature parabola (like parabola C) and $(D_j)_{LSQ} \pm (\delta D_j)_{LSQ}$ agrees with $(D_j)_{CEN} \pm (\delta D_j)_{CEN}$; j =2, 3, 4. Therefore, the intercept and the slope of the fitted line LSQ agrees with those of CEN as indicated in Fig.4-6. Accordingly, reliable results are obtained from the new procedure of the least squares method (Table 4-1). Similarly, using the new procedure for the example presented in Fig. 4-8, the accuracy of $(D_4)_{LSQ}$ is greatly improved as indicated in (Table 4-2, example b) and Fig. 4-10. This figure shows the effect of the curvature of the fitted parabola on $(\delta D_4)_{LSQ}$. The flat parabola F produced by the 11 point fit increases $(\delta D_4)_{LSQ}$ to about 17 times $(\delta D_4)_{CEN}$. On the other hand, the new procedure yields parabola H which improves the ratio $(\delta D_4)_{LSQ}/(\delta D_4)_{CEN}$ to about one (Table 4-2, example b).

The results shown in Figures 4-9, 4-10 and Tables 4-1, 4-2 demonstrate that the new procedure :

(i) minimizes χ^2_j;

(ii) improves the uncertainties of the least squares method results to be :
$(\delta D_j)_{LSQ} \approx (\delta D_j)_{CEN}$
$\delta M_{LSQ} \approx \delta M_{CEN}$;

(iii) improves the accuracy of the least squares method results to be :
$|(D_j)_{LSQ} - (D_j)_{CEN}| \leq \sqrt{(\delta D_j)^2_{LSQ} + (\delta D_j)^2_{CEN}}$
$|\overline{\Delta M}_{LSQ} - \overline{\Delta M}_{CEN}| \leq \sqrt{\delta M^2_{LSQ} + \delta M^2_{CEN}}$

The problems mentioned in this section took place during the analysis of the data collected from the mass spectral peaks of $^{181}Ta^{35}Cl_2$ - $^{179}Hf^{35}Cl^{37}Cl$ (June, 1978), $^{183}WO_2{}^{35}Cl$ - $^{178}Hf^{35}Cl^{37}Cl$ (Aug.-Sept., 1978), ^{130}Te - ^{130}Xe (Jan. 1986) and $^{208}Pb^{35}Cl$ - $^{206}Pb^{37}Cl$ (Dec., 1986 - Jan., 1987). Similar problems to those described in this work were experienced in Kozier's work but with values of N smaller than eleven channels. With the improvement mentioned in this section, reliable results were obtained from the computer matching techniques. Computer matching resumed successfully (Nov. 1987). The first experiment using this improvement is the (Pb - Tl) measurements (chapter 5), in which only computer runs were collected. In this experiment, the average precision of the new data determined by the least squares method (4.48 parts in 10^9) is better than that obtained from the centroid method (5.41 parts in 10^9) by a factor of 1.2 (Tables 5-1a and 5-1b). Both values are better than that of the visual runs gathered for (Te-Xe) measurements (Dyck, 1990) by a factor of about 3. This significant improvement encouraged us to measure the spacings of the doublets : ^{76}Ge - ^{76}Se, $^{74}Ge^{35}Cl$ - $^{72}Ge^{37}Cl$, $^{76}Ge^{35}Cl$ - $^{74}Ge^{37}Cl$ and $^{78}Se^{35}Cl$ - $^{76}Se^{37}Cl$ by the computer-matching method ($^{76}Se^{35}Cl$ - $^{74}Ge^{37}Cl$, $^{78}Se^{35}Cl$ - $^{76}Ge^{37}Cl$ and ^{74}Se - ^{74}Ge are in progress). This set of measurements have been undertaken to improve our knowledge of the energies available for the double beta decays of ^{76}Ge and ^{74}Se (Hykawy, 1990).

Conclusion :

(1) For a computer run, the optimum value N_m of a range of N channels is selected according to the following criterion :

χ^2 function should be minimized for quadrants 2, 3 and 4 of each one of the eight matches and N_m is selected at the lowest value of $\overline{\chi^2}_{min}$ of this run.

(2) Reversing the sign of the curvature of a fitted parabola affects the accuracy of a peak separation determined by the least squares method $(D_j)_{LSQ}$. For a fitted parabola of negative curvature, $(D_j)_{LSQ}$ is far from $(D_j)_{CEN}$ when the sign of the curvature is changed to be positive.

(3) The magnitude of the curvature of a fitted parabola affects the uncertainty $(\delta D_j)_{LSQ}$.

$(\delta D_j)_{LSQ} \gg (\delta D_j)_{CEN}$ for a flat parabola.

References for chapter (4)

Barber, R. C., Meredith, J. O., Bishop, R. L., Duckworth, H. E., Kettner, M. E. & van Rookhuyzen, P. (1967). Proceeding of the Third Int. Conf. on Atomic Masses, ed. by R. C. Barber (Winnipeg : University of Manitoba Press), p.717.

Benson, J. L. & Johnson, W. H. (1966). Phys. Rev., 141, 1112.

Bevington, P. R. (1969). Data Reduction and Error Analysis For The Physical Sciences (McGraw-Hill Book Co., New York).

Bishop, R. L. & Barber, R. C. (1970). Rev. of Sci. Instr., 42, 327.

Campbell, L. L. (1956). Can. J. Phys., 34, 929.

Dyck, G. R., Sidky, M. H., Hykawy, J. G., Lander, C. A., Sharma, K. S., Barber, R. C. & Duckworth, H. E. (1990). Accepted for Publication for Phys. Lett.

Hykawy, J. G., Nxumalo, J. N., Sidky, M. H., Barber, R. C., Sharma, K. S., Duckworth, H. E. & Lander, C. A. (1990). To be published.

Kozier, K. S. (1977). PhD. Thesis, Winnipeg : University of Manitoba.

Macdougall, J. D., McLatchie, W., Whineray, S. & Duckworth, H. E. (1966). Z. Naturforshg, 21A, 63.

Meredith, J. O. (1971). PhD. Thesis, Winnipeg : University of Manitoba.

Meredith, J. O., Southon, F. C. G., Barber, R. C., Williams, P. & Duckworth, H. E. (1972). Int. J. of Mass Spec. and Ion Physics, 10, 359.

Sharma, K. S., Kozier, K. S., Barnard, J. W., Barber, R. C., Haque, S. S. & Duckworth, H. E. (1977). Can. J. of Phys., 55, 506.

Southon, F. C. G. (1973). PhD. Thesis, Winnipeg : University of Manitoba.

Stevens, C. M. & Moreland, P. E. (1967). Proceedings of the Third Int. Conf. on Atomic Masses, ed. by R. C. Barber (Winnipeg : University of Manitoba Press), p.673.

Table 4-1

Results of mass differences determined by the centroid and least squares (old and new procedures) methods for eight matches of a computer run obtained from the mass spectral peaks of ^{130}Te - ^{130}Xe

Match	$(\Delta M_i)_{CEN}$ (μu)	$(\Delta M_i)_{LSQ}$ (μu) (old procedure)	$(\Delta M_i)_{LSQ}$ (μu) (new procedure)
NAF (i=1)	2709.21	2702.40	2701.70
NSF (i=2)	2729.37	2732.36	2734.95
NSR (i=3)	2699.74	2702.14	2702.23
NAR (i=4)	2706.27	2714.19	2714.52
BAR (i=5)	2681.53	2691.38	2691.55
BSR (i=6)	2695.11	2910.27*	2691.94
BSF (i=7)	2670.59	2682.72	2680.51
BAF (i=8)	2698.26	2691.55	2691.90
**	2698.76 ± 6.28	2728.38 ± 26.55	2701.16 ± 5.99

* : mass difference $(\Delta M_6)_{LSQ}$ of match 6 determined by the old procedure of the least squares method in which the $(\chi^2_4)_\nu$ function of quadrant 4 is maximized (Fig. 4-7)

** : results of a computer run determined by the centroid $(\overline{\Delta M}_{CEN} \pm \delta M_{CEN})$ and least squares $(\overline{\Delta M}_{LSQ} \pm \delta M_{LSQ})$ methods

Table 4-2

Comparison between the accuracy and the uncertainty of a peak separation determined by the least squares method using the old (I) and new (II) procedures

Example	$(D_4)_{CEN} \pm (\delta D_4)_{CEN}$ *	Procedure	$(D_4)_{LSQ} \pm (\delta D_4)_{LSQ}$ **	Accuracy : $(D_4)_{LSQ} - (D_4)_{CEN} \pm \sqrt{(\delta D_4)^2_{LSQ} + (\delta D_4)^2_{CEN}}$
a	34.84 ± 1.00	I	-33.70 ± 1.85	-68.54 ± 2.10
		II	34.09 ± 1.35	-0.75 ± 1.68
b	-28.32 ± 0.88	I	132.30 ± 14.75	160.62 ± 14.78
		II	-26.67 ± 1.40	1.65 ± 1.65

*, ** : Separation between peaks in quadrants 4 and 1 determined by the centroid (*) and least squares (**) methods (in channels)

I, II : Old and new procedures used to minimize χ^2_j function

a : Example of a peak in quadrant 4 belong to a match (match 6 in Table 4-1) obtained from the mass spectral peaks of ^{130}Te - ^{130}Xe in which χ^2_4 function is maximized (the raw data of quadrant 4 are fitted to a negative curvature parabola A as shown in part I of Fig. 4-7)

b : Example of a peak in quadrant 4 belong to a match obtained from the mass spectral peaks of $^{208}Pb^{35}Cl$ - $^{206}Pb^{37}Cl$ in which the raw data of quadrant 4 are fitted to a flat parabola (parabola F shown in part I of Fig. 4-8) whose curvature is negative and its vertex lies far from the region of the raw data

FIGURE 4-1a

Asymmetric error signal

(mismatched peaks)

FIGURE 4-1b

Symmetric signal

(matched condition for visual matching)

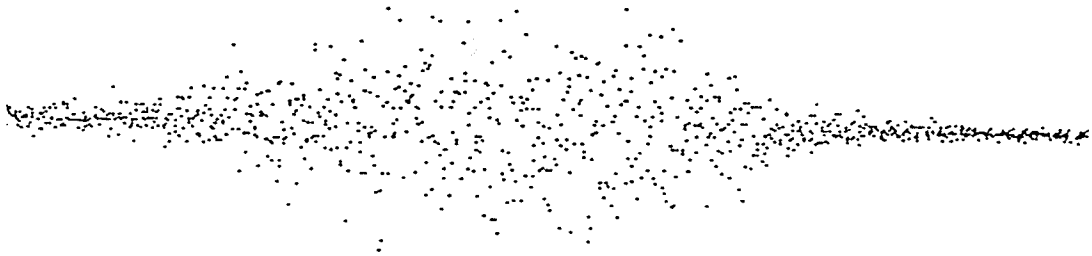

FIGURE 4-2

Memory contents of the MCA for Normal, Add, Forward (NAF configuration)

A, B, C and D are used to calculate the baseline. Peak limits are shown (●) at 20% of the peak height. In quad. 1, 2, 3 and 4 the electrostatic analyzer voltage V_e is changed by the amounts ΔV_e, δV_1, 0 and δV_2, respectively.

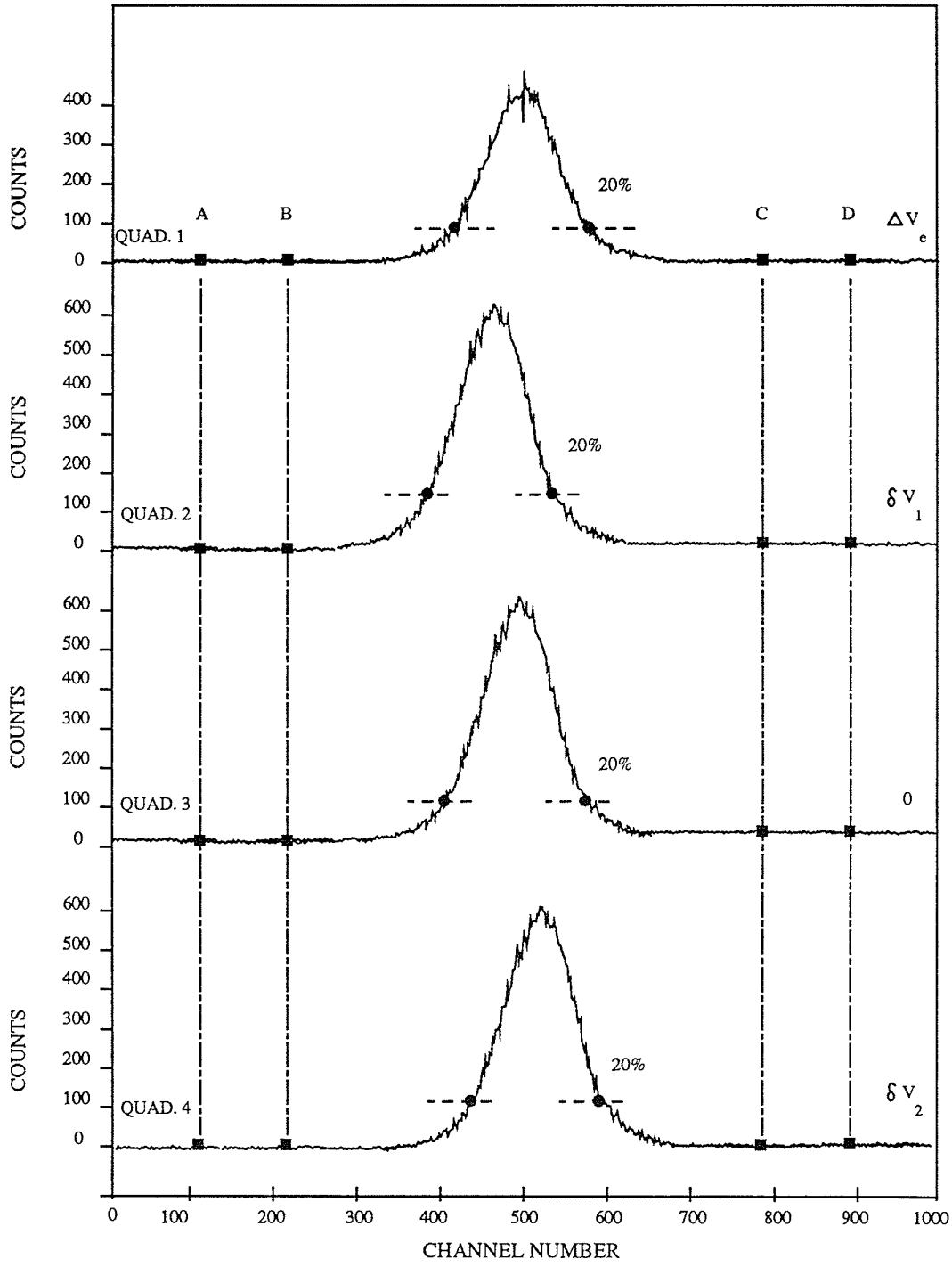
COUNTS
QUAD. 1
A
B
20%
C
D
ΔV e
QUAD. 2
δV 1
QUAD. 3
0
QUAD. 4
δV 2
0 100 200 300 400 500 600 700 800 900 1000
CHANNEL NUMBER

FIGURE 4-3

Flow chart of the data analysis program

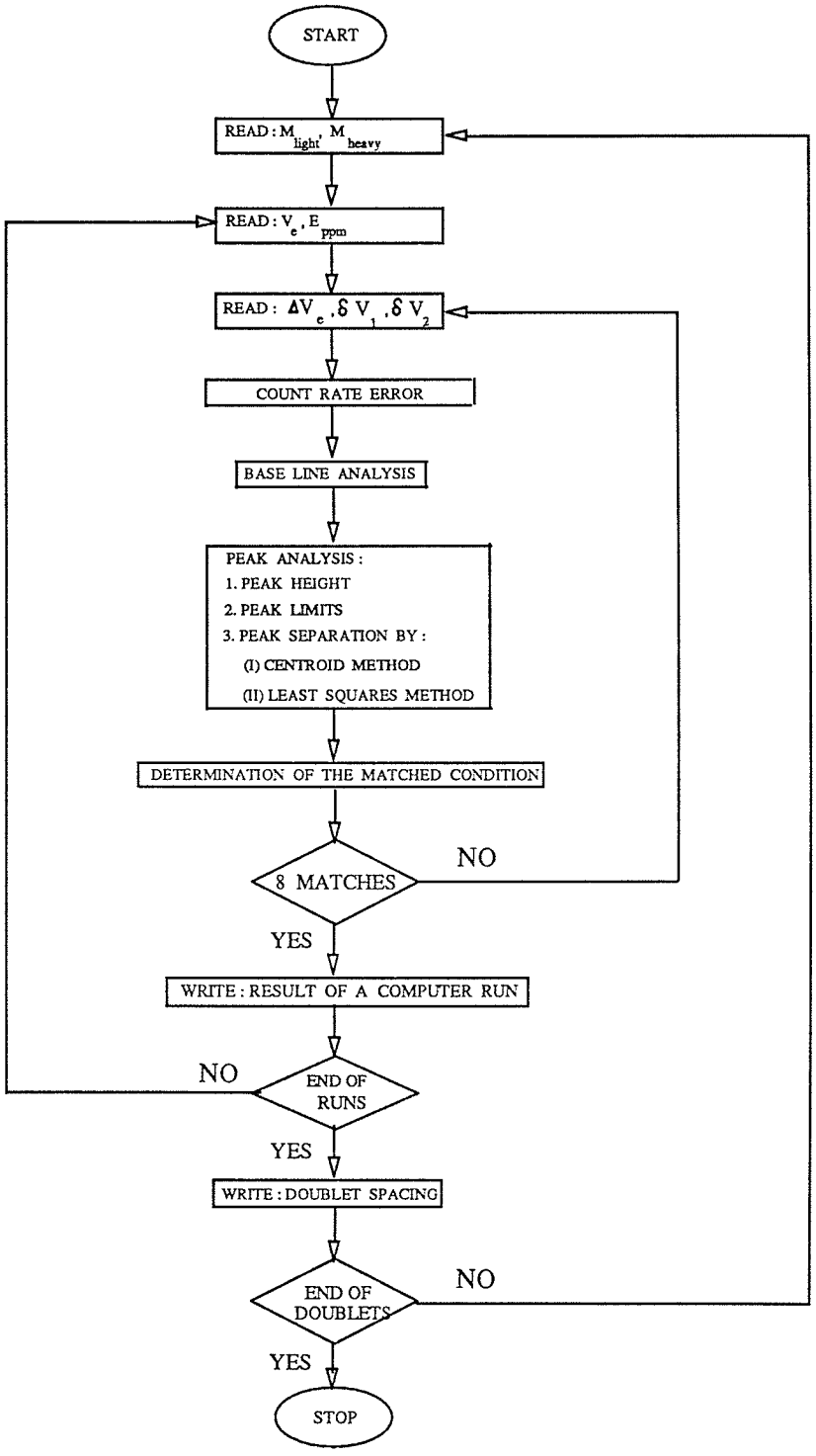
START
READ : M_{light}, M_{heavy}
READ : V_e, E_{ppm}
READ : ΔV_e, δV_1, δV_2
COUNT RATE ERROR
BASE LINE ANALYSIS
PEAK ANALYSIS :
1. PEAK HEIGHT
2. PEAK LIMITS
3. PEAK SEPARATION BY :
(I) CENTROID METHOD
(II) LEAST SQUARES METHOD
DETERMINATION OF THE MATCHED CONDITION
8 MATCHES
NO
YES
WRITE : RESULT OF A COMPUTER RUN
NO
END OF RUNS
YES
WRITE : DOUBLET SPACING
END OF DOUBLETS
NO
YES
STOP

FIGURE 4-4

Variation of $(\chi^2_3)_\nu$ with the peak displacement

Example obtained from the mass spectral peaks of H_3 - DH to show the variation of $(\chi^2_3)_\nu$ (reduced value of the sum of the squares of the differences between the counts in quad. 1 and 3) with the displacement d_3 (distance between the centroids of the peaks in quad. 1 and 3). d_3 is varied by moving the peak in quad. 3 (peak 3) relative to that in quad. 1 (peak 1) at increments of one channel. $(\chi^2_3)_\nu$ is calculated within a range of channels R. This range corresponds to the peak counts of quad. 1 as shown in part I. In part II, peak 3 is displaced at a distance $(d_3) > W/2$ such that the range R corresponds to the background of that peak. When $|d_3| < W/2$, a fraction, f, of peak 3 is included in the range R as shown in part III. In part IV, $(\chi^2_3)_\nu$ values are plotted versus d_3. $(\chi^2_3)_\nu$ function near the minimum is obtained by fitting a parabola to $(\chi^2_3)_\nu$ values within a range of N channels as shown in Fig. 4-5. The raw data are obtained by moving peak 3 symmetrically on both sides of peak 1 (e.g. in part II, peak 3 moves from d_3 = 140 channel to d_3 = -140 channel to obtain a total sum of : 140 - (-140) + 1 = 281 points, as shown in part IV).

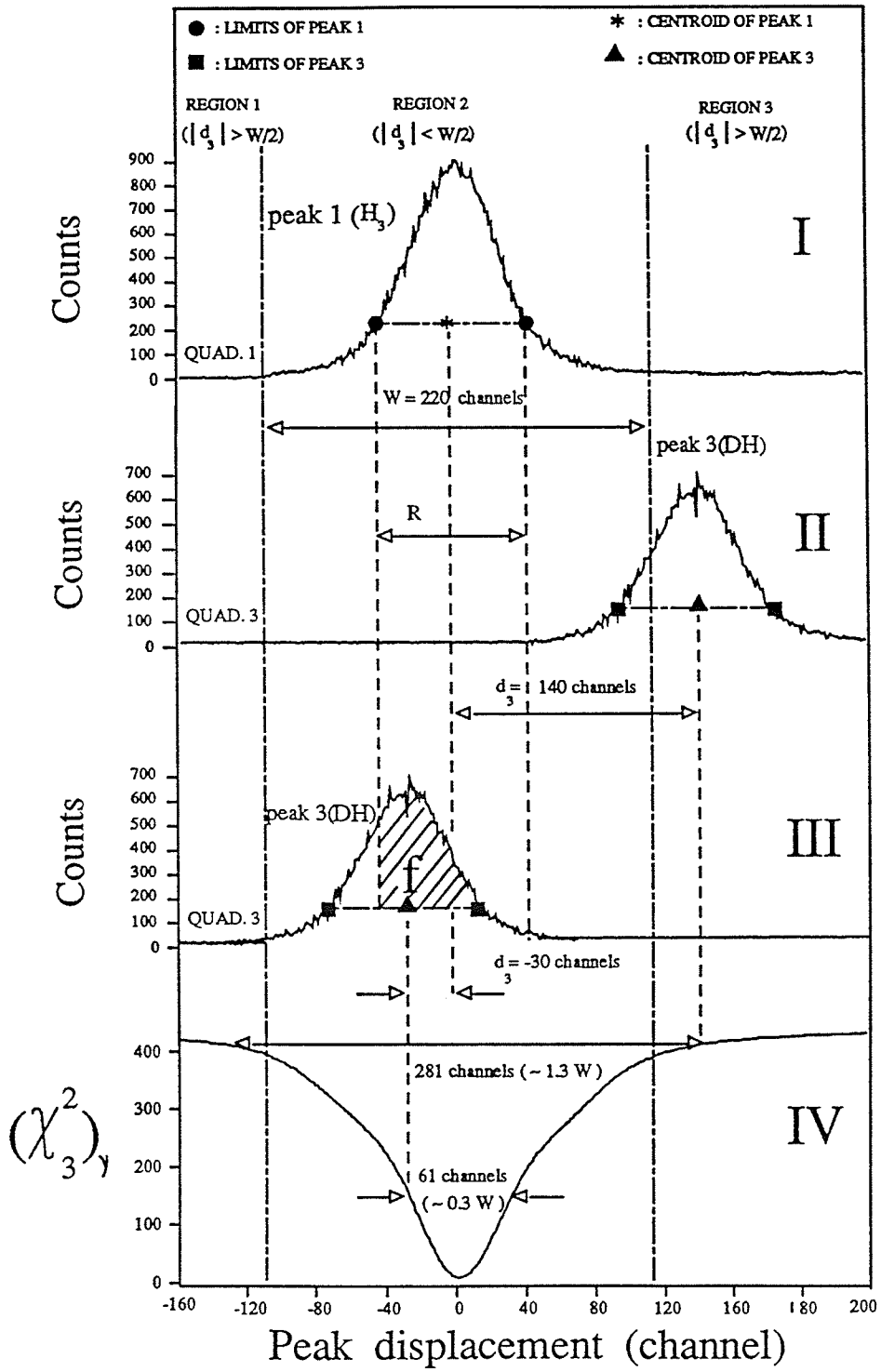
● : LIMITS OF PEAK 1
■ : LIMITS OF PEAK 3
✱ : CENTROID OF PEAK 1
▲ : CENTROID OF PEAK 3
REGION 1
(| d3 | > W/2)
REGION 2
(| d3 | < W/2)
REGION 3
(| d3 | > W/2)
Counts
peak 1 (H3)
I
QUAD. 1
W = 220 channels
peak 3(DH)
R
II
QUAD. 3
d3 = 140 channels
peak 3(DH)
III
f
QUAD. 3
d3 = -30 channels
281 channels (~ 1.3 W)
IV
61 channels
(~ 0.3 W)
(χ²3)y
Peak displacement (channel)

FIGURE 4-5

Fitting a positive curvature parabola to 11 values of $(\chi^2_3)_v$ within a range of 11 channels. The parabola's vertex (●) lies within this range of channels

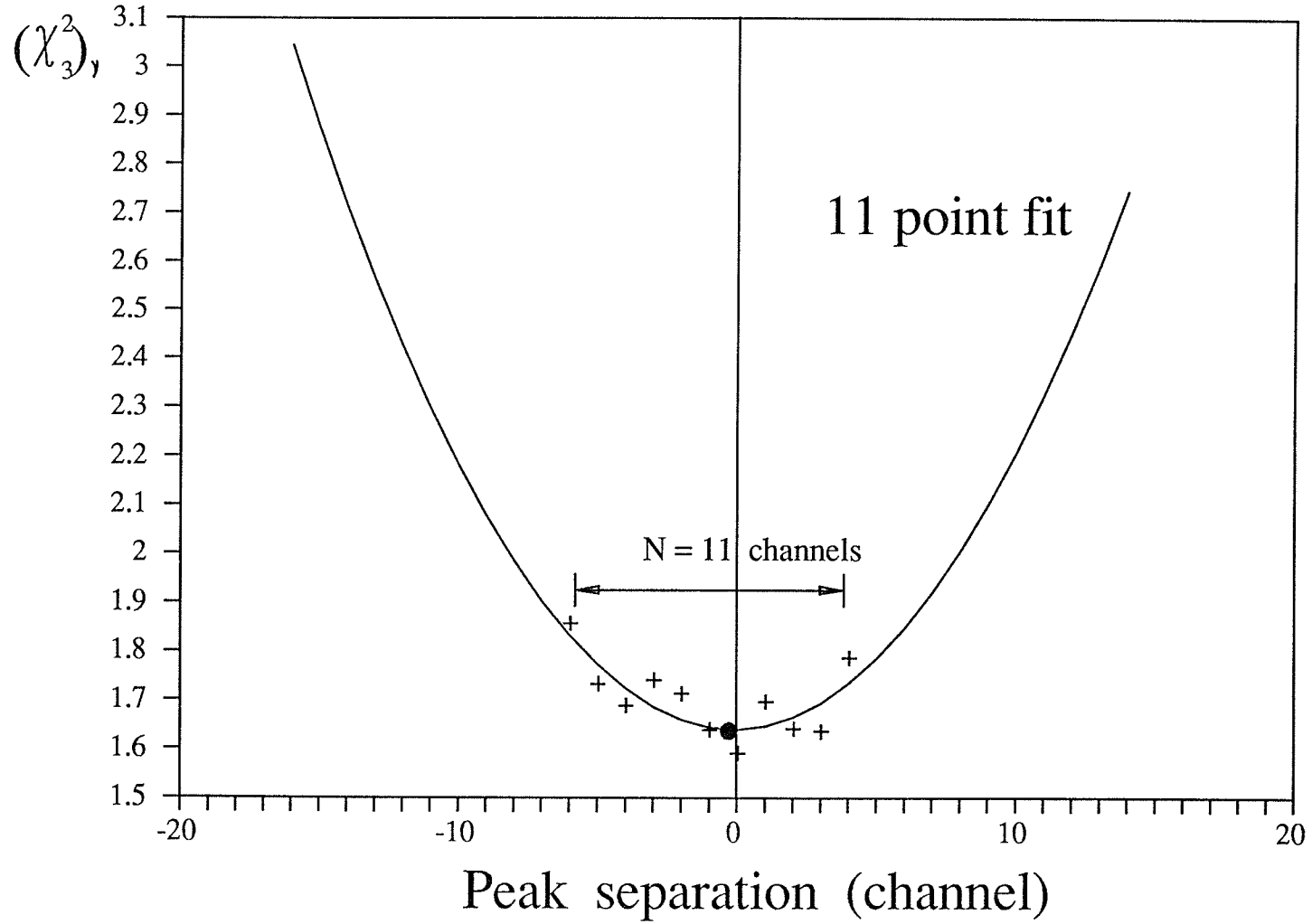
$(\chi^2_3)_\gamma$
3.1
3
2.9
2.8
2.7
2.6
2.5
2.4
2.3
2.2
2.1
2
1.9
1.8
1.7
1.6
1.5
-20
-10
0
10
20
11 point fit
N = 11 channels
Peak separation (channel)

FIGURE 4-6

Fitting 3 pairs of split voltages δV_1, 0, δV_2 and peak separations to a straight line

Results obtained from centroid ($\bullet$) and least squares ($*$) methods are fitted to lines CEN and LSQ. The matched conditions determined by the centroid and least squares methods are $(\delta V_0)_{CEN}$ and $(\delta V_0)_{LSQ}$, respectively.

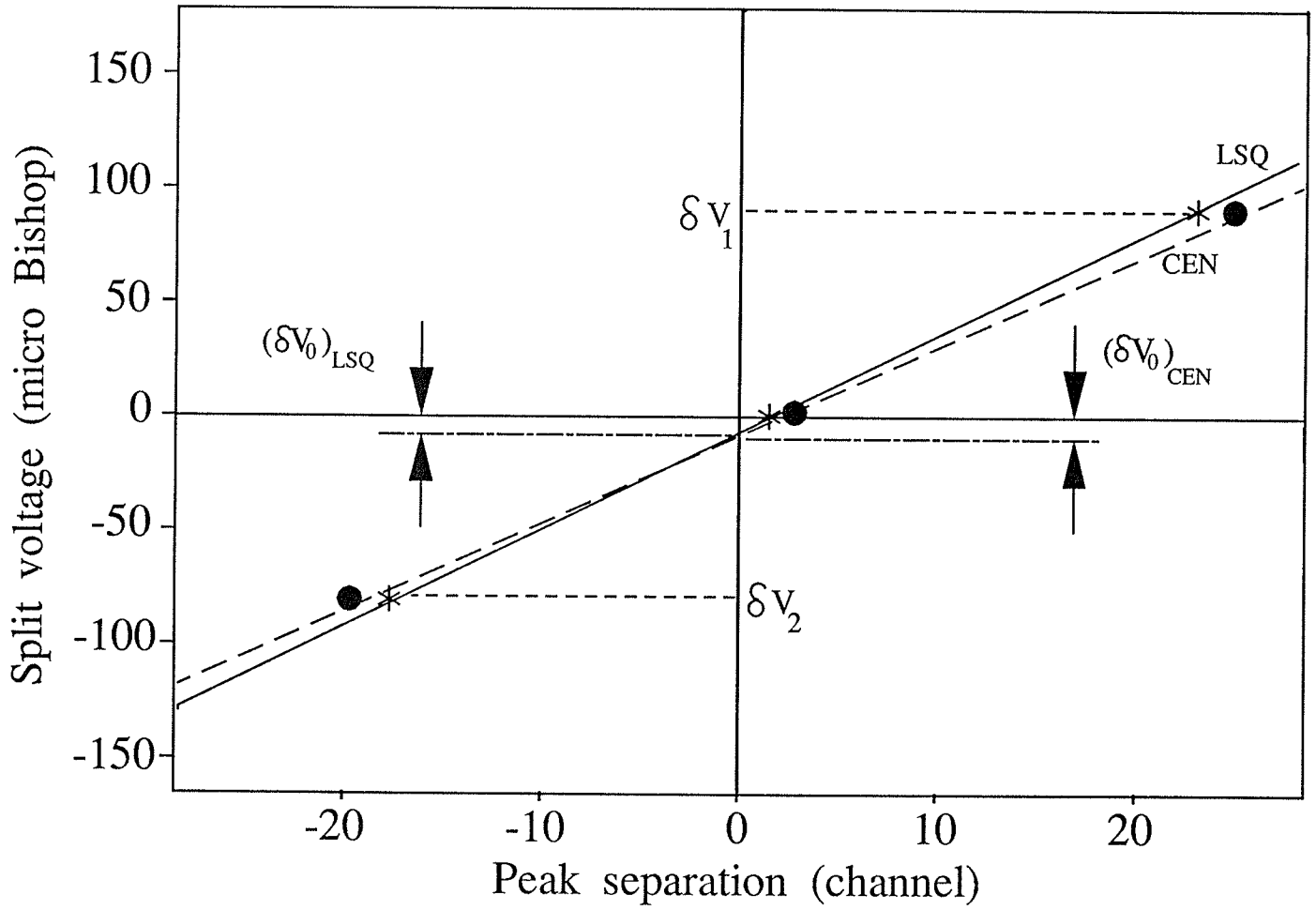
150
100
50
0
-50
-100
-150
-20
-10
0
10
20
Split voltage (micro Bishop)
Peak separation (channel)
LSQ
CEN
δ V1
δ V2
(δV0)LSQ
(δV0)CEN

FIGURE 4-7

The effect of reversing the sign of the curvature of χ_j^2 function on the determination of the matched condition by the least squares method $(\delta V_0)_{LSQ}$

Example of a match obtained from the mass spectral peaks of ^{130}Te - ^{130}Xe to explain the effect of reversing the sign of the curvature of the χ_j^2 function on the determination of the matched condition by the least squares method $(\delta V_0)_{LSQ}$. The raw data (+ + +) are obtained within a range of 11 channels (N = 11 channels) which represents 2.7% of the peak width W (W = 405 channels). The 11 values of $(\chi_4^2)_v$ are fitted to a negative curvature parabola A as shown in part I. To minimize $(\chi_4^2)_v$, it was suggested that the curvature of parabola A should be reversed, thus another parabola B is produced.

The peak separation of quad. 4 determined by the least squares method $(D_4)_{LSQ}$ disagrees with that obtained from the centroid method $(D_4)_{CEN}$. The peak separations of quad. 2, 3 and 4 are plotted versus the split voltages δV_1, 0, δV_2 as shown in part II. The points of quad. 2, 3 and 4 obtained from the centroid method (•) are fitted to a line CEN. The line LSQ excludes the points obtained from the least squares method (*). The matched condition determined by the centroid method $(\delta V_0)_{CEN}$ disagrees with $(\delta V_0)_{LSQ}$.

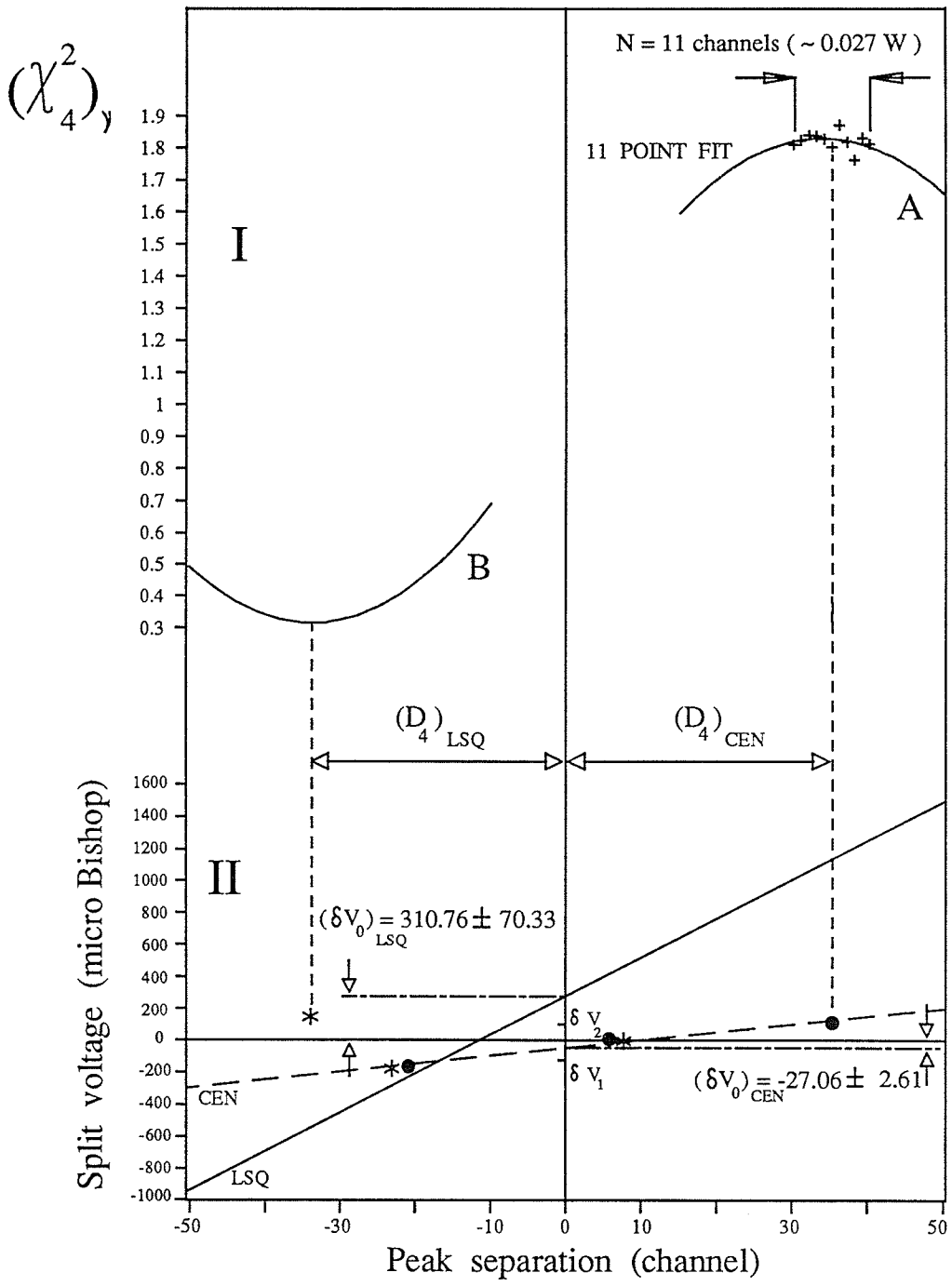
$(\chi^2_4)_y$
N = 11 channels (~ 0.027 W)
11 POINT FIT
A
I
B
II
$(D_4)_{LSQ}$
$(D_4)_{CEN}$
$(\delta V_0)_{LSQ} = 310.76 \pm 70.33$
δV_2
δV_1
$(\delta V_0)_{CEN} = -27.06 \pm 2.61$
CEN
LSQ
Split voltage (micro Bishop)
Peak separation (channel)

FIGURE 4-8

The effects of fitting χ_j^2 values to a flat parabola whose curvature is negative and whose vertex lies far from the region of the raw data on the accuracy and the uncertainty of a peak separation $(D_j)_{LSQ}$ determined by the least squares method

Example of a match obtained from the mass spectral peaks of $^{208}Pb\,^{35}Cl$ - $^{206}Pb\,^{37}Cl$ to show the effects of fitting χ_j^2 values to a flat parabola, whose curvature is negative and whose vertex lies far from the region of the raw data, on the accuracy and the uncertainty of $(D_j)_{LSQ}$. The raw data (+ + +) are obtained within a range of 11 channels (N = 11 channels) which represents 2.5% of the peak width W (W = 437 channels). The 11 values of $(\chi_4^2)_v$ are fitted to a flat parabola F which has a negative curvature as shown in part I. The vertex of parabola F is at ~ – 130 channel (not shown). To minimize $(\chi_4^2)_v$, the curvature of parabola F is reversed, thus parabola G is produced whose vertex $(D_4)_{LSQ}$~130 channel as shown. $(D_4)_{LSQ}$ is 6 times the magnitude of $(D_4)_{CEN}$. The determination of the uncertainty of $(D_4)_{LSQ}$ (—*—) is based on the curvature of the flat parabola F. The peak separations of quad. 2, 3 and 4 are plotted versus the split voltages $\delta V_1, 0, \delta V_2$ as shown in part II. The points obtained from the centroid method (●) are fitted to a line CEN. The line LSQ passes through the points (*) of quad. 2, 3 and excludes —*— of quad. 4. The matched condition determined by the least squares method $(\delta V_0)_{LSQ}$ agrees with that obtained from the centroid method $(\delta V_0)_{CEN}$.

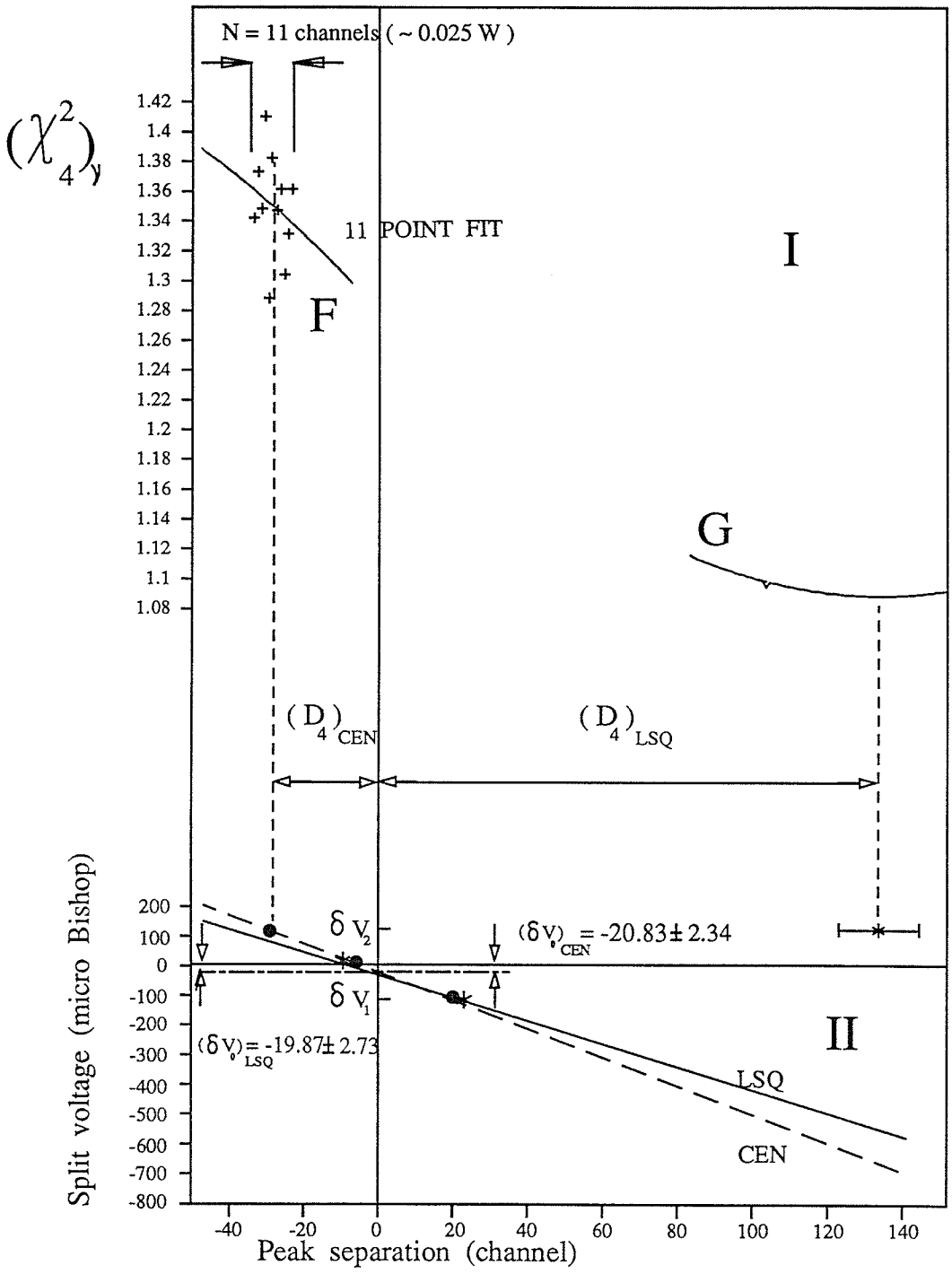
N = 11 channels (~ 0.025 W)
$(\chi^2_4)_y$
11 POINT FIT
F
I
G
II
$(D_4)_{CEN}$
$(D_4)_{LSQ}$
δV_2
δV_1
$(\delta V_0)_{CEN} = -20.83 \pm 2.34$
$(\delta V_0)_{LSQ} = -19.87 \pm 2.73$
LSQ
CEN
Split voltage (micro Bishop)
Peak separation (channel)

FIGURE 4-9

Comparison between the old (parabola B) and new (parabola C) procedures used to minimize the χ_j^2 function in the case of fitting the raw data to a negative curvature parabola A (χ_j^2 is maximized locally). Parabolae A and B are obtained from the example shown in Fig. 4-7. The values of $(D_4)_{LSQ}$ based on the old ($*$: vertex of parabola B) and new ($\blacksquare$: vertex of parabola C) procedures are shown. The accuracies of these values are obtained by comparing their positions with $(D_4)_{CEN}$.

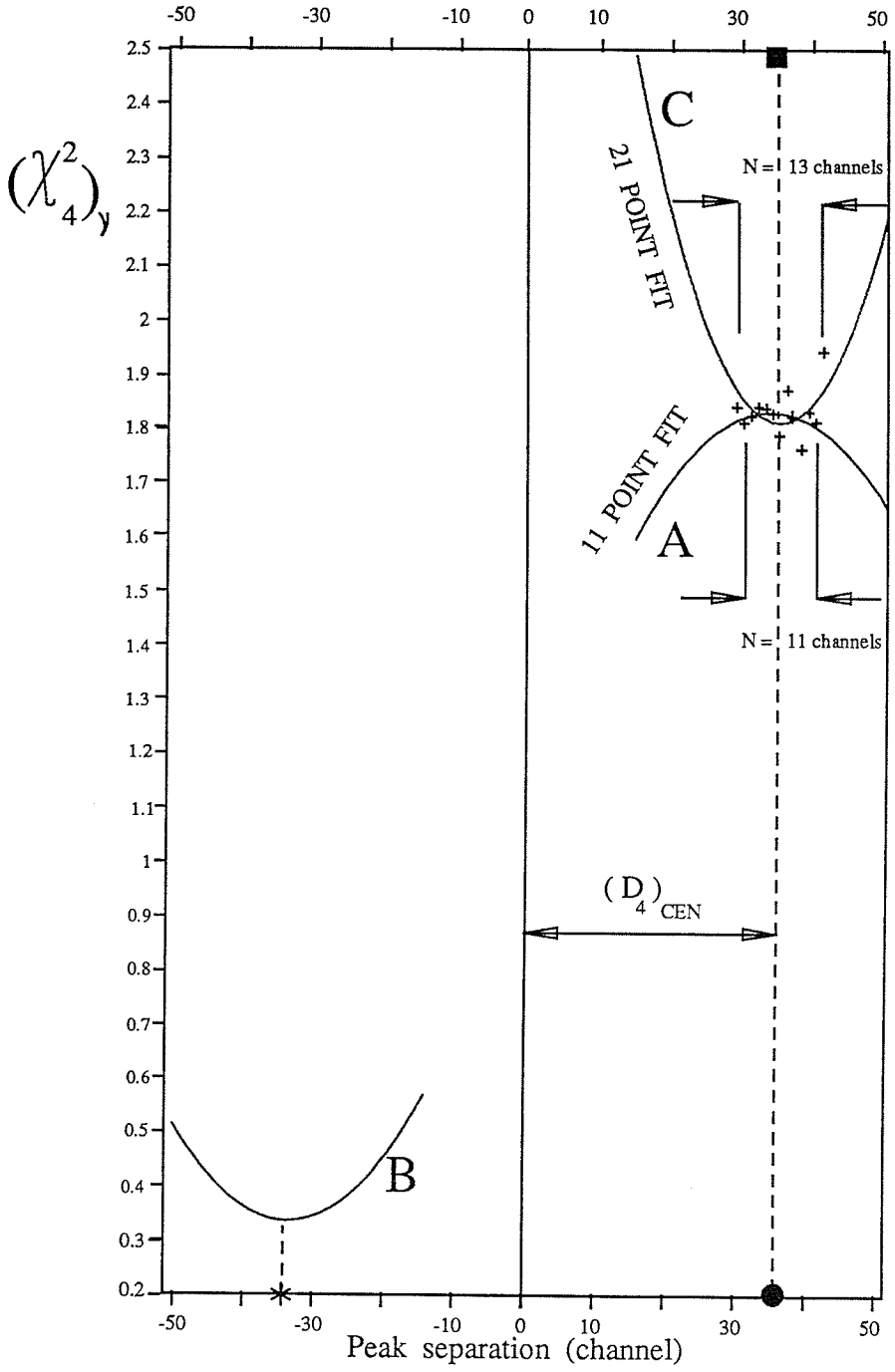
$(\chi^2_4)_y$
-50
-30
-10
0
10
30
50
2.5
2.4
2.3
2.2
2.1
2
1.9
1.8
1.7
1.6
1.5
1.4
1.3
1.2
1.1
1
0.9
0.8
0.7
0.6
0.5
0.4
0.3
0.2
C
21 POINT FIT
N = 13 channels
11 POINT FIT
A
N = 11 channels
$(D_4)_{CEN}$
B
Peak separation (channel)

FIGURE 4-10

Comparison between the accuracy and the uncertainty of $(D_j)_{LSQ}$ determined from the old (∗ : vertex of parabola G) and new (■ : vertex of parabola H) procedures in the case of fitting the raw data to a flat parabola F whose curvature is negative and whose vertex lies far from the region of the raw data. Parabolae F and G are obtained from the example shown in Fig. 4-8. The locations of ∗ and ■ relative to ● indicate the accuracy of $(D_4)_{LSQ}$ obtained from the old and new procedures relative to $(D_4)_{CEN}$. The uncertainties of —∗— and ■ are based on the curvatures of parabolae G and H.

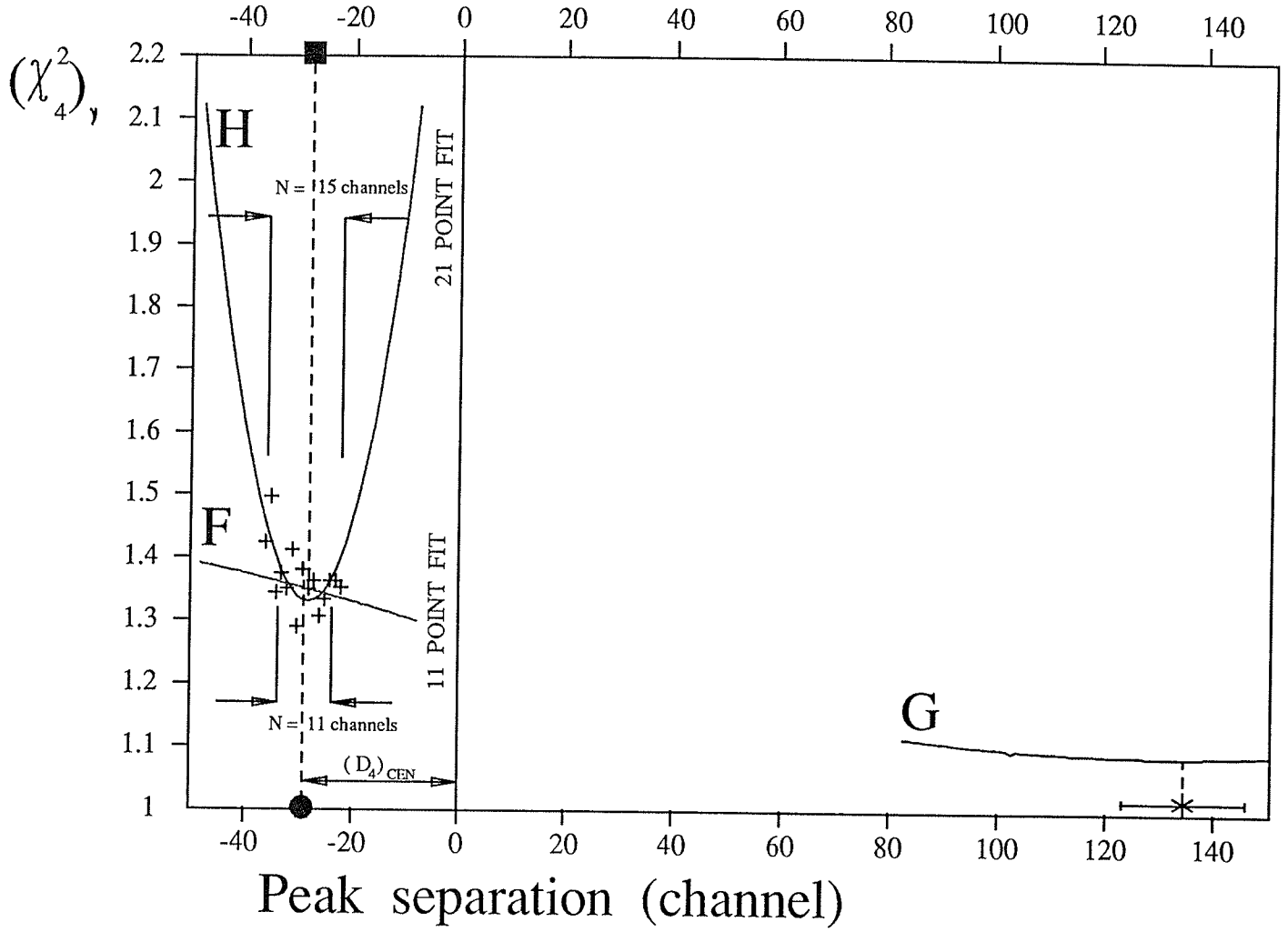
$(\chi^2_4)_\gamma$
2.2
2.1
2
1.9
1.8
1.7
1.6
1.5
1.4
1.3
1.2
1.1
1
-40
-20
0
20
40
60
80
100
120
140
H
N = 15 channels
21 POINT FIT
F
11 POINT FIT
N = 11 channels
$(D_4)_{CEN}$
G
Peak separation (channel)

CHAPTER (5)

NEW ATOMIC MASS DETERMINATIONS

The observed solar neutrino flux, measured using conventional neutrino detectors, is a factor of about 3 lower than the value expected by theoretical models. This discrepancy may be due, in part, to the high threshold energies for the reaction used to detect the neutrinos. It has been suggested (Freedman, 1976) that the reaction : $\nu + {}^{205}\mathrm{Tl} \rightarrow {}^{205}\mathrm{Pb} + e^-$, which has a low threshold energy, may provide a good mechanism on which a neutrino detector may be based. The threshold energy E_{th} of the neutrino capture reaction in ^{205}Tl is determined in terms of the Q-value Q_{EC} of the electron capture reaction for the ground state of ^{205}Pb (eqn. 6-9). This Q-value represents the ^{205}Pb - ^{205}Tl atomic mass difference.

In an effort to determine this mass difference, the Manitoba II spectrometer has been used to measure the spacings of four chloride doublets among selected isotopes of Tl and Pb. Each of these doublet spacings was determined by the least squares computer-assisted matching method. The separations of these doublets range from 1/30,000 to 1/55,000 of their mass. The spectrometer was operated with a resolution (at about 10% of peak height) in the range 1/100,000 to 1/180,000. This measurement program represents the first work which was undertaken after installation of the new magnet facilities (see sec. 3-4) and improvements to the analysis procedure (see sec. 4-3) were carried out.

5-1 Experimental details

Tl^+ and Pb^+ ions were formed from the fragmentation of the molecules TlCl and $PbCl_2$. The sample material was contained in a copper tube outside the ion source.

In order to correct for the presence of known systematic effects (Southon, 1977) which are proportional to the doublet width, calibrations were made by measuring a wide doublet (ΔM = 1 to 2 u), whose spacing is well known, and the correction was applied, to the narrow doublet under consideration (for more details see sec. 2-3-2). This correction remains fairly constant over a period of a few hours and is redetermined for every second or third run. This correction ranged from 0.1 to 0.5 μu (well within the uncertainty of any individual measurement) for all the measurements reported here.

As described before, every run consists of eight independent measurements, X_{ik}, carried out with different configurations of the instrument (sec. 4-2-1). The result of the i^{th} run, X_i, is taken to be the average of these eight values :

$$X_i = \sum_{k=1}^{8} X_{ik}/8 \qquad (5\text{-}1)$$

The uncertainty associated with this average is given by :

$$\sigma_i = \sqrt{\sum_{k=1}^{8} (X_{ik} - X_i)^2/8(8-1)} \qquad (5\text{-}2)$$

For a set of N runs with results $X_i \pm \sigma_i$, the final result is taken to be $\langle X \rangle$, the weighted average of all X_i :

$$\langle X\rangle = \frac{\sum_{i=1}^{N} X_i(1/\sigma_i^2)}{\sum_{i=1}^{N}(1/\sigma_i^2)} \qquad (5\text{-}3)$$

The uncertainty associated with this value is chosen to be the larger of the internal error σ_{int} or the external error σ_{ext}, where

$$\sigma_{int}^2 = 1/\sum_{i=1}^{N}(1/\sigma_i^2) \qquad (5\text{-}4)$$

$$\sigma_{ext}^2 = \frac{\left(\sum_{i=1}^{N}(X_i - \langle X\rangle)^2/\sigma_i^2\right)}{(N-1)\sum_{i=1}^{N}(1/\sigma_i^2)} \qquad (5\text{-}5)$$

The quantity $\sigma_{ext}/\sigma_{int}$ is defined as Birge ratio. In this work, this ratio is close to unity and the values of σ_{int} and σ_{ext} are approximately the same (Tables 5-1a and 5-1b). This behaviour indicates that the uncertainties have been realistically estimated.

The new values for the doublet spacings are given in Tables 5-1a and 5-1b. They were determined on the basis of 8 to 25 computer runs each. For the special case of doublet $^{206}Pb\ ^{35}Cl$ - $^{204}Pb\ ^{37}Cl$, a set of 10 computer runs were gathered for the natural sample of that doublet. The mass differences $\langle X\rangle_{LSQ}$ and $\langle X\rangle_{CEN}$ determined by the least squares and centroid methods were :

$\langle X\rangle_{LSQ} = 4369.92\ \mu u$, $(\sigma_{int})_{LSQ} = 2.03\ \mu u$, $(\sigma_{ext})_{LSQ} = 2.59\ \mu u$.

$\langle X\rangle_{CEN} = 4371.55\ \mu u$, $(\sigma_{int})_{CEN} = 2.02\ \mu u$, $(\sigma_{ext})_{CEN} = 2.61\ \mu u$.

In an attempt to improve the uncertainties an enriched sample of $PbCl_2$ (6% ^{204}Pb) was used to improve the intensity ratio relative to a natural sample (1.5% ^{204}Pb) from 54.10 ± 1.31 : 1 to about 10.84 ± 0.05 : 1. At that time there was a great interset to achieve this improvement,

so, Manitoba II was operated 24 hours continuously and 15 computer runs were collected. The final uncertainties shown in Tables 5-1a and 5-1b (based on all 25 runs) are greatly improved in comparison with those (based on 10 runs) obtained from the natural sample.

The precision of the new data determined by the least squares method (Table 5-1a) is better than that obtained from the centroid method (Table 5-1b) except for doublet B. The results obtained from this work (Table 5-1a) agree with the values taken from the 1983 Atomic Mass Evaluation (Wapstra, 1985) and represent a substantial improvement in precision, except for doublets A and C, as shown in Fig. 5-1. In this figure, our new determinations (least squares method computer runs) are compared to values (centroid method computer runs and visual runs) presented in earlier work by Derenchuk et al (Derenchuk, 1985). In every case, our new results are consistent with the earlier results of Derenchuk (Derenchuk, 1985). It should be noted that the strongest agreement occurs for doublet A where our earlier datum was solely the result of computer matching. Our new values (Table 5-1a) represent a factor of 1.32 improvement in precision over the previous values.

The schematic diagram (Fig. 5-2) indicates that the mass doublets A, B, C and D can be combined with additional reaction data (Table 5-2) to form closed loops 1, 2, 3, 4 and 5 which can be used to test the consistency of the data. The loops are :

$$\text{Loop 1} = (^{208}\text{Pb} - ^{206}\text{Pb}) + (^{206}\text{Pb} - ^{207}\text{Pb}) + (^{207}\text{Pb} - ^{208}\text{Pb})$$

$$= [(^{37}\text{Cl} - ^{35}\text{Cl}) + (^{208}\text{Pb}\,^{35}\text{Cl} - ^{206}\text{Pb}\,^{37}\text{Cl})] - [n - Q\,(^{206}\text{Pb}\,(n,\gamma)\,^{207}\text{Pb})] - [n - Q\,(^{207}\text{Pb}\,(n,\gamma)\,^{208}\text{Pb})]$$

Loop 2 = $(^{206}Pb - ^{204}Pb) + (^{204}Pb - ^{205}Pb) + (^{205}Pb - ^{206}Pb)$

= $[(^{37}Cl - ^{35}Cl) + (^{206}Pb\ ^{35}Cl - ^{204}Pb\ ^{37}Cl)] - [n - Q\ (^{204}Pb\ (n,\gamma)\ ^{205}Pb)] - [n + Q\ (^{206}Pb\ (\gamma,n)\ ^{205}Pb)]$

Loop 3 = $(^{207}Pb - ^{205}Tl) + (^{205}Tl - ^{204}Tl) + (^{204}Tl - ^{204}Pb) + (^{204}Pb - ^{205}Pb) + (^{205}Pb - ^{206}Pb) + (^{206}Pb - ^{207}Pb)$

= $[(^{37}Cl - ^{35}Cl) + (^{207}Pb\ ^{35}Cl - ^{205}Tl\ ^{37}Cl)] + [n + Q\ (^{205}Tl\ (\gamma,n)\ ^{204}Tl)] + [Q\ (^{204}Tl\ (\beta)\ ^{204}Pb)] - [n - Q\ (^{204}Pb\ (n,\gamma)\ ^{205}Pb)] - [n + Q\ (^{206}Pb\ (\gamma,n)\ ^{205}Pb)] - [n - Q\ (^{206}Pb\ (n,\gamma)\ ^{207}Pb)]$

Loop 4 = $(^{205}Tl - ^{203}Tl) + (^{203}Tl - ^{204}Tl) + (^{204}Tl - ^{205}Tl)$

= $[(^{37}Cl - ^{35}Cl) + (^{205}Tl\ ^{35}Cl - ^{203}Tl\ ^{37}Cl)] - [n - Q\ (^{203}Tl\ (n,\gamma)\ ^{204}Tl)] - [n + Q\ (^{205}Tl\ (\gamma,n)\ ^{204}Tl)]$

Loop 5 = $(^{208}Pb - ^{206}Pb) + (^{206}Pb - ^{204}Pb) + (^{204}Pb - ^{204}Tl) + (^{204}Tl - ^{203}Tl) + (^{203}Tl - ^{205}Tl) + (^{205}Tl - ^{207}Pb) + (^{207}Pb - ^{208}Pb)$

= $[(^{37}Cl - ^{35}Cl) + (^{208}Pb\ ^{35}Cl - ^{206}Pb\ ^{37}Cl)] + [(^{37}Cl - ^{35}Cl) + (^{206}Pb\ ^{35}Cl - ^{204}Pb\ ^{37}Cl)] - [Q\ (^{204}Tl\ (\beta)\ ^{204}Pb)] + [n - Q\ (^{203}Tl\ (n,\gamma)\ ^{204}Tl)] - [(^{37}Cl - ^{35}Cl) + (^{205}Tl\ ^{35}Cl - ^{203}Tl\ ^{37}Cl)] - [(^{37}Cl - ^{35}Cl) + (^{207}Pb\ ^{35}Cl - ^{205}Tl\ ^{37}Cl)] - [n - Q\ (^{207}Pb\ (n,\gamma)\ ^{208}Pb)]$

The closures of these loops are calculated by using our new measurements (Table 5-1a), the additional data (Table 5-2) and the auxiliary data (Table 5-3). The results of these calculations (Table 5-4) for loops 1, 2, 3 and 4 indicate the consistency of each doublet with other

measurements obtained from (n,γ) reactions and β decays, while the closure of loop 5 shows the consistency of all the doublets together with other precise reaction data. The data C, m, r and h shown in Figure 5-2 form a closed loop. The raw values of these data (Table 5-2) are used as input values for the least squares adjustment shown in Table 5-7. While these values fail to close the loop (-6.588 ± 4.754 μu) formed by them, their output values (Table 5-7) closes this loop to (-0.001 ± 1.838 μu). This may be explained by comparing the input and output values for each one of the data C, m, r, and h (Table 5-7). These comparisons indicate that there is no significant difference between those values for C, m and h, while for datum r the output value is larger than the input value by about 6.74 keV (7.24 μu). This value represents a major contribution to the difference between the closures (-6.588 ± 4.754 μu) and (-0.001 ± 1.838 μu) calculated by using the input and output values of C, m, r and h. A similar discrepancy is noted when the input values are compared with the more extensive 1983 Atomic Mass Evaluation (Wapstra, 1985). It has been recommended (Freedman, 1988) to redetermine the Q-value of the reaction ^{206}Tl (β) ^{206}Pb which represents datum r. For these reasons the loop fromed by the data C, m, r and h is not used in this work to check the consistency of our new datum C.

5-2 Description of the least squares evaluation

The experimental data for the mass differences, whether derived from mass spectroscopy or from nuclear reaction or decay Q-value determinations, may be considered as a set of N measured values, $Y_I \pm \sigma_I$, each of which is a linear combination of n atomic masses, M_j. This may be written for the I^{th} measured value in the following way :

$$\sum_{j=1}^{n} A_{Ij} M_j = Y_I \pm \sigma_I \qquad (5\text{-}6)$$

where I = 1, 2, ..., N and j = 1, 2, ..., n and the coefficients A_{Ij} are, in general, either 0 or ± 1.

A set of estimates, Y_I^*, for the observed values, Y_I, may be calculated from a set of estimates for the masses, M_j^*. From these values one can define the residuals, r_I, as :

$$r_I = Y_I^* - Y_I \qquad (5\text{-}7)$$

As has been discussed by Sharma (Sharma, 1977), the estimates for the masses, M_j^*, may be chosen through a least squares evaluation, such that the weighted sum of the residuals is minimized :

$$\chi^2 = \sum_{I=1}^{N} (r_I/\sigma_I)^2 \qquad (5\text{-}8)$$

To check the consistency of the input data, the generalized Birge ratio, which is defined as $\sqrt{\chi^2/f}$ (Sharma, 1977), may be calculated and compared with its expected value $1 \pm \sqrt{1/2f}$ where f is the number of degrees of freedom of the system. If the generalized Birge ratio is significantly larger than the expected value, the input data must be examined for inconsistencies. The consistency of the I^{th} datum may be checked by calculating the consistency factor of that datum, $\sqrt{\chi_I^2}$. This factor is the ratio between the estimated residual r_I calculated from the least squares adjustment and the experimental error σ_I. If this ratio is significantly larger than 1.0, it can be concluded that the experimental error σ_I has not been estimated correctly, and the I^{th} datum is identified as an inconsistent one. Local consistency of the input data may be obtained by replacing the error σ_I by r_I or, equivalently, multiplying σ_I by the consistency factor $\sqrt{\chi_I^2}$ of that datum (Wapstra, 1985).

5-3 Electron capture decay energy of the ground state of ^{205}Pb

The schematic diagram (Fig. 5-2) of the input data pertinent to the ^{205}Pb - ^{205}Tl mass difference, shows that there are four different ways, involving our new data and other measurements, of calculating this mass difference. The values determined from these paths Q_1, Q_2, Q_3 and Q_4 are as follows :

Q_1 = (^{205}Pb - ^{204}Pb) - (^{204}Tl - ^{204}Pb) - (^{205}Tl - ^{204}Tl)

= [n - Q (^{204}Pb (n,γ) ^{205}Pb)] - [Q (^{204}Tl (β) ^{204}Pb)] - [n + Q (^{205}Tl (γ,n) ^{204}Tl)]

Using the reaction data given in Table 5-2 :

$Q_1 \pm \delta Q_1 = 53.03 \pm 3.01$ keV

The main contribution to the uncertainty $\delta Q_1 = 3.01$ keV is from the error associated with the Q-value of the reaction ^{205}Tl (γ,n) ^{204}Tl which is used to determine the mass difference ^{205}Tl - ^{204}Tl. This mass difference can be calculated from alternative path involving the mass differences ^{204}Tl - ^{203}Tl and ^{205}Tl - ^{203}Tl. Thus, another value, Q_2 ,for the mass difference ^{205}Pb - ^{205}Tl is produced.

Q_2 = (^{205}Pb - ^{204}Pb) - (^{204}Tl - ^{204}Pb) + (^{204}Tl - ^{203}Tl) - (^{205}Tl - ^{203}Tl)

= [n - Q (^{204}Pb (n,γ) ^{205}Pb)] - [Q (^{204}Tl (β) ^{204}Pb)] + [n - Q (^{203}Tl (n,γ) ^{204}Tl)] - [(^{37}Cl - ^{35}Cl) + (^{205}Tl ^{35}Cl - ^{203}Tl ^{37}Cl)]

Using our new value for the doublet ^{205}Tl ^{35}Cl - ^{203}Tl ^{37}Cl (Table 5-1a), the reaction data (Table 5-2) and the auxiliary data (Table 5-3) :

$Q_2 \pm \delta Q_2 = 51.45 \pm 1.43$ keV

The comparison of the mass differences used to calculate Q_1 and Q_2 indicates that the mass difference ^{205}Tl - ^{204}Tl is replaced by the mass differences ^{205}Tl - ^{203}Tl and ^{204}Tl - ^{203}Tl. Therefore, the significant improvement in the uncertainty of the ^{205}Pb - ^{205}Tl mass difference

from $\delta Q_1 = 3.01$ keV to $\delta Q_2 = 1.43$ keV is clearly due to the precise measurements of the doublet ^{205}Tl ^{35}Cl - ^{203}Tl ^{37}Cl ($\delta M = 0.90$ μu) (this work) and the Q-value of the reaction ^{203}Tl (n,γ) ^{204}Tl ($\delta Q = 0.30$ keV) (Colenbrander, 1974).

An independent value, Q_3 ,is obtained from :

Q_3 = -(^{206}Pb - ^{205}Pb) - (^{206}Tl - ^{206}Pb) + (^{206}Tl - ^{205}Tl)

= -[n + Q (^{206}Pb (γ,n) ^{205}Pb)] - [Q (^{206}Tl (β) ^{206}Pb)] + [n - Q (^{205}Tl (n,γ) ^{206}Tl)]

Using the reaction data given in Table 5-2 :

$Q_3 \pm \delta Q_3 = 56.60 \pm 5.02$ keV

The reaction data used in the above equation produce a value for Q_3 larger than Q_1, Q_2 and the 1983 Atomic Mass Evaluation value $Q_{M.T}$ by about 3 keV and an error δQ_3 higher than δQ_1, δQ_2 and $\delta Q_{M.T}$ (Table 5-5). The mass differences used to calculate Q_3 can be obtained from another path as follows :

(^{206}Pb - ^{205}Pb) = (^{206}Pb - ^{204}Pb) - (^{205}Pb - ^{204}Pb)

- (^{206}Tl - ^{206}Pb) + (^{206}Tl - ^{205}Tl) = (^{206}Pb - ^{207}Pb) + (^{207}Pb - ^{205}Tl)

Thus, another value Q_4 for the mass difference ^{205}Pb - ^{205}Tl is produced :

Q_4 = (^{205}Pb - ^{204}Pb) - (^{206}Pb - ^{204}Pb) + (^{206}Pb - ^{207}Pb) + (^{207}Pb - ^{205}Tl)

= [n - Q (^{204}Pb (n,γ) ^{205}Pb)] - [(^{37}Cl - ^{35}Cl) + (^{206}Pb ^{35}Cl - ^{204}Pb ^{37}Cl)] - [n - Q (^{206}Pb (n,γ) ^{207}Pb)] + [(^{37}Cl - ^{35}Cl) + (^{207}Pb ^{35}Cl - ^{205}Tl ^{37}Cl)]

Using our new values for the doublets ^{206}Pb ^{35}Cl - ^{204}Pb ^{37}Cl, ^{207}Pb ^{35}Cl - ^{205}Tl ^{37}Cl (Table 5-1a) and the reaction data given in (Table 5-2) :

$Q_4 \pm \delta Q_4 = 53.27 \pm 2.06$ keV

which is in a good agreement with $Q_1 \pm \delta Q_1$, $Q_2 \pm \delta Q_2$ and $Q_{M.T} \pm \delta Q_{M.T}$ (Table 5-5). Our new data for the doublets ^{206}Pb ^{35}Cl - ^{204}Pb ^{37}Cl, ^{207}Pb ^{35}Cl - ^{205}Tl ^{37}Cl and the Q-values of

the reactions ^{204}Pb (n,γ) ^{205}Pb, ^{206}Pb (n,γ) ^{207}Pb (Hungerford, 1983) improve the accuracy and the precision of the ^{205}Pb - ^{205}Tl mass difference from $Q_3 \pm \delta Q_3 = 56.60 \pm 5.02$ keV to $Q_4 \pm \delta Q_4 = 53.27 \pm 2.06$ keV.

To obtain the best Q-value of ^{205}Pb (e.c.) ^{205}Tl, a least squares adjustment has been performed on all available atomic mass data including our new data in Table 5-1a and the reaction data in Table 5-2. These data may be represented by a set of 14 linear combinations of the atomic masses ^{204}Pb, ^{205}Pb, ^{206}Pb, ^{207}Pb, ^{208}Pb, ^{203}Tl, ^{204}Tl, ^{205}Tl and ^{206}Tl. The generalized Birge ratio R of the initial least squares adjustment (Table 5-6) is 3.31, clearly in disagreement with the value $R = 1 \pm 0.29$ expected on the basis of 6 degrees of freedom. This discrepancy results from the particular datum, p ,whose χ^2 contribution represents about 55% of the overall χ^2.

This discrepant datum represents the Q-value (Q_x) of the decay $e^- + {}^{205}\mathrm{Pb} \rightarrow {}^{205}\mathrm{Tl} + \nu$ obtained from a measurement of the intensity ratio of M shell to L shell X rays in the decay of the ground state of ^{205}Pb (Pengra, 1978). The theoretical, relative capture probabilities for the L and M shells indicate that the capture is primarily from the $p_{3/2}$ subshell (Pengra, 1978). The given value of $Q_x \pm \delta Q_x$ (41.4 ± 1.1 keV) includes a correction factor 1.02 ± 0.01 based on a comparison with the corresponding factor for the $s_{1/2}$ subshell. The decay energy $Q_x \pm \delta Q_x$ disagrees with the values $Q_1 \pm \delta Q_1, Q_2 \pm \delta Q_2, Q_3 \pm \delta Q_3, Q_4 \pm \delta Q_4$ and their weighted average $Q_{AV} \pm \delta Q_{AV}$ (Table 5-5) as shown in Fig. 5-3. $Q_x \pm \delta Q_x$ has been rejected from the 1983 Atomic Mass Evaluation (Wapstra, 1985), where it is described as well documented data inconsistent with its adjusted value $Q_{M.T} \pm \delta Q_{M.T}$ (Fig. 5-3). Accordingly, for our final least squares adjustment (Table 5-7), the input uncertainty of datum p ,was multiplied by a consistency factor equal to the square root of its χ^2 contribution (Wapstra, 1985). The generalized Birge ratio for this adjustment, R = 1.12, is greatly improved and agrees with

the expected value within the anticipated limits ($0.71 < R < 1.29$). The magnitude of R indicates the overall consistency of the data included in the adjustment. The decay energy of ^{205}Pb determined from this work (51.87 ± 0.84 keV) agrees with the 1983 Atomic Mass Evaluation value (53.5 ± 1.6 keV).

References for chapter (5)

Barkman, J. N., McFee, J. E., Kennett, T. J. & Prestwich, W. V. (1979). Z.Physik A, 289, 325.

Colenbrander, A. H. & Kennett, T. J. (1974). Can. J. Phys., 52, 1215.

Derenchuk, V. P., Ellis. R. J., Sharma. K. S., Barber, R. C. & Duckworth, H. E. (1985). Can. J. Phys., 63, 966.

Freedman, M. S., Stevens, C. M., Horwitz, E. P., Fuchs, L. M., Lerner, J. L., Goodman, L. S., Child, W. J. & Hessler, J. (1976). Science, 193, 1117.

Freedman, M. S. (1988). Proc. of the International Conference on Solar Neutrino Detection with ^{205}Tl, and Related Topics. Nucl. Instr. Meth., A271, No. 2, 267.

Hungerford, P., von Egidy, T., Schmidt, H. H., Kerr, S. A., Borner, H. G. & Monnand, E. (1983). Z. Phys.A - Atoms and Nuclei, 313, 349.

Pengra, J. G., Genz, H. & Fink, R. W. (1978). Nucl. Phys., A302, 1.

Sharma, K. S., Meredith, J. O., , Barber, R. C., Kozier, K. S., Haque, S. S., Barnard, J. W. , Southon, F. C. G., Williams, P. & Duckworth, H. E. (1977). Can. J. Phys., 55, 1360.

Southon, F. C. G., Meredith, J. O., , Barber, R. C. & Duckworth, H. E. (1977). Can. J. Phys., 55, 383.

Wapstra, A. H. & Audi, G. (1985). The 1983 Atomic Mass Evaluation, Nucl. Phys., A432, 1.

Wiesner, W., Flothmann, D. & Gils, H. J. (1972). Nucl. Phys., A191, 166.

Wolfson, J. L. & Collier, A. J. (1968). Nucl. Phys., A112, 156.

Table 5-1a

New atomic mass differences determined by the least squares method

Code	Doublet	Number of Computer runs	Weighted average $\langle X \rangle_{LSQ}$ (μu)	$(\sigma_{int})_{LSQ}$ (μu)	$(\sigma_{ext})_{LSQ}$ (μu)	Birge ratio
A	$^{208}Pb^{35}Cl$ - $^{206}Pb^{37}Cl$	9	5137.39	0.37	0.51	1.40
B	$^{206}Pb^{35}Cl$ - $^{204}Pb^{37}Cl$	25	4368.64	0.62	0.94	1.52
C	$^{207}Pb^{35}Cl$ - $^{205}Tl^{37}Cl$	10	4419.18	1.19	1.98	1.66
D	$^{205}Tl^{35}Cl$ - $^{203}Tl^{37}Cl$	8	5033.33	0.73	0.90	1.23

Table 5-1b

New atomic mass differences determined by the centroid method

Code	Doublet	Number of Computer runs	Weighted average $\langle X \rangle_{CEN}$ (μu)	$(\sigma_{int})_{CEN}$ (μu)	$(\sigma_{ext})_{CEN}$ (μu)	Birge ratio
A	$^{208}Pb^{35}Cl$ - $^{206}Pb^{37}Cl$	9	5137.00	0.54	0.72	1.32
B	$^{206}Pb^{35}Cl$ - $^{204}Pb^{37}Cl$	25	4368.81	0.49	0.86	1.74
C	$^{207}Pb^{35}Cl$ - $^{205}Tl^{37}Cl$	10	4417.52	1.28	2.24	1.75
D	$^{205}Tl^{35}Cl$ - $^{203}Tl^{37}Cl$	8	5030.91	0.74	1.42	1.92

Table 5-2

Additional data

Type	Code	Description	Q-value (keV)	Reference
Reaction data	f	^{204}Pb (n,γ) ^{205}Pb	6731.57 ± 0.15	(Hungerford, 1983)
	g	^{206}Pb (γ,n) ^{205}Pb	−8087.00 ± 3.00	(Barkman, 1979)
	h	^{206}Pb (n,γ) ^{207}Pb	6737.76 ± 0.18	(Hungerford, 1983)
	j	^{207}Pb (n,γ) ^{208}Pb	7367.90 ± 0.10	(Hungerford, 1983)
	k	^{203}Tl (n,γ) ^{204}Tl	6655.80 ± 0.30	(Colenbrander, 1974)
	l	^{205}Tl (γ,n) ^{204}Tl	−7548.00 ± 3.00	(Barkman, 1979)
	m	^{205}Tl (n,γ) ^{206}Tl	6503.40 ± 0.40	(Colenbrander, 1974)
	o	^{204}Tl (β) ^{204}Pb	763.40 ± 0.20	(Wolfson, 1968)
	p	^{205}Pb (ε) ^{205}Tl	41.40 ± 1.10	(Pengra, 1978)
	r	^{206}Tl (β) ^{206}Pb	1527.00 ± 4.00	(Wiesner, 1972)

Table 5-3

Auxiliary data *		
^{37}Cl =	36965902.619 ± 0.112	μu
^{35}Cl =	34968852.728 ± 0.069	μu
^{37}Cl - ^{35}Cl =	1997049.890 ± 0.110	μu
^{1}H =	1007825.035 ± 0.012	μu
^{2}H =	2014101.779 ± 0.024	μu
^{12}C =	12000000.000	μu
^{13}C =	13003354.826 ± 0.017	μu
^{14}N =	14003074.002 ± 0.026	μu
n =	1008664.904 ± 0.014	μu
1u =	931501.200 ± 0.300	keV

* (Wapstra, 1985)

Table 5-4

Loop Closures

Loop	Data forming the loop (Fig. 5-2)	Closure (μu)
1	A, h, j	0.41 ± 0.57
2	B, f, g	-3.01 ± 3.36
3	C, l, o, f, g, h	-2.75 ± 5.04
4	D, k, l	1.70 ± 3.36
5	A, B, o, k, D, C, j	-1.55 ± 2.46

Table 5-5

^{205}Pb decay energy (^{205}Pb-^{205}Tl mass difference) from different paths

Data forming the path (Fig. 5-2)	Q-value (keV)
f, o, l	$Q_1 \pm \delta Q_1 = 53.03 \pm 3.01$
f, o, k, D	$Q_2 \pm \delta Q_2 = 51.44 \pm 1.43$
g, r, m	$Q_3 \pm \delta Q_3 = 56.60 \pm 5.02$
f, B, h, C	$Q_4 \pm \delta Q_4 = 53.27 \pm 2.06$
Weighted average	$Q_{AV} \pm \delta Q_{AV} = 52.38 \pm 1.07$
Mass table *	$Q_{M.T} \pm \delta Q_{M.T} = 53.50 \pm 1.60$

* (Wapstra, 1985)

Table 5-6

Initial least squares adjustment

Code	Description	Input values $Y_I \pm \sigma_I$	Output values $Y_o \pm \sigma_o$	* χ_i^2	** 1983 Mass table
A	$^{208}Pb^{35}Cl$ - $^{206}Pb^{37}Cl$	5137.39 ± 0.51	5137.07 ± 0.19	0.399	5136.97 ± 0.24
B	$^{206}Pb^{35}Cl$ - $^{204}Pb^{37}Cl$	4368.64 ± 0.94	4370.21 ± 0.81	2.761	4370.30 ± 1.60
C	$^{207}Pb^{35}Cl$ - $^{205}Tl^{37}Cl$	4419.18 ± 1.98	4415.36 ± 0.97	3.728	4421.10 ± 1.80
D	$^{205}Tl^{35}Cl$ - $^{203}Tl^{37}Cl$	5033.33 ± 0.90	5036.33 ± 0.66	11.141	5031.00 ± 1.70
f	Q(^{204}Pb (n,γ) ^{205}Pb)	6731.57 ± 0.15	6731.70 ± 0.15	0.714	6731.57 ± 0.15
g	Q(^{206}Pb (γ,n) ^{205}Pb)	−8087.00 ± 3.00	−8088.22 ± 0.00	0.165	−8088.20 ± 1.50
h	Q(^{206}Pb (n,γ) ^{207}Pb)	6737.76 ± 0.18	6737.69 ± 0.17	0.137	6737.78 ± 0.18
j	Q(^{207}Pb (n,γ) ^{208}Pb)	7367.90 ± 0.10	7367.89 ± 0.10	0.013	7367.90 ± 0.10
k	Q(^{203}Tl (n,γ) ^{204}Tl)	6655.80 ± 0.30	6656.11 ± 0.29	1.081	6655.82 ± 0.30
l	Q(^{205}Tl (γ,n) ^{204}Tl)	−7548.00 ± 3.00	−7543.31 ± 0.67	2.444	−7548.50 ± 1.50
m	Q(^{205}Tl (n,γ) ^{206}Tl)	6503.40 ± 0.40	6503.50 ± 0.82	0.058	6503.50 ± 0.40
o	Q(^{204}Tl (β) ^{204}Pb)	763.40 ± 0.20	763.56 ± 0.20	0.636	763.41 ± 0.20
p	Q(^{205}Pb (ε) ^{205}Tl)	41.40 ± 1.10	48.05 ± 0.67	36.583	53.50 ± 1.60
r	Q(^{206}Tl (β) ^{206}Pb)	1527.00 ± 4.00	1536.67 ± 1.03	5.841	1531.20 ± 1.60

A, B, C and D are in (μ*u*) ; f, g, h, j, k, l, m, o, p and r are in (keV)

* $\chi_i^2 = \left(\frac{Y_I - Y_o}{\sigma_I}\right)^2$; ** (Wapstra, 1985)

Table 5-7

Final least squares adjustment

Code	Description	Input values $Y_I \pm \sigma_I$	Output values $Y_o \pm \sigma_o$	* χ_i^2	** 1983 Mass table
A	$^{208}Pb^{35}Cl$ - $^{206}Pb^{37}Cl$	5137.39 ± 0.51	5137.05 ± 0.19	0.456	5136.97 ± 0.24
B	$^{206}Pb^{35}Cl$ - $^{204}Pb^{37}Cl$	4368.64 ± 0.94	4369.41 ± 0.82	0.670	4370.30 ± 1.60
C	$^{207}Pb^{35}Cl$ - $^{205}Tl^{37}Cl$	4419.18 ± 1.98	4418.51 ± 1.05	0.116	4421.10 ± 1.80
D	$^{205}Tl^{35}Cl$ - $^{203}Tl^{37}Cl$	5033.33 ± 0.90	5032.92 ± 0.79	0.208	5031.00 ± 1.70
f	Q(^{204}Pb (n,γ) ^{205}Pb)	6731.57 ± 0.15	6731.58 ± 0.15	0.005	6731.57 ± 0.15
g	Q(^{206}Pb (γ,n) ^{205}Pb)	−8087.00 ± 3.00	−8089.07 ± 0.00	0.477	−8088.20 ± 1.50
h	Q(^{206}Pb (n,γ) ^{207}Pb)	6737.76 ± 0.18	6737.71 ± 0.17	0.063	6737.78 ± 0.18
j	Q(^{207}Pb (n,γ) ^{208}Pb)	7367.90 ± 0.10	7367.89 ± 0.10	0.015	7367.90 ± 0.10
k	Q(^{203}Tl (n,γ) ^{204}Tl)	6655.80 ± 0.30	6655.76 ± 0.30	0.020	6655.82 ± 0.30
l	Q(^{205}Tl (γ,n) ^{204}Tl)	−7548.00 ± 3.00	−7546.83 ± 0.82	0.151	−7548.50 ± 1.50
m	Q(^{205}Tl (n,γ) ^{206}Tl)	6503.40 ± 0.40	6503.47 ± 0.83	0.028	6503.50 ± 0.40
o	Q(^{204}Tl (β) ^{204}Pb)	763.40 ± 0.20	763.39 ± 0.20	0.005	763.41 ± 0.20
p	Q(^{205}Pb (ε) ^{205}Tl)	41.40 ± 6.65	51.87 ± 0.84	2.475	53.50 ± 1.60
r	Q(^{206}Tl (β) ^{206}Pb)	1527.00 ± 4.00	1533.74 ± 1.10	2.837	1531.20 ± 1.60

A, B, C and D are in (μu) ; f, g, h, j, k, l, m, o, p and r are in (keV)

* $\chi_i^2 = \left(\frac{Y_I - Y_o}{\sigma_I}\right)^2$; ** (Wapstra, 1985)

FIGURE 5-1

Comparison of our new data (●) with our previous data (∗) (Derenchuk, 1985) and the mass table values (■) (Wapstra, 1985)

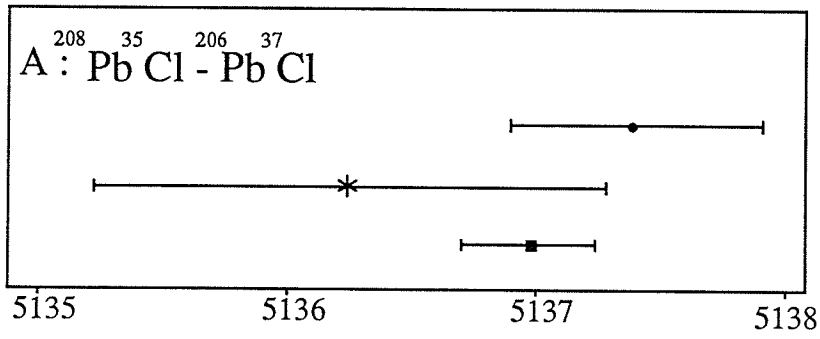

μu

5137.39± 0.51

5136.23 ± 1.08

5136.97 ± 0.24

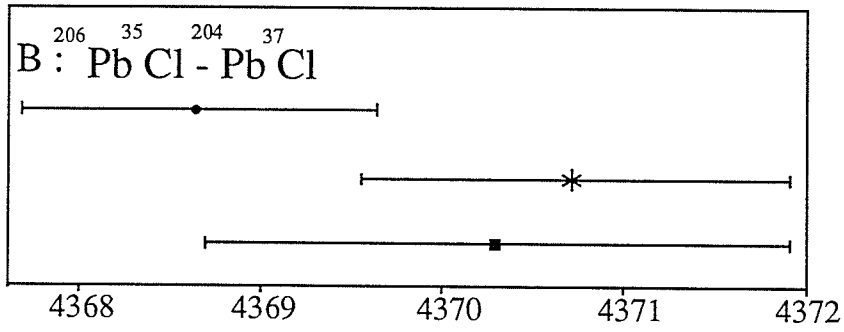

4368.64 ± 0.94

4370.72 ± 1.17

4370.30 ± 1.60

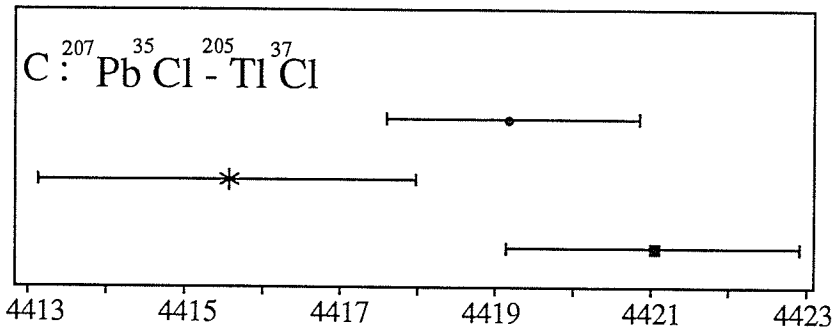

4419.18 ± 1.98

4415.60 ± 2.40

4421.10 ± 1.80

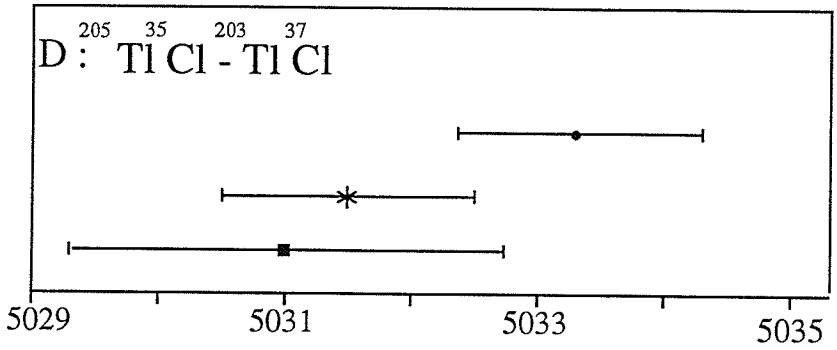

5033.33 ± 0.90

5031.43 ± 1.07

5031.00 ± 1.70

FIGURE 5-2

Schematic diagram of the input data

Naturally occurring nuclides are indicated by solid bars. Different types of input data are used :

Mass doublets : A, B , C , D

(n,γ) reactions : j , h , f , m , k

(γ,n) reactions : g , l

β decays : r , o

electron capture : p

The uncertainty associated with each datum is shown within a circle. For the special case of datum p, the input uncertainty shown ($*$) in this figure is multiplied by a consistency factor which increases this value to 6.65 keV (Table 5-7).

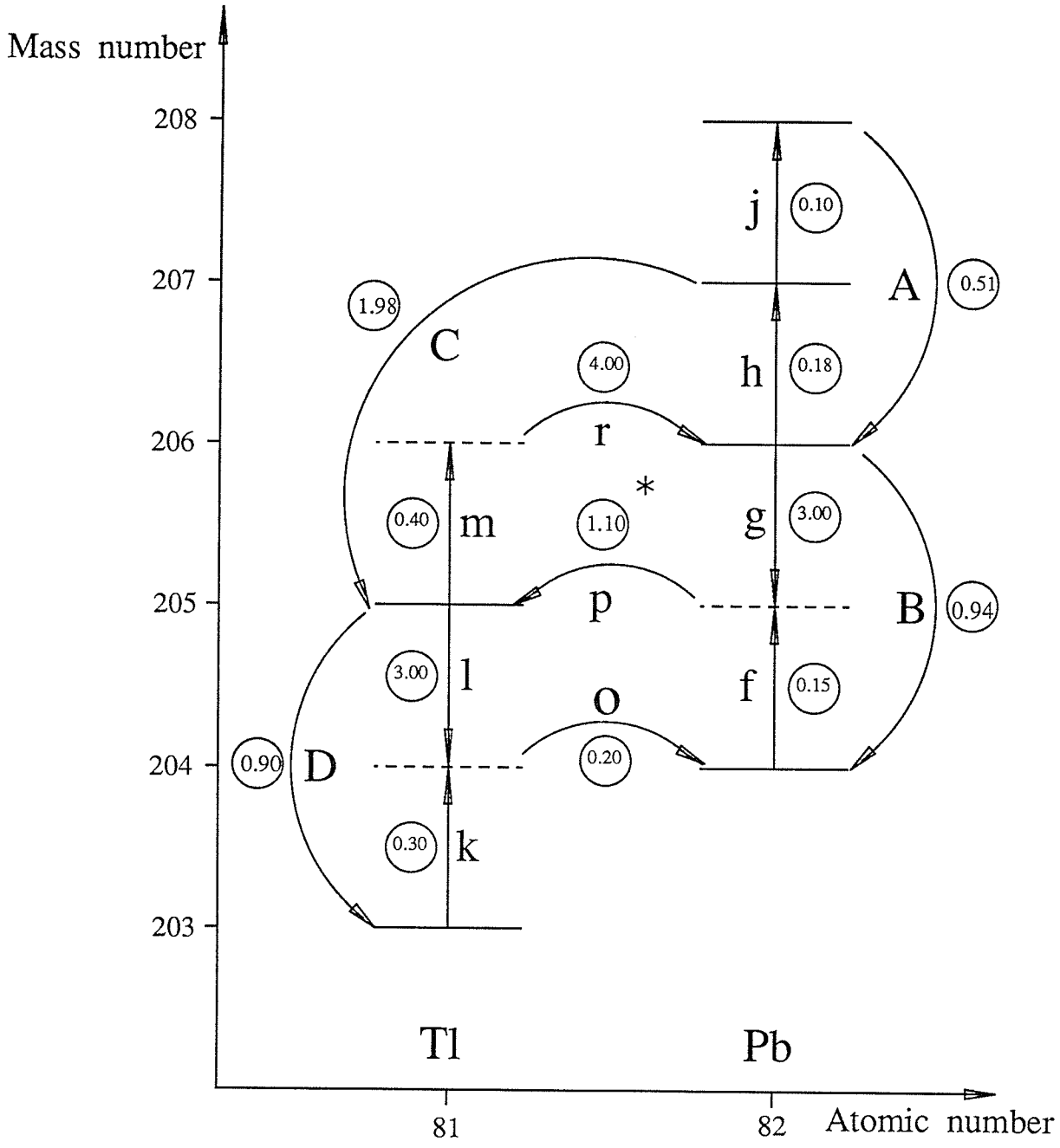
Mass number
208
207
206
205
204
203
j
0.10
A
0.51
1.98
C
4.00
h
0.18
r
*
0.40
m
1.10
g
3.00
p
B
0.94
3.00
l
f
0.15
o
0.90
D
0.20
0.30
k
Tl
Pb
81
82
Atomic number

FIGURE 5-3

Comparison between the ^{205}Pb - ^{205}Tl mass difference values calculated from input data involving : mass doublets, (n,γ), (γ,n) reactions and β decays with other values obtained from X-ray measurements and the 1983 Atomic Mass Evaluation.

Q_1, Q_2, Q_3 and Q_4 are different values of the ^{205}Pb - ^{205}Tl mass difference (electron capture Q-value for ^{205}Pb) calculated from different paths of the schematic diagram (Fig. 5-2). Q_{AV} is the weighted average of Q_1, Q_2, Q_3 and Q_4. The decay energy of ^{205}Pb obtained from the 1983 mass table $Q_{M.T}$ (●) and X-ray measurements Q_X (■) are shown.

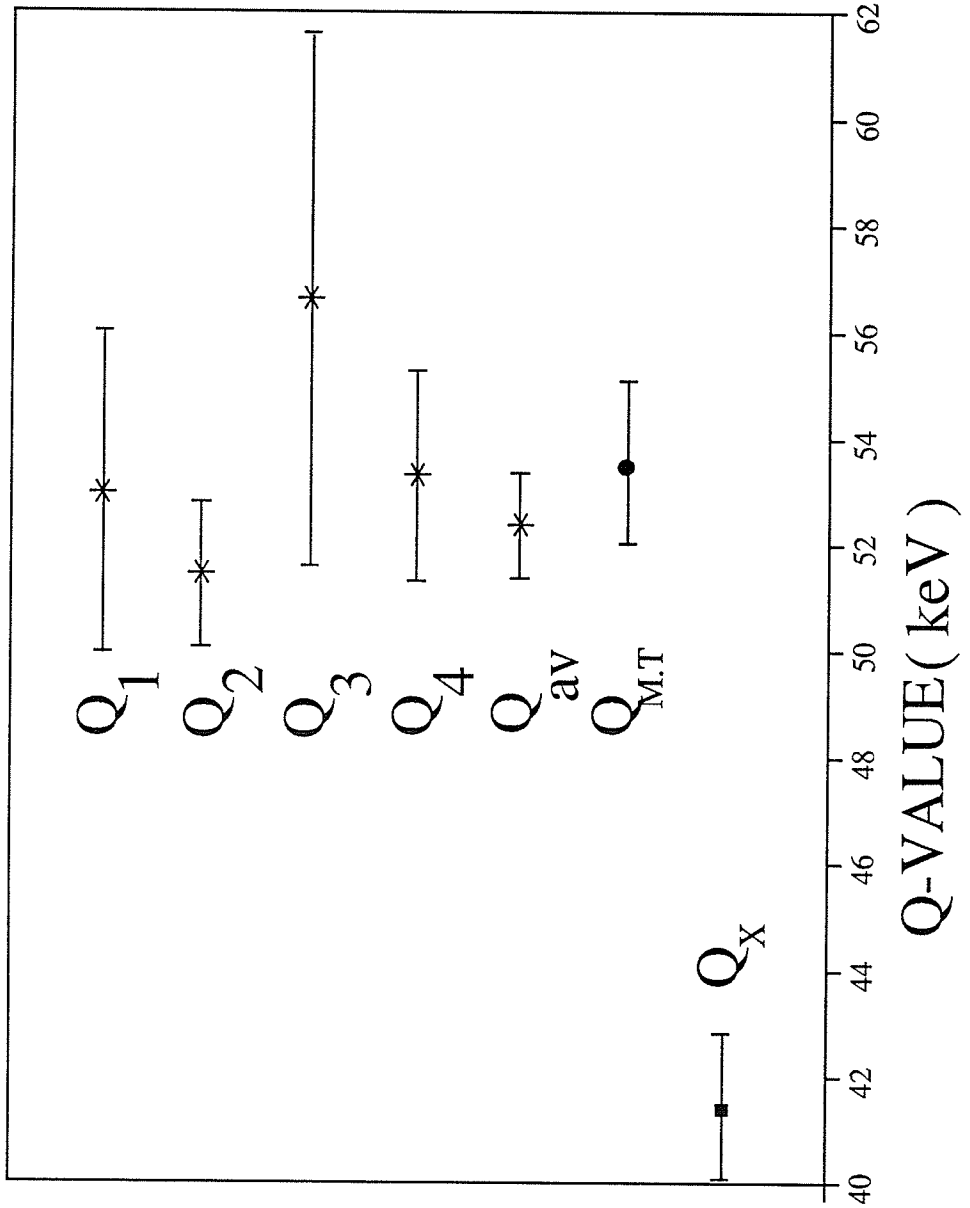
Q-VALUE(keV)
40
42
44
46
48
50
52
54
56
58
60
62
Q_X
$Q_{M.T}$
Q_{av}
Q_4
Q_3
Q_2
Q_1

CHAPTER (6)

SIGNIFICANCE OF THE NEW ATOMIC MASS DIFFERENCES

6-1 Introduction

Most scientists believe that we understand the process by which the sun's heat is produced -- that is , in thermonuclear reactions that fuse light elements into heavier ones, thus converting mass into energy. However, no one has found an easy way to test the extent of our understanding because the sun's thermonuclear furnace is deep in the interior, where it is hidden by an enormous mass of cooler material (Bahcall, 1976). It is assumed that the sun shines because of fusion reactions similar to those envisioned for terrestrial fusion reactors. These reactions produce neutrinos which have the ability to penetrate from the solar interior to the surface and escape to space. Thus, detection of solar neutrinos on Earth represents a direct and quantitative way to test the theory of nuclear energy generation in the sun.

Davis et al (Davis, 1968) carried out an experiment at the Homestake Mine in Lead, South Dakota to detect solar neutrinos. This experiment was based on the neutrino capture reaction : $\nu + {}^{37}Cl \rightarrow {}^{37}Ar + e^-$ which has a threshold energy of 820 keV. This reaction excludes a large portion of the solar neutrino spectrum. The measured ^{37}Ar production rate above background was 0.38 ± 0.05 atoms/day (Rowley, 1985). On the other hand, the standard solar model predicts a ^{37}Ar production rate of 1.1 ± 0.4 atoms/day (Bahcall, 1985). It would be desirable to check this result with a more appropriate detection mechanism. For this reliability check we would need another neutrino capture reaction which has :

(i) a low energy threshold, $\ll$ 400 keV, to gain sensitivity to the intense neutrinos produced in the (proton-proton) reaction (Bahcall, 1976);

(ii) an adequate and well known capture cross section;

(iii) a very long product half-life, so that the product would have accumulated and have been retained in a suitable target mineral over geologic time; but less than 10^8 years, so that it would not have survived from primordial generation; and

(iv) tolerable yields of competing reactions giving the same product in situ (Freedman, 1976).

These requirements are satisfied by the reaction : $\nu + {}^{205}Tl \rightarrow {}^{205}Pb + e^-$ which has a threshold energy of 51.87 ± 0.84 keV (this work).

6-2 The feasibility of the geochemical ^{205}Pb solar neutrino experiment

The neutrino capture in ^{205}Tl : $\nu + {}^{205}Tl \rightarrow {}^{205}Pb + e^-$ yields the $1/2^-$ excited state of ^{205}Pb. This reaction, is followed by a fast isomeric decay to the $5/2^-$ ground state of ^{205}Pb (Fig. 6-1). The electron capture decay of the ground state of ^{205}Pb (half-life is 16-million year) effectively traps the neutrino capture event. A probably suitable thallium ore, lorandite (Tl As S_2), is found in the Alshar mine in Yugoslavia (Freedman, 1976). The microscopic, neutrino-induced, quantities of ^{205}Pb atoms could be detected via accelerator mass spectrometry (AMS) to determine the neutrino-induced transition probabilities. For 100 detected events one million ^{205}Pb atoms are needed for the ion source sample assuming that an ion source efficiency times the transmission probability ~10^{-4} is possible. This requirement corresponds to about 11 mg of lead, representing about 7.6 kg of lorandite, or about 1.1 ton

of mined ore. These numbers are minimum quantities for one single run (Ernst, 1986).

The transition probability can be determined using completely stripped $^{205}Tl^{81+}$ decaying into the K shell of ^{205}Pb (Fig. 6-1). The SIS 18 synchrotron facility together with the experimental storage ring ESR associated with the UNILAC in Darmstadt, which are under construction, offer the possibility to generate bare $^{205}Tl^{81+}$, to store them and to study their beta decay into the K shell by measuring the number of ^{205}Pb ions produced.

The amount of the cosmic-ray-induced background reaction ^{205}Tl (p,n) ^{205}Pb can be estimated by determining the depth of the mine over the last ten million years. This can be done by measuring with AMS the μ^- induced content of radioisotopes (Kubik, 1984) in the region of the Alshar mine and by comparing these contents with reference measurements.

6-3 Proposal for ^{205}Tl solar neutrino detector

^{205}Tl has been proposed to be a solar neutrino detector. The purpose of this proposal is to measure the neutrino capture cross section, $\sigma(E_\nu, Q_{ec})$, of the reaction :

$$\nu + {}^{205}Tl^{0} \rightarrow {}^{205}Pb^{1+} + e^{-} \qquad (6\text{-}1)$$

$\sigma(E_\nu, Q_{ec})$ is given by (Freedman, 1988) :

$$\sigma(E_\nu, Q_{ec}) = 5.14 \times 10^{-41}(E_\nu - Q_{ec} + 0.511)\frac{\sqrt{(E_\nu - Q_{ec} + 0.511)^2 - (0.511)^2}}{(ft)_{ec}} \quad cm^2 \qquad (6\text{-}2)$$

where :

E_ν : neutrino energy in MeV,

Q_{ec} : the electron capture Q-value of the $1/2^-$ excited state of ^{205}Pb and

$(ft)_{ec}$: ft value of the orbital electron capture decay of the 1/2$^-$ excited state of ^{205}Pb.

Q_{ec} is determined in terms of the electron capture decay energy Q_{EC} of the 5/2$^-$ ground state of ^{205}Pb and the excitation energy E_{exc} of the 1/2$^-$ excited state (Fig. 6-1) :

$$Q_{ec} = Q_{EC} + E_{exc} \tag{6-3}$$

$(ft)_{ec}$ is expressed in terms of the nuclear matrix element M_{ec} as :

$$(ft)_{ec} \propto 1/M_{ec}^2 \tag{6-4}$$

The neutrino capture in atomic ^{205}Tl (reaction 6-1) explores the same nuclear wave functions of initial and final states as does the beta decay of the nucleus $^{205}Tl^{81+}$:

$$^{205}Tl^{81+} \rightarrow {}^{205}Pb^{81+} + \bar{\nu} \tag{6-5}$$

Therefore, the nuclear matrix elements M_{ec}, M_β of reactions (6-1), (6-5) are the same ($M_{ec} = M_\beta$). The production rate R_β of $^{205}Pb^{81+}$ of reaction (6-5) is related to M_β by :

$$R_\beta \propto M_\beta^2 \tag{6-6}$$

Equations (6-4) and (6-6) yield the following relation (Freedman, 1988) :

$$M_{ec}^2 = M_\beta^2 = R_\beta(ions/\sec.) \times 7.77 \times 10^{-3}/2.06 = 6170/(ft)_{ec} \tag{6-7}$$

Using the relations (6-3) and (6-7), eqn. (6-2) can be written in the form :

$$\sigma(E_\nu, Q_{EC}) = 0.87 \times 10^{-50} R_\beta (E_\nu - Q_{EC} - E_{exc} + 0.511)\sqrt{(E_\nu - Q_{EC} - E_{exc} + 0.511)^2 - (0.511)^2} \quad cm^2 \tag{6-8}$$

where : R_β is measured in (ions/hour) and E_ν, Q_{EC}, E_{exc} are in (MeV)

The threshold energy E_{th} of reaction (6-1) can be determined from (6-8) to be :

$$E_{th} = Q_{EC} + E_{exc} \tag{6-9}$$

Thus, measuring the rate of accumulation R_β of $^{205}Pb^{81+}$ in reaction (6-5) gives directly the cross section $\sigma(E_\nu, Q_{EC})$ of reaction (6-1). The current value of the uncertainty δQ_{EC} is less than 2.0 keV so that the contribution of that error can be neglected with respect to E_ν in eqn. (6-8). Thus :

$$\delta\sigma(E_\nu, Q_{EC})/\sigma(E_\nu, Q_{EC}) = \delta R_\beta / R_\beta \qquad (6\text{-}10)$$

In reaction 6-5, the production rate R_β of $^{205}Pb^{81+}$ is calculated in terms of the decay energy Q_β of that decay (Freedman, 1988) :

$$R_\beta \propto Q_\beta^2 \qquad (6\text{-}11)$$

Q_β is determined in terms of the atomic mass difference between $^{205}Tl^0$ and $^{205}Pb^0$ which represents the electron capture decay energy Q_{EC} of the $^{205}Pb^0$ ground state. From conservation of energy in Fig. 6-1 :

$$Q_\beta + Q_{EC} = (B.E.)_{Tl} - (B.E.)_{Pb} - E_{exc} + (B.E.)_{1s} \qquad (6\text{-}12a)$$

where :

$(B.E.)_{Tl}$ = 551.0 keV (Desclaux, 1973)

$(B.E.)_{Pb}$ = 568.3 keV (Desclaux, 1973)

$(B.E.)_{1s}$ = 101.4 keV (Johnson, 1985)

E_{exc} = 2.3 keV (Schmorak, 1978)

$$Q_\beta + Q_{EC} = 81.8 \quad keV \qquad (6\text{-}12b)$$

Substituting from (6-12b) in (6-11) :

$$R_\beta \propto (81.8 - Q_{EC})^2 \qquad (6\text{-}13)$$

The error δR_β which arises from the uncertainty of the electron capture decay Q-value, δQ_{EC}, is given by :

$$\delta R_\beta / R_\beta = 2\delta Q_{EC}/(81.8 - Q_{EC}) \qquad (6\text{-}14)$$

6-4 Results and discussion

It is interesting to calculate the relative uncertainty $\delta R_\beta / R_\beta$ (eqn. 6-14) and see the variation of the production rate R_β with the electron capture decay Q-value, Q_{EC} (eqn. 6-13). δR_β and R_β are calculated for several values of Q_{EC} obtained from different sources with one of them being the value determined by our group for the electron capture decay Q-value for the ground state of ^{205}Pb. The calculations have been carried out using a given value of R_β (Freedman, 1988). The results of these calculations are presented in Table 6-1 and are shown in Fig. 6-2.

The substantional improvement in the precision of Q_{EC} achieved by our group (δQ_{EC} = 0.84 keV) in comparison with the precision (δQ_{EC} = 1.6 keV) obtained from the 1983 Atomic Mass Evaluation (Wapstra, 1985) reduces the uncertainty δR_β in the production rate R_β by a factor of about 2. The cross section uncertainty is expected to be improved by the same factor (see eqn. 6-10). The Q_{EC} obtained from X-ray measurement (Pengra, 1978) is lower than the adjusted value of our group by 10.48 keV; this reduction increases the production rate R_β by about 80%.

The cross section $\sigma(E_\nu, Q_{EC})$ is calculated from eqn. 6-8 for a range of neutrino energies ($E_{th} \le E_\nu \le 0.41 MeV$). The calculations are plotted for two different values of Q_{EC} (^{205}Pb -

^{205}Tl mass difference) in Fig. 6-3. This figure shows the sensitivity of the cross section to the accuracy of the ^{205}Pb - ^{205}Tl mass difference. For a neutrino energy E_ν, the reduction of the mass difference by 10.48 keV increases the cross section by a factor of about 1.85.

References for chapter (6)

Bahcall, J. N. & Davis, R., Jr. (1976). Science, 191, 264.

Bahcall, J. N. (1985). Solar Neutrinos and Neutrino Astronomy (Homestake, 1984), AIP Conf. Proc., 126, 60.

Davis, R., Jr. (1968). Phys. Rev. Lett., 20, 1205.

Desclaux, J.-P. (1973). ADNDT, 12, 311.

Ernst, H., Korschinek, G., Kubik, P., Mayer, W., Morinaga, H., Nolte, E., Ratzinger, U., Henning, W., Kutschera, W., Muller, M. & Schull, D. (1986). Proceedings of the international symposium, Osaka, Japan, ed. by T. Kotani, H. Ejiri & E. Takasugi, p.452 (Nuclear beta decays and neutrino World Scientific, Singapore, 1986).

Freedman, M. S., Stevens, C. M., Horwitz, E. P., Fuchs, L. M., Lerner, J. L., Goodman, L. S., Child, W. J. & Hessler, J. (1976). Science, 193, 1117.

Freedman, M. S. (1988). Proc. of the International Conference on Solar Neutrino Detection with ^{205}Tl, and Related Topics. Nucl. Instr. Meth., A271, No. 2, 267.

Kubik, P., Korschinek, G., Nolte, E., Ratzinger, U., Ernst, H., Teichmann, S., Morinaga, H., Wild, E. & Hille, P. (1984). Nucl. Instr. and Meth. B, 5, 326.

Johnson, W. R. & Soff, G. (1985). At. Data Nucl. Data Tables, 33, 405.

Pengra, J. G., Genz, H. & Fink, R. W. (1978). Nucl. Phys. A, 302, 1.

Rowley, J. K. (1985). Solar Neutrinos and Neutrino Astronomy (Homestake, 1984), AIP Conf. Proc., 126, 1.

Schmorak, M. R. (1978). Nucl. Data Sheets, 23, 287.

Wapstra, A. H. & Audi, G. (1985). The 1983 Atomic Mass Evaluation, Nucl. Phys. A, 432, 1.

Table 6-1

The production rate ($R_\beta \pm \delta R_\beta$) of Pb^{81+} ions calculated for three values of the electron capture decay energy ($Q_{EC} \pm \delta Q_{EC}$) (^{205}Pb - ^{205}Tl atomic mass difference)

$Q_{EC} \pm \delta Q_{EC}$ (keV)	$\frac{\delta Q_{EC}}{Q_{EC}}$	$R_\beta \pm \delta R_\beta \times 10^3 (ions/hour)$ (eqn. 6-13)	$\frac{\delta R_\beta}{R_\beta}$ (eqn. 6-14)
$53.50 \pm 1.60^{a)}$	2.99 %	$3.640^{d)} \pm 0.412$	11.31 %
$41.40 \pm 1.10^{b)}$	2.66 %	7.418 ± 0.404	5.45 %
$51.87 \pm 0.84^{c)}$	1.62 %	4.071 ± 0.228	5.61 %

a) : (Wapstra, 1985)

b) : (Pengra, 1978)

c) : (This work)

d) : (Freedman, 1988)

FIGURE 6-1

Energetics of ^{205}Tl - ^{205}Pb

$\_1/2^+$: ground state of $^{205}Tl^0$

$\_1/2^-$: excited state of $^{205}Pb^0$

$\_5/2^-$: ground state of $^{205}Pb^0$

$(B.E.)_{Tl}$: Total electronic binding energy of the 81 electrons in $^{205}Tl^0$

$(B.E.)_{Pb}$: Total electronic binding energy of the 82 electrons in $^{205}Pb^0$

$(B.E.)_{1s}$: Hydrogenic, 1s, binding energy in $^{205}Pb^{81+}$

Q_{ec} : Q-value of the electron capture decay ($\leftarrow - - -$) of the $1/2^-$ excited state of $^{205}Pb^0$ to the $1/2^+$ ground state of $^{205}Tl^0$ (inverse reaction of $\nu + {}^{205}Tl \rightarrow {}^{205}Pb + e$)

Q_{EC} : Q-value of the electron capture decay ($\leftarrow \cdots \cdot$) of the $5/2^-$ ground state of $^{205}Pb^0$ to the $1/2^+$ ground state of $^{205}Tl^0$ (first forbidden transition)

E_{exc} : excitation energy of the $1/2^-$ excited state

$1/2^-$ / $5/2^-$: isomeric decay of the $1/2^-$ excited state of $^{205}Pb^0$ to the $5/2^-$ ground state of $^{205}Pb^0$

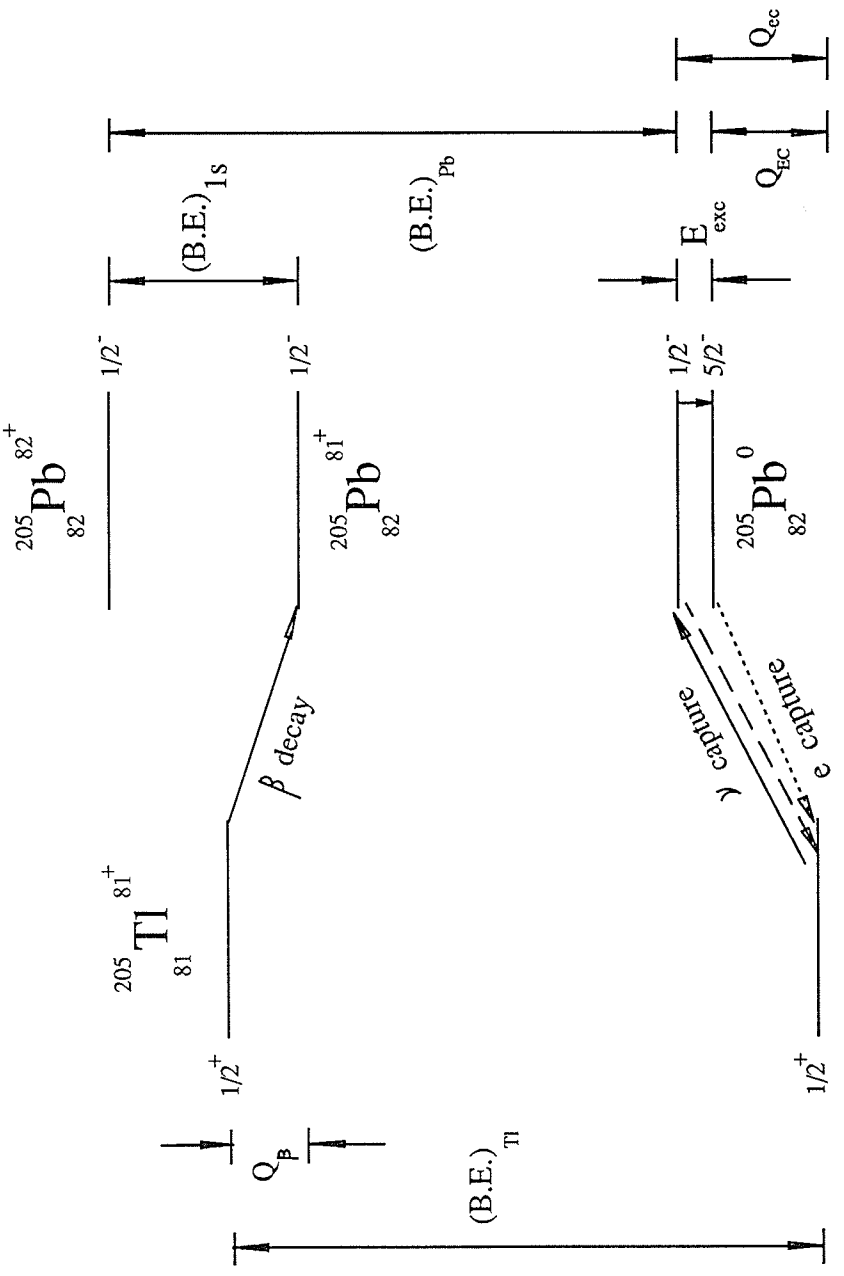
$^{205}_{82}Pb^{82+}$
$^{205}_{81}Tl^{81+}$
$^{205}_{82}Pb^{81+}$
$^{205}_{82}Pb^{0}$
$^{205}_{81}Tl^{0}$
1/2+
1/2-
5/2-
(B.E.)Tl
(B.E.)1s
(B.E.)Pb
Q_β
E_{exc}
Q_{EC}
Q_{ec}
β decay
γ capture
e capture

FIGURE 6-2

Variation of the production rate of ^{205}Pb ions produced from the β decay of ^{205}Tl ions with the Q-value Q_{EC} of the reaction : e + ^{205}Pb → ^{205}Tl + ν. Q_{EC} represents the atomic mass difference ^{205}Pb -^{205}Tl assuming that ^{205}Pb and ^{205}Tl are in their ground states (Fig. 6-1). Three values of this mass difference obtained from different sources are shown with the corresponding values of the production rate :

..... : X-ray measurements (Pengra, 1978)

___ : This work

- - - : 1983 Mass Table (Wapstra, 1985)

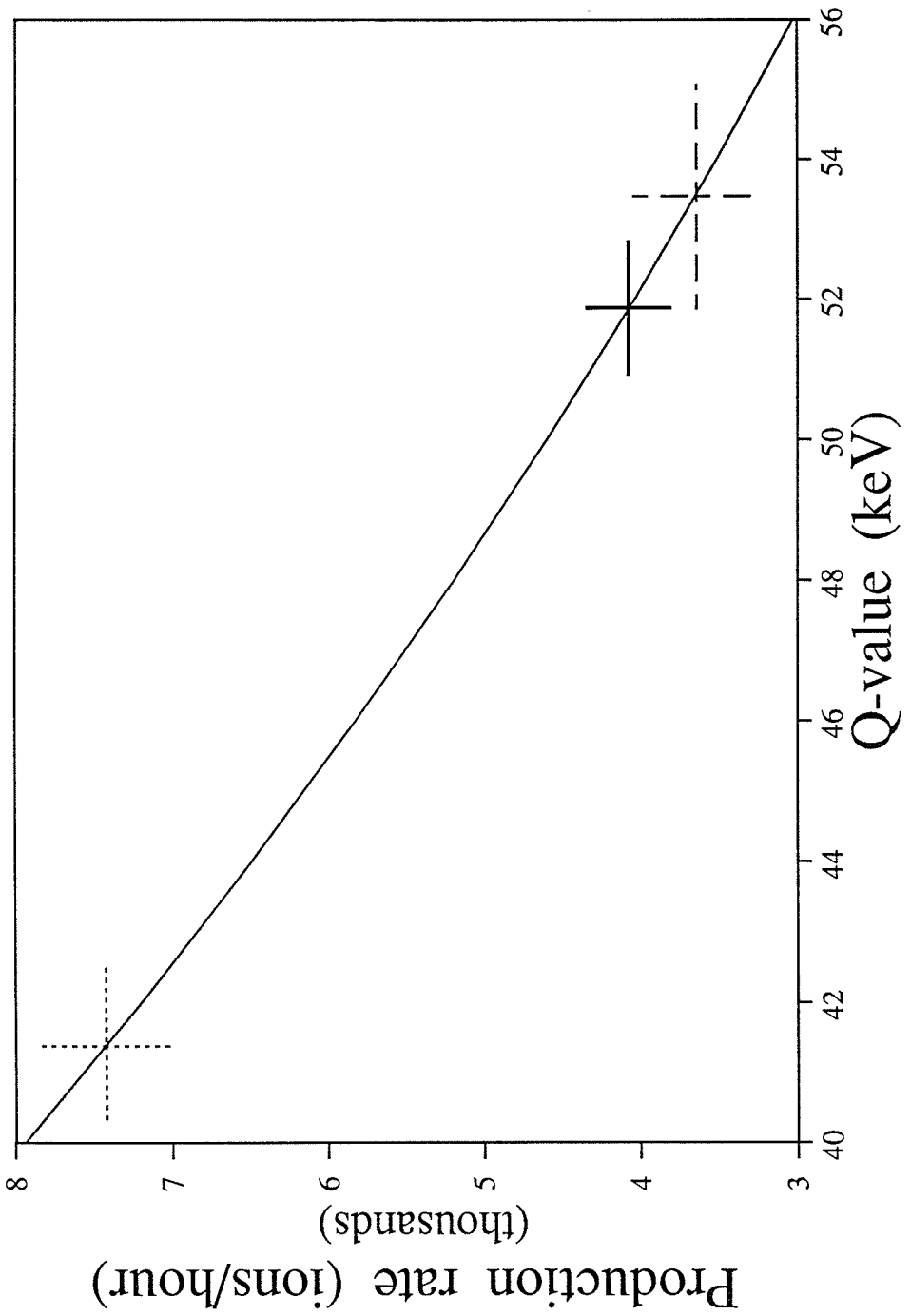
Production rate (ions/hour)
(thousands)
8
7
6
5
4
3
Q-value (keV)
40
42
44
46
48
50
52
54
56

FIGURE 6-3

Variation of the neutrino capture cross section $\sigma(E_\nu, Q_{EC})$ of the reaction $\nu + {}^{205}Tl \rightarrow {}^{205}Pb + e$ with the neutrino energy E_ν for two values of the Q-value Q_{EC} (the atomic mass difference ${}^{205}Pb - {}^{205}Tl$). The threshold energy E_{th} of the reaction $\nu + {}^{205}Tl \rightarrow {}^{205}Pb + e$ is determined in terms of Q_{EC} (eqn. 6-9) to be :

(1) 43.7 keV (■) based on X-ray measurements

(2) 54.17 keV (●) based on this work

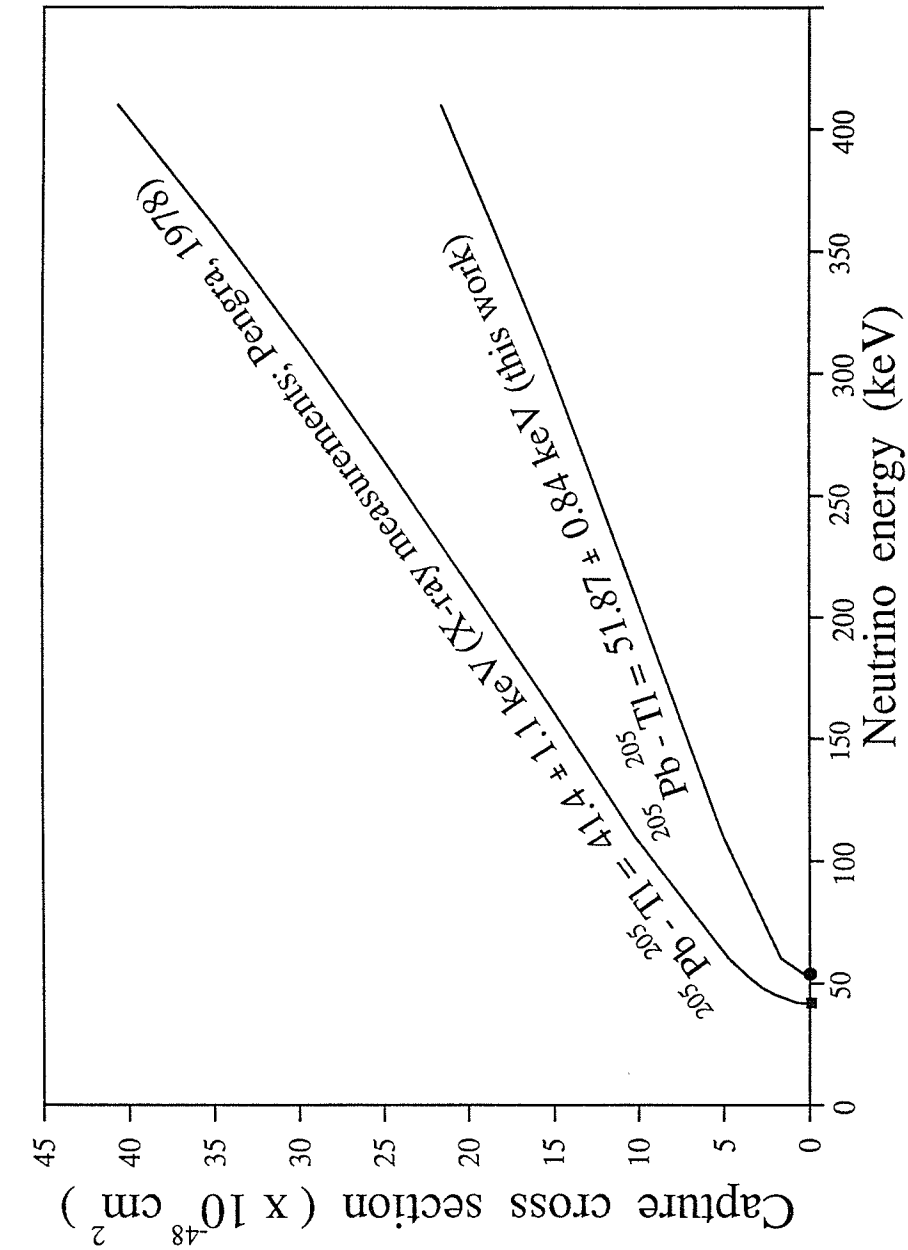
Capture cross section (x 10^{-48} cm^2)
Neutrino energy (keV)
0
5
10
15
20
25
30
35
40
45
0
50
100
150
200
250
300
350
400
^{205}Pb - ^{205}Tl = 41.4 ± 1.1 keV (X-ray measurements; Pengra, 1978)
^{205}Pb - ^{205}Tl = 51.87 ± 0.84 keV (this work)

APPENDIX A

A-1 COMPUTER PROGRAM FOR THE DATA ANALYSIS

```
000001 C*********************************************************************
000002        PROGRAM RESANAL
000003 C*********************************************************************
000004 C       This program came on cards from ancient times, passed down from
000005 C       generation to generation, mutating each time. It is now a monster.
000006 C       30nov88 - save and recall MARKS.
000007 C       28FEB89 - Make everything implicit double precision.
000008 C                 Change all SQRT to DSQRT, FLOAT to DFLOAT, ABS to DABS.
000009 C       1mar89 - Change output file slightly - add a few more digits
000010 C                here and there, since we now use REAL*8.
000011 C       5may89 - change NPS to 11 from 41. This is the number of points used
000012 C                to fit a parabola to the chi-squared values for the least
000013 C                squares match of two peaks. Was set to 41 in the past to
000014 C                eliminate upside down parabolas that came from matching peaks
000015 C                of very different intensities. With most peaks, chi-squared
000016 C                values are very smooth, and 11 points gives a good fit. With
000017 C                41 points, we were fitting to the sides of the chi curve rather
000018 C                than the base, getting a minimum that was displaced by 3
000019 C                channels or so from the true minimum.
000020 C       22jan90- Made a number of small changes. Took out fixed default marks
000021 C                and inserted routine AUTOMARKSCALE which makes good marks if
000022 C                there are no old ones and sets the scale factor for the peaks
000023 C                too. Also fixed use of GERASE when re-plotting - faster, even
000024 C                though everything has to be re-drawn. Added 'goto mark' option
000025 C                to XHAIR and hopefully bullet-proofed it a bit.
000026 C       24jan90- Get 0/1 display/auto flag from file.
000027 C                Get NPS, number of points for parabolic fit from file with
000028 C                logical name PEAKPARM. Get FSET for auto marks from
000029 C                samefile. Should have line in calling .COM file like:
000030 C                      $ ASSIGN/USER peakparam.dat PEAKPARM
000031 C                First line of data file is ignored, then flag IDL, then
000032 C                integer NPS on  next line, then FACTOR on fourth line.
000033 C*********************************************************************************
000034
000035       IMPLICIT REAL*8 (A-H),(O-Z)
000036       REAL*8 VEE,EMLT,EMHV,FSET
000037       INTEGER OUT,OOT,ISC(2)
000038       CHARACTER DUMCH*1
000039       DIMENSION VDM(4,1024),CHA(1024),XMOM(4),PP(4),SG(4),DLV(3),
000040      &          NIONS(4),CS(3),ES(3),EDV(3),DLTM(8),ERDM(8),RP05(20)
000041       DIMENSION DELEM(20),EDELEM(20),DLTEM(20),EDLTEM(20),DIFC(3),RC(3)
000042       DIMENSION PWC(4),VMAXC(4),VMAXR(4),VAR(4,1024),SV(1024),VCH(1024)
000043       DIMENSION A(4,1024),SH(3),ESH(3),DLTM2(8),ERDM2(8),ASM(4,1024)
000044       DIMENSION DLTEM2(20),EDLTM2(20),DELEM2(20),ERDLM2(20),VSM(1024)
000045       DIMENSION AVRT1(20),ERRT1(20),AVRT2(20),ERRT2(20),VRW(1024)
000046       DIMENSION RAT1(8),RAT2(8),XS2(8),AVXS2(20),ERXS2(20)
000047       DIMENSION MARKS(4,2)
000048       DIMENSION IDATA(4096), ID(4)
000049 C
000050       DOUBLE PRECISION AVE
000051       LOGICAL QUIT
000052 C
000053       COMMON /DATA_A/ IDATA, ILIN, QUIT,ID
000054       COMMON /DATA_B/ MARKS,FSET
000055       COMMON / DATA_C / ISC
000056 ********************************************************************************
000057        WRITE(6,*) 'Welcome to RESANAL.'
000058        ISC(1) = -4
000059        ISC(2) = -4
000060        INP=8
000061        OUT=9
000062        OOT=10
000063        IOT=OUT
000064        OPEN(UNIT=INP,FILE='D.ANALYZE',STATUS='OLD',READONLY)
000065        OPEN(UNIT=OUT,FILE='R.ANALYZE',STATUS='UNKNOWN')
000066        OPEN(UNIT=OOT,FILE='D.ALTERED',STATUS='NEW')
000067        OPEN(UNIT=7,FILE='PEAKPARM',STATUS='OLD')
000068 C        ISMTH IS SMOOTHING CODE .
000069 C              0   NO SMOOTHING
000070 C              1   A NINE POINT SMOOTHING IS USED FOR THE BASE-LINE ANALYSIS
000071 C                  AND FOR THE PEAK ANALYSIS.
000072 C              2   A FIVE POINT MOVING AVERAGE IS USED TO SMOOTH .
```

```
000073 |C              3   A NINE POINT SMOOTHING IS USED FOR THE BASE-LINE ANALYSIS.
000074 |C              4   A NINE POINT SMOOTHING IS USED FOR THE PEAK ANALYSIS.
000075 |C       PCB IS THE PERCENT CUT-OFF FOR THE BASE-LINE ANALYSIS .
000076 |      ISMTH = 4
000077 |      NIQ=1024
000078 |      NCPS = 8
000079 |      PCB = 5.0
000080 |      PC  = 20.0              ! Percent cut off of peak height for centroid.
000081 |C*************************************************************************
000082 |C      WRITE(6,*) 'Enter number of pts for parabolic fit ',
000083 |C     *'(11 or more is good):'
000084 |C      READ (5,*) NPS          ! see 5may89.
000085 |C*************************************************************************
000086 |       READ(7,900) DUMCH
000087 |900    FORMAT(A)
000088 |       READ(7,*) IDL   !0 for display, 1 for auto.
000089 |       READ(7,*) NPS
000090 |       IF(NPS.LE.0)THEN
000091 |         WRITE(*,*) 'NPS value from file PEAKPARM too small:',NPS
000092 |         WRITE(*,*) 'Reset to 11.'
000093 |         NPS = 11
000094 |       END IF
000095 |       IF(MOD(NPS,2).EQ.0)THEN
000096 |         WRITE(*,*) 'NPS value from file PEAKPARM was even:',NPS
000097 |         WRITE(*,*) 'For symmetrical smoothing, it must be odd.'
000098 |         WRITE(*,*) 'Reset to',NPS+1
000099 |         NPS = NPS + 1
000100 |       END IF
000101 |       READ(7,*) FSET
000102 |       IF(FSET.LE.0)THEN
000103 |         WRITE(*,*) 'FSET value from file PEAKPARM too small:',FSET
000104 |         WRITE(*,*) 'Reset to 3.0.'
000105 |         FSET = 3.0
000106 |       END IF
000107 |       CLOSE(7)
000108 |C*************************************************************see 22jan90
000109 |      IF ( ISMTH .EQ. 0 )   NCPS=4
000110 |      DO 10 I=1,1024
000111 |10    CHA(I) = I
000112 |      READ ( INP,504 ) NDUBS
000113 |      WRITE(OOT,504) NDUBS
000114 |      DO 999 NDUB = 1,NDUBS
000115 |        READ ( INP,503 ) NRUNS,NCP,((DIFC(I),RC(I)),I=1,3)
000116 |        WRITE(OOT,503) NRUNS,NCP,((DIFC(I),RC(I)),I=1,3)
000117 |        DO 21 IM=1,NRUNS
000118 |          READ ( INP,502) NRECS,IZRANL,IADD,VEE,EMLT,EMHV,PPM,EPPM,ISADD
000119 |          WRITE(OOT,502) NRECS,IZRANL,IADD,VEE,EMLT,EMHV,PPM,EPPM,ISADD
000120 |          WRITE ( OUT,601 )
000121 |         WRITE ( OUT,620 ) ISMTH,NCPS
000122 |         WRITE ( OUT,605 ) EMLT,EMHV,VEE,IADD
000123 |
000124 |          M1=64
000125 |          MA=192
000126 |          MB=832
000127 |          M2=960
000128 |
000129 |        IF(IDL.EQ.1)THEN
000130 |          WRITE(*,*) 'Number of points for parabolic smoothing is',NPS
000131 |        ELSE
000132 |11        WRITE(*,*) 'Enter new value for NPS:  (odd only please)'
000133 |          READ(5,*) NPS
000134 |          IF(MOD(NPS,2).EQ.0)THEN
000135 |            WRITE(*,*) 'NPS value was even:',NPS
000136 |            WRITE(*,*) 'For symmetrical smoothing, it must be odd.'
000137 |            GOTO 11
000138 |          END IF
000139 |         WRITE(6,*) 'Enter 0 for display or 1 to process all spectrae:'
000140 |         READ (5,*) IDL
000141 |        END IF
000142 |*****************************************************************************
000143 |C         *************  DO ANALYSIS RECORD BY RECORD  ****************
000144 |          DO 15 IJ=1,NRECS
000145 |      READ(INP,501)NRECN,IT,CAL,BDV,SDV01,SDV03,MARKS
000146 |      WRITE(*,501)NRECN,IT,CAL,BDV,SDV01,SDV03
000147 |         WRITE ( OUT,805 ) NPS
```

```
000148 |
000149 |          IF (IDL.EQ.0) GO TO 737
000150 |          GO TO 739
000151 | 737        CALL GETDAT ( NRECN )
000152 |            GO TO 78
000153 | 739        CALL GETFIL ( NRECN )
000154 | 78       WRITE(OOT,501)NRECN,IT,CAL,BDV,SDV01,SDV03,MARKS
000155 |          K1=MARKS(1,1)
000156 |          KA=MARKS(2,1)
000157 |          KB=MARKS(3,1)
000158 |          K2=MARKS(4,1)
000159 |C
000160 |          I1=MARKS(1,2)
000161 |          IA=MARKS(2,2)
000162 |          IB=MARKS(3,2)
000163 |          I2=MARKS(4,2)
000164 |C
000165 |          IF(IT .GT. 4) GO TO 101
000166 |            SDV1=SDV01+DFLOAT(ISADD)
000167 |            SDV3=SDV03-DFLOAT(ISADD)
000168 |          GO TO 102
000169 |  101      SDV1=SDV01-DFLOAT(ISADD)
000170 |            SDV3=SDV03+DFLOAT(ISADD)
000171 |  102     CONTINUE
000172 |          WRITE ( OUT,608 )  NRECN , IT ,K1,KA,KB,K2,I1,IA,IB,I2
000173 |          NIQ=1024
000174 |          ISF=NIQ/1024
000175 |          L1=M1
000176 |          LA=MA
000177 |          LB=MB
000178 |          L2=M2
000179 |C
000180 |          IF ( K1 .EQ. 0 )     GO TO 59
000181 |            K1=K1*ISF
000182 |            KA=KA*ISF
000183 |            KB=KB*ISF
000184 |            K2=K2*ISF
000185 |  59      CONTINUE
000186 |C
000187 |          IF (I1 .EQ. 0)GO TO 591
000188 |            I1=I1*ISF
000189 |            IA=IA*ISF
000190 |            IB=IB*ISF
000191 |            I2=I2*ISF
000192 |  591     CONTINUE
000193 |C
000194 |          NCH=4*NIQ
000195 |        DO  201 J=1,4
000196 |        DO  201 I=1,1024
000197 | 201    VDM(J,I)=DFLOAT(IDATA(I+1024*(J-1)))
000198 |
000199 |   20     ID1=ID(1)
000200 |          ID2=ID(2)
000201 |          ID3=ID(3)
000202 |          ID4=ID(4)
000203 |C
000204 |C       CORRECT FOR COUNTING LOSSES
000205 |C        RESOLVING TIME IS A POLYNOMIAL FUNCTION OF THE OBSERVED COUNT-RATE .
000206 |C         OBS.COUNT RATE IN KHZ.
000207 |C         DWELL TIME = 11 MICROSEC/CHANNEL
000208 |C         H = RHO / ( 11*NUMBER OF SWEEPS )
000209 |            IF (VDM(4,1024) .LE. 0. )VDM(4,1024)=4000.
000210 |  37        NOS=VDM(4,1024)/4
000211 |            WRITE(OUT,888)NOS
000212 |            HPRIME = 1000./( 13.*DFLOAT(NOS))
000213 |            HP = HPRIME/1000.
000214 |            SMS = 0
000215 |            SMB = 0
000216 |C
000217 |C      ******  DO BASELINE AND CENTROID ANALYSIS BY QUADRANTS ******
000218 |C
000219 |          DO 12 NQ=1,4
000220 |            ICT = 0
000221 |C
000222 |C       CORRECT FOR DEADTIME EFFECTS
```

```
000223 C
 727          CALL DTC (HP,HPRIME,VDM,NIQ,NQ,VCH,VAR)
000225
000226 C
000227 C      ******          END OF DEADTIME CORRECTION.      ******
000228 C
000229           CALL BLINE(OUT,ISMTH,NQ,NIQ,NCPS,CAL,ICT,PCB,0,K1,KA,
000230      &               KB,K2,I1,IA,IB,I2,L1,LA,LB,L2,VCH,A,JA,JB,
000231      &               J3,J4,J1,J2,BSL1,ED1,BSL2,ED2,BSL)
000232
000233
000234
000235 C      ******          END OF BASELINE SEARCH           ******
000236 C
000237       CALL QUAD(NRECN,ISMTH,NQ,NCPS,PC,CHA,VDM,VCH,JA,JB,J3,J4,
000238      &          MN1,MN2,VMAXC,VMAXR,PW,PWB,PW50,PW5,PWC,
000239      &          NIONS,PP,SG,AVE,N1,N2,ION,SV,CLP)
000240
000241
000242
000243  47     CALL STATS ( CHA,VCH,N1,N2,AVE,XMOM,TV,SGMA,A3,A4 )
000244
000245  67      PP(NQ) = AVE
000246          SG(NQ) = SGMA
000247       WRITE(OUT,607)J1,BSL1,ED1,JA,N1,N2,JB,BSL2,ED2,J2,BSL,ION,AVE,SGMA
000248       WRITE(OUT,*)' PEAK SHAPE : SKEWNESS = ',A3,' PEAKEDNESS = ',A4
000249 C
000250 C     ******       END OF LOCATING BY QUADRANTS      ******
000251    12    CONTINUE
000252 C*****************************************************************
000253        CS(1)=PP(2)-PP(1)-ZC1
000254        CS(3)=PP(4)-PP(1)-ZC3
000255        CS(2)=PP(3) - PP(1)
000256        NS1 = NIONS(1)
000257        NS2 = ( NIONS(2)+NIONS(3)+NIONS(4) )
000258        AVN = NS2/3.
000259        RI = AVN/NS1
000260
000261       CALL MATCH (OUT,VAR,A,NPS,CS,MN1,MN2,RI,SH,ESH,RAV,CHIAV)
000262
000263        DLV(1) =  SDV1
000264        DLV(2) = 0.
000265        DLV(3) =  SDV3
000266        EDV(1) = 0.1
000267        EDV(2) = 0.1
000268        EDV(3) = 0.1
000269        EBDV = 0.1
000270
000271       CALL DFT (IZRANL,NRECN,NCP,PC,PCB,IADD,BDV,SDV1,SDV3,EMLT,
000272      &          EMHV,VEE,IOT,IJ,NOS,RC,DIFC,MN1,MN2,VMAXC,VMAXR,
000273      &          PW,PWB,PW50,PW5,PWC,NIONS,PP,SG,SMS,SMB,VAR,A,
000274      &          SH,ESH,RAV,CHIAV,
000275      &          DLTM,EMM,ERDM,RAT1,RP05,DLTM2,ERDM2,RAT2,XS2,RATR)
000276    15 CONTINUE
000277 C
000278 C***********          END OF ANALYSIS BY RECORDS       ****************
000279 C
000280       IF ( IZRANL .NE. 0 )    GO TO 21
000281 C
000282       CALL AVESDV ( 1,NRECS,DLTM,AVDLM,ERDLM,ED)
000283       WRITE(OUT,601)
000284       WRITE ( OUT,610 ) AVDLM,ERDLM
000285       CALL AVESDV ( 1,NRECS,RAT1,ARAT1,ERAT1,E1 )
000286       CALL AVESDV ( 1,NRECS,RAT2,ARAT2,ERAT2,E2 )
000287       CALL AVESDV ( 1,NRECS,XS2,AXS2,EXS2,EX2 )
000288
000289       WRITE(*,*) 'RAT1= ',ARAT1,'RAT2= ',ARAT2,'XS2= ',AXS2
000290 C
000291       CALL WTDAVG ( DLTM,ERDM,NRECS,1,OUT,DELTAM,SGDM )
000292 C
000293       CRPPM = DELTAM*PPM/1000000.
000294       WRITE ( OUT,613 ) CRPPM
000295       EDLTEM(IM) = DSQRT ( ERDLM*ERDLM +(AVDLM*EPPM/1000000.)**2 )
000296       DLTEM(IM) = AVDLM + CRPPM
```

```
000297 |      DELEM(IM) = DELTAM + CRPPM
000298 |      EDELEM(IM) = DSQRT (SGDM*SGDM + (DELTAM*EPPM/1000000.)**2 )
000299 |      WRITE ( OUT,611 ) DLTEM(IM) , EDLTEM(IM)
000300 |      WRITE ( OUT,611 ) DELEM(IM) , EDELEM(IM)
000301 |C
000302 |      CALL AVESDV ( 1,NRECS,RP05,ARP5,ERP5,ED)
000303 |C
000304 |      ARP5 = ARP5 * 1000. * EMM / AVDLM
000305 |      ERP5 = ERP5 * 1000. * EMM / AVDLM
000306 |      WRITE ( OUT,616 ) ARP5,ERP5
000307 |      CALL AVESDV(1,NRECS,DLTM2,ADLM2,EDLM2,ED2)
000308 |      WRITE(OUT,889)
000309 |      WRITE(OUT,610) ADLM2,EDLM2
000310 |      CALL WTDAVG(DLTM2,ERDM2,NRECS,1,OUT,DELTA2,SGDM2)
000311 |      EDLTM2(IM)=EDLM2
000312 |      DLTEM2(IM)=ADLM2+CRPPM
000313 |      DELEM2(IM)=DELTA2+CRPPM
000314 |      ERDLM2(IM)=SGDM2
000315 |      WRITE(OUT,611)DLTEM2(IM),EDLTM2(IM)
000316 |      WRITE(OUT,611)DELEM2(IM),ERDLM2(IM)
000317 |      WRITE ( OUT,621 ) ARAT1,ERAT1
000318 |      WRITE ( OUT,622 ) ARAT2,ERAT2,AXS2,EXS2
000319 |      AVRT1(IM) = ARAT1
000320 |      ERRT1(IM) = ERAT1
000321 |      AVRT2(IM) = ARAT2
000322 |      ERRT2(IM) = ERAT2
000323 |      AVXS2(IM) = AXS2
000324 |      ERXS2(IM) = EXS2
000325 |   21 CONTINUE
000326 |C
000327 |      WRITE ( OUT,615 )
000328 |      CALL AVESDV ( 1,NRUNS,DLTEM,AVDLTM,ERDLTM,ED)
000329 |      WRITE ( OUT,610 ) AVDLTM,ERDLTM
000330 |      CALL WTDAVG ( DLTEM,EDLTEM,NRUNS,1,OUT,FINEM,EFINEM )
000331 |      CALL WTDAVG ( DELEM,EDELEM,NRUNS,1,OUT,FINEM,EFINEM )
000332 |      CALL AVESDV(1,NRUNS,DLTEM2,AVDLM2,ERADM2,ERD2)
000333 |      WRITE(OUT,610) AVDLM2, ERADM2
000334 |      CALL WTDAVG(DLTEM2,EDLTM2,NRUNS,1,OUT,FM,EFM)
000335 |      CALL WTDAVG(DELEM2,ERDLM2,NRUNS,1,OUT,FM,EFM)
000336 |      CALL WTDAVG ( AVRT1,ERRT1,NRUNS,1,OUT,AT1,EAT1 )
000337 |      CALL WTDAVG ( AVRT2,ERRT2,NRUNS,1,OUT,AT2,EAT2 )
000338 |      CALL WTDAVG ( AVXS2,ERXS2,NRUNS,1,OUT,AX,EAX )
000339 |  999 CONTINUE
000340 |C
000341 |C
000342 |C      FORMAT STATEMENTS FOLLOW .
000343 |C
000344 |  501 FORMAT (   I6,I2,F4.1,F6.1,2F6.1,8I4,2I3)
000345 |  502 FORMAT ( 2I2,I8,3F9.4,2F6.0,I5 )
000346 |  503 FORMAT ( 2I4,F8.1,3(F8.1,F8.5) )
000347 |  504 FORMAT ( I4 )
000348 |  601 FORMAT ('1')
000349 |  603 FORMAT (F12.3,' +-',F6.3,'    VS   ',F8.1,' +-',F4.1 )
000350 |  604 FORMAT ('0        CHANNELS                    DELTA V',
000351 |     2 (4X,F12.4,' +-',F7.3) )
000352 |  605 FORMAT ('0',3F10.5,I10,15X,'            BL      IONS     CENTRE')
000353 |  805 FORMAT ('0  THE NUMBER OF POINTS FOR PARABOLIC FITTING = ',I5)
000354 |  607 FORMAT(2X,I6,F8.1,' +-',F9.3,4I6,F8.1,' +-',F9.3,I6,F12.2,I10,
000355 |     2       F11.3,' +-',F8.3,2F9.4,F7.4)
000356 |  608 FORMAT ( '0',I6,'   TYPE',I5,3X,8I6)
000357 |  610 FORMAT ('0  STRAIGHT AVERAGE =',F13.3,F10.3 )
000358 |  611 FORMAT ('0     CORRECTED VALUE = ',F13.3,' +-',F10.3 )
000359 |  613 FORMAT ('0   PROPORTIONAL CORRECTION =',F7.3 )
000360 |  615 FORMAT ('1      WEIGHTED MEAN OF ALL RUNS ' )
000361 |  616 FORMAT ('0   AVERAGE RESOLVING POWER AT5.0% =',2F5.1,' THOUSAND')
000362 |  620 FORMAT ('0 SMOOTHING CODE =',I3,' NUMBER OF CONSECUTIVE POINTS =',
000363 |     @ I4 )
000364 |  621 FORMAT ( '0  CENTROID RATIO= ',F10.5,' +- ',F8.5 )
000365 |  622 FORMAT ( '0  LSTSQRS RATIO = ',F10.5,' +- ',F8.5,'  AVG CHISQR='
000366 |     @ ,F10.5,' +- ',F8.5 )
000367 |  888 FORMAT(' ','NUMBER OF SWEEPS=',I8)
000368 |  889 FORMAT('0','LEAST SQUARES VALUES:')
000369 |C
```

```
000370        CLOSE(INP)
000371        CLOSE(OUT)
000372        CLOSE(OOT)
000373        STOP
000374        END
000375
000376  C*************************************************************************
000377        SUBROUTINE DTC (HP,HPRIME,VDM,NIQ,NQ,VCH,VAR)
000378  C*************************************************************************
000379        IMPLICIT REAL*8 (A-H),(O-Z)
000380
000381  C     THIS ROUTINE EVALUATES THE DEAD TIME CORRECTION
000382
000383        DIMENSION VDM(4,1024),VCH(1024),VAR(4,1024)
000384        DO 48 I=1,1024
000385        V0 = VDM(NQ,I)
000386        IF ( V0 .LT.1 ) V0 = 1
000387        X0 = V0 * HPRIME
000388  C  X0 IS OBSERVED COUNTING RATE , ADJUSTED SO MIN. COUNT IS 1 .
000389        RHO = .09347 + .01069*X0 - .00004273*X0*X0 + .0000000623*X0*X0*X0
000390
000391        H = HP*RHO
000392
000393  C        VCH  IS CORRECTED COUNTS .
000394        VCH(I)=VDM(NQ,I)/(1.-VDM(NQ,I)*H)
000395  C
000396  C        VAR IS NOW TO BE USED AS VARIANCE OF VCH .
000397        VAR(NQ,I)=VCH(I)*(1.+VCH(I)*H)
000398        IF(VAR(NQ,I).LT.1.) VAR(NQ,I)=1.
000399  C
000400  C*************************************************************************
000401  C       DEFEAT DEADTIME CORRECTION.
000402  C       VCH(I)=VDM( NQ, I)
000403  C        VAR( NQ, I) = VCH (I)
000404  C        IF( VAR( NQ, I) .LT. 1. ) VAR( NQ, I) = 1.
000405  C*************************************************************************
000406  C
000407     48 CONTINUE
000408           RETURN
000409           END
000410
000411
000412  C*************************************************************************
000413        SUBROUTINE BLINE(OUT,ISMTH,NQ,NIQ,NCPS,CAL,ICT,PCB,IBL,K1,KA,
000414       &                 KB,K2,I1,IA,IB,I2,L1,LA,LB,L2,VCH,A,JX,JY,
000415       &                 JU,JV,JZ,JW,BSL1,ED1,BSL2,ED2,BSL)
000416  C*************************************************************************
000417        IMPLICIT REAL*8 (A-H),(O-Z)
000418
000419  C          THIS ROUTINE SEARCHES FOR THE BASELINE
000420                INTEGER OUT
000421                DIMENSION VCH(1024),SV(1024),A(4,1024)
000422
000423                DO 42 I=1,1024
000424     42         SV(I) = VCH(I)
000425                IF ( ISMTH .NE. 2 )  GO TO 43
000426                SV(1) = VCH(1)
000427                SV(2) = VCH(2)
000428                SV(1023) = VCH(1023)
000429                SV(1024) = VCH(1024)
000430                DO 41 I=3,1022
000431                SV(I) = ( VCH(I-2)+VCH(I-1)+VCH(I)+VCH(I+1)+VCH(I+2) )/5.
000432  41           CONTINUE
000433  43           CONTINUE
000434
000435  C        M.S: TWO SMOOTHING CODE OPTIONS FOR SMOOTHING OVER 9 POINTS
000436
000437             IF ((ISMTH .EQ.1).OR.(ISMTH.EQ.3))  GO TO 44
000438  C
000439             GO TO 47
000440     44      CALL NINESM ( 1,1024,VCH,SV )
000441  C          COMPUTE BASELINE
000442
000443   47        CONTINUE
```

```
000444 |
000445 |            IF ( NQ .GT. 1 )      GO TO 100
000446 |            IF ( K1 .NE. 0 )    GO TO 25
000447 |            J1=L1
000448 |            J2=L2
000449 |            JA=LA
000450 |            JB=LB
000451 |            CALL STRIP (OUT,IBL,VCH,J1,JA,JB,J2,NQ,NIQ )
000452 |            GO TO 27
000453 |    25      J1=K1
000454 |            J2=K2
000455 |            JA=KA
000456 |            JB=KB
000457 |            CALL STRIP (OUT,IBL,VCH,J1,JA,JB,J2,NQ,NIQ )
000458 |            GO TO 27
000459 |   100      IF ( I1 .NE. 0 )     GO TO 31
000460 |              I1=L1
000461 |              I2=L2
000462 |              IA=LA
000463 |              IB=LB
000464 |    31      CONTINUE
000465 |            J1 = I1
000466 |            J2 = I2
000467 |            JA = IA
000468 |            JB = IB
000469 |            CALL STRIP (OUT,IBL,VCH,J1,JA,JB,J2,NQ,NIQ )
000470 |    27    CONTINUE
000471 |          CALL AVESDV ( J1,JA,VCH,BSL1,SDX1,ED1 )
000472 |          CALL AVESDV ( JB,J2,VCH,BSL2,SDX2,ED2 )
000473 |          LDM1=JA-J1+1
000474 |          LDM2=J2-JB+1
000475 |          BSL=(BSL1*LDM1+BSL2*LDM2)/(LDM1+LDM2)
000476 |          ICT = ICT + 1
000477 |          IF ( ICT .GE. 2 )     GO TO 26
000478 |C
000479 |          CALL CUT3 ( SV,BSL,PCB,JA,JB,J3,J4,NCPS,IMX,CL,1 )
000480 |C
000481 |C     USE NEW-FOUND LIMITS TO RECALCULATE BSL
000482 |          IAMX=(IMX-J3)
000483 |C         IAMX IS LEFT HALF-WIDTH
000484 |          J5 = J3 - IAMX
000485 |          IF ( J5 .LE. JA )      GO TO 45
000486 |            JA = J5
000487 |    45    CONTINUE
000488 |          IBMX=J4-IMX
000489 |C         IBMX IS RIGHT HALF-WIDTH
000490 |          J6 = J4 + IBMX
000491 |          IF ( J6 .GE. JB )    GO TO 46
000492 |            JB = J6
000493 |    46    CONTINUE
000494 |          GO TO 27
000495 |    26    CONTINUE
000496 |          DO 14 I=1,NIQ
000497 |            VCH(I) = ( VCH(I)-BSL ) * CAL
000498 |            A(NQ,I) = VCH(I)
000499 |            IF(A(NQ,I).LT.0.) A(NQ,I)=0.
000500 |    14    CONTINUE
000501 |          JX=JA
000502 |          JY=JB
000503 |          JU=J3
000504 |          JV=J4
000505 |          JZ=J1
000506 |          JW=J2
000507 |          RETURN
000508 |          END
000509 |
000510 |C*************************************************************************
000511 |       SUBROUTINE QUAD(NRECN,ISMTH,NQ,NCPS,PC,CHA,VDM,VCH,JA,JB,J3,J4,
000512 |      &                 MN1,MN2,VMAXC,VMAXR,PW,PWB,PW50,PW5,PWC,
000513 |      &                 NIONS,PP,SG,AVE,N1,N2,ION,SV,CLP)
000514 |C*************************************************************************
000515 |       IMPLICIT REAL*8 (A-H),(O-Z)
000516 |
000517 |C          THIS ROUTINE EVALUATES NEW LIMITS FOR PEAK ANALYSIS
```

```
000518
000519       DIMENSION CHA(1024),VDM(4,1024),VCH(1024),SV(1024),
000520      &          VMAXC(4),VMAXR(4),NIONS(4),PWC(4),PP(4),SG(4)
000521
000522                DO 42 I=1,1024
000523     42         SV(I) = VCH(I)
000524
000525                IF ( ISMTH .NE. 2 )  GO TO 43
000526                SV(1) = VCH(1)
000527                SV(2) = VCH(2)
000528                SV(1023) = VCH(1023)
000529                SV(1024) = VCH(1024)
000530                DO 41 I=3,1022
000531                SV(I) = ( VCH(I-2)+VCH(I-1)+VCH(I)+VCH(I+1)+VCH(I+2) )/5.
000532 41           CONTINUE
000533 43           CONTINUE
000534
000535 C         M.S: TWO SMOOTHING CODE OPTIONS FOR SMOOTHING OVER 9 POINTS
000536
000537              IF ((ISMTH .EQ.1).OR.(ISMTH.EQ.4))  GO TO 44
000538 C
000539              GO TO 47
000540     44       CALL NINESM ( 1,1024,VCH,SV )
000541 C
000542     47    CONTINUE
000543 C
000544           CALL CUT3 ( SV,0.0,5.0,JA,JB,J51,J52,NCPS,IMX,CL,2 )
000545           CALL CUT3 ( SV,0.0,50.0,J3,J4,M50,N50,NCPS,IMX,CL,3)
000546           CALL CUT3 ( SV,0.0,PC,JA,JB,N1,N2,NCPS,IMX,CLP,4 )
000547
000548           IF ( NQ .NE. 1 )  GO TO 49
000549             MN1 = N1
000550             MN2 = N2
000551     49    CONTINUE
000552 C
000553 C  CALCULATE CORRECTED AND OBSERVED COUNTS AND COUNTING RATES
000554 C  AT PEAK MAXIMUM .
000555 C  USE AN ELEVEN POINT AVERAGE .
000556 C
000557           S1=0.
000558           S2 = 0.
000559           DO 50 L=1,11
000560             K=L-6
000561             S1 = S1 + VCH(IMX+K)
000562     50      S2 = S2 + VDM(NQ,IMX+K)
000563           VMAXC(NQ) = S1/11.
000564           VMAXR(NQ) = S2/11.
000565           PW = N2-N1+1
000566           PWB = J4-J3+1
000567           PW50 = N50-M50+1
000568           PW5 = J52 - J51 + 1
000569           PWC(NQ) = PW5
000570           ION = 0
000571           DO 11 I=N1,N2
000572             ION = ION + VCH(I)
000573     11    CONTINUE
000574           NIONS(NQ) = ION
000575           RETURN
000576           END
000577
000578 C*****************************************************************************
000579       SUBROUTINE DFT (IZRANL,NRECN,NCP,PC,PCB,IADD,BDV,SDV1,SDV3,EMLT,
000580      &                EMHV,VEE,IOT,IJ,NOS,RC,DIFC,MN1,MN2,VMAXC,VMAXR,
000581      &                PW,PWB,PW50,PW5,PWC,NIONS,PP,SG,SMS,SMB,VAR,A,
000582      &                SH,ESH,RAV,CHIAV,
000583      &                DLTM,EMM,ERDM,RAT1,RP05,DLTM2,ERDM2,RAT2,XS2,RATR)
000584 C*****************************************************************************
000585       IMPLICIT REAL*8 (A-H),(O-Z)
000586
000587
000588 C     THIS ROUTINE EVALUATES THE MASS DIFFERENCE BY THE CENTROID METHOD
000589
000590       DIMENSION VAR(4,1024),A(4,1024),RC(3),DIFC(3),CS(3),DLV(3),EDV(3),
000591      &    ES(3),VMAXC(4),VMAXR(4),NIONS(4),PP(4),SG(4),PWC(4),RP05(8),
000592      &    DLTM(8),ERDM(8),DLTM2(8),ERDM2(8),RAT1(8),RAT2(8),XS2(8)
```

```
000593 |
000594 |       OUT=IOT
000595 |       NS1 = NIONS(1)
000596 |       PW1 = PWC(1)
000597 |       CALL AVESDV (2,4,PWC,PW2,EPW,ED )
000598 |       NS2 = ( NIONS(2)+NIONS(3)+NIONS(4) )
000599 |       AVN = NS2/3.
000600 |       NS2 = AVN
000601 |       RATIO = NS1 / AVN
000602 |       RI = AVN/NS1
000603 |       IF ( RATIO .GT. 1. )      GO TO 23
000604 |       SMS = SMS + NS1
000605 |       SMB = SMB + NS2
000606 |       PWS = PW1
000607 |       PWB = PW2
000608 |       RATIO = 1. / RATIO
000609 |       LRG = 2
000610 |       GO TO 24
000611 |    23  SMS = SMS + NS2
000612 |       SMB = SMB + NS1
000613 |       PWS = PW2
000614 |       PWB = PW1
000615 |       LRG = 1
000616 |    24  CONTINUE
000617 |       EPW = EPW * 1.7
000618 |       WRITE ( OUT,617 ) PWB,PWS,EPW
000619 |       WRITE ( OUT,625 ) ( VMAXC(I) , I=1,4)
000620 |       VMAX3 = ( VMAXC(2)+VMAXC(3)+VMAXC(4) )/3.
000621 |       CR1 = VMAXC(1)*90.909/NOS
000622 |       CR2 = VMAX3*90.909/NOS
000623 |       RATC = CR1/CR2
000624 |       IF ( RATC .LT. 1. )  RATC = 1./RATC
000625 |       WRITE ( OUT,626 ) CR1,CR2,RATC
000626 |       ZC0 = 0.
000627 |       WRITE ( OUT,623 ) ( VMAXR(I) , I=1,4 )
000628 |       VMAX3 = ( VMAXR(2)+VMAXR(3)+VMAXR(4) )/3.
000629 |       CR1 = VMAXR(1)*90.909/NOS
000630 |       CR2 = VMAX3*90.909/NOS
000631 |       RATR = CR1/CR2
000632 |       IF ( RATR .LT. 1. )  RATR = 1./RATR
000633 |       WRITE ( OUT,624 ) CR1,CR2,RATR
000634 |       ZC1 = 0.
000635 |       ZC3 = 0.
000636 |       EZC0 = 0.
000637 |       EZC1 = 0.
000638 |       EZC3 = 0.
000639 |       IF ( IZRANL .NE. 0 )     GO TO 13
000640 |13     CONTINUE
000641 |
000642 |
000643 |       CS(1)=PP(2)-PP(1)-ZC1
000644 |       CS(3)=PP(4)-PP(1)-ZC3
000645 |       CS(2) = PP(3) - PP(1)
000646 |       ES(2) = DSQRT ( SG(3)*SG(3) + SG(1)*SG(1) )
000647 |       ES(1) = DSQRT ( SG(2)*SG(2) + EZC1*EZC1 + SG(1)*SG(1) )
000648 |       ES(3) = DSQRT ( SG(4)*SG(4) + EZC3*EZC3 + SG(1)*SG(1) )
000649 |       DLV(1) =  SDV1
000650 |       DLV(2) = 0.
000651 |       DLV(3) =  SDV3
000652 |       EDV(1) = 0.1
000653 |       EDV(2) = 0.1
000654 |       EDV(3) = 0.1
000655 |       EBDV = 0.1
000656 |       WRITE ( OUT,604 ) BDV,EBDV
000657 |       WRITE ( OUT,603 ) ( CS(IW),ES(IW),DLV(IW),EDV(IW),IW=1,3 )
000658 |       IF ( IZRANL .NE. 0 )     GO TO 115
000659 |C
000660 |      CALL WTFIT3 ( 3,CS,ES,DLV,EDV,YNT,S1,EYT,ES1,1,IOT,20,CHISQ)
000661 |C
000662 |       IF ( BDV .GT. 0. )  DELV = ( -YNT + BDV ) + IADD
000663 |       IF ( BDV .LT. 0. )  DELV =-( -YNT + BDV ) + IADD
000664 |       EV1 = EYT
000665 |       IF ( BDV .GT. 0. )   DLTM(IJ) = DELV * EMLT / VEE
000666 |       IF ( BDV .LT. 0. )   DLTM(IJ) = DELV * EMHV / VEE
000667 |       EMM = ( EMLT + EMHV ) / 2.
000668 |       ERDM(IJ) =  EV1 * EMM / VEE
```

```
000669          RAT1(IJ) = RATIO
000670          S1 = DABS ( S1 )
000671          RP = DELV / ( PW*S1 )
000672          RPB = DELV / ( PWB*S1 )
000673          RP50 = DELV / ( PW50*S1 )
000674          RP5 = DELV / ( PW5*S1 )
000675          RP05(IJ) = RP5
000676          WRITE ( OUT,602 ) DLTM(IJ),ERDM(IJ)
000677          ERR = ( PW*EMM*S1) / (VEE*DSQRT(24.*SMS) )
000678          ERR = DSQRT ( 1.+1./RATIO ) * ERR * (1. + ES1/S1 )
000679          IRES = RP * 1000    * EMM /  DLTM(IJ)
000680          NROLD = NRECN
000681  C
000682  C        CORRECT FOR THE EFFECTS OF CONTAMINANT PEAKS IF ANY.
000683  C
000684          IF ( NCP .EQ. 0 )       GO TO 17
000685  C
000686          DO 16 IC = 1,NCP
000687  C
000688  C        LOAD RATIO OF THE INTENSITY OF THE CURRENT CONTAMINANT PEAK TO
000689  C        THE MAIN PEAK. DIFC IS THE SEPARATION BETWEEN THE CONTAMINANT
000690  C        AND THE MAIN PEAK.
000691  C
000692           RC1 = RC(IC)
000693           DIF1 = DIFC(IC)
000694  C
000695           RT = RP5 * DABS(DIF1) / DLTM(IJ)
000696           WRITE ( OUT,614 ) RP5 , RT
000697           CALL CONTAM ( IRES, RT,RC1,DIF1,C1 )
000698           WRITE ( OUT,612 ) C1
000699     16    DLTM(IJ) = DLTM(IJ) + C1
000700     17    CONTINUE
000701          WRITE ( OUT,609 ) IRES , PC,PCB,RPB,PC,RP,RP50
000702          WRITE ( OUT,606 ) RATIO , ERR ,SMS,PW
000703          WRITE ( OUT,650 )
000704  C
000705          CALL WTFIT3 ( 3,SH,ESH,DLV,EDV,YINT,S2,EYNT,ES2,1,IOT,20,CHISQR )
000706  C
000707          IF ( BDV .GT. 0. )     DELV =  (-YINT + BDV ) + IADD
000708          IF ( BDV .LT. 0. )     DELV = -(-YINT + BDV ) + IADD
000709          EV1 = EYNT
000710          IF ( BDV .GT. 0. )     DLTM2(IJ) = DELV*EMLT/VEE
000711          IF ( BDV .LT. 0. )     DLTM2(IJ) = DELV*EMHV/VEE
000712          ERDM2(IJ) = EV1*EMM/VEE
000713          WRITE ( OUT,602 ) DLTM2(IJ),ERDM2(IJ)
000714          RAT2(IJ) = RAV
000715          XS2(IJ) = CHIAV
000716
000717     602 FORMAT ('0              *****     DELTA M = ',F13.5,' +-',F9.5,'
000718        2MICRO UNITS      ***** ' )
000719     603 FORMAT (F12.3,' +-',F6.3,'    VS   ',F8.1,' +-',F4.1 )
000720     604 FORMAT ('0        CHANNELS                    DELTA V',
000721        2 (4X,F12.4,' +-',F7.3) )
000722     606 FORMAT('0',8X, 'RATIO = ',F8.2,' TO 1   ERR =',F7.3,' MICRO UNITS
000723        2     IONS IN SMALL PEAK =',F10.0,'    PEAK WIDTH =',F6.1 )
000724     609 FORMAT ('0',8X,'RESOLUTION = 1 PART IN',I7,' THOUSAND , AT',
000725        2 F5.1,'%'
000726        3'   RESOLVING POWER AT',F4.1,'% =',F6.2,'  , AT',F5.1,'% =',F6.2,
000727        4'   , AT 50%=',F6.2 )
000728     612 FORMAT ('0    CONTAMINANT CORRECTIONS :',  F8.3 )
000729     614 FORMAT ('0   RP0 =',F5.2, '   RATIO TO CONTAMINANT SEP =',F5.2 )
000730     617 FORMAT ('0  PEAK WIDTHS AT 5.0% : ', 2F6.0,' +-',F5.1 )
000731     623 FORMAT ('    RAW MAXIMUM COUNTS ',4F8.1 )
000732     624 FORMAT ('    RAW COUNT RATES ',2F8.2,'  KHZ   , RATIO=',F10.4 )
000733     625 FORMAT ( '0  CORRECTED MAXIMUM COUNTS ',4F8.1 )
000734     626 FORMAT ('   CORRECTED COUNT RATES ',2F8.2,'  KHZ   , RATIO=',F10.4)
000735     650 FORMAT ('0' )
000736
000737     115 RETURN
000738         END
000739
```

```
000740 |
000741 |C*****************************************************************
000742 |      SUBROUTINE CONTAM ( IRES, RT,RC,DIF,C )
000743 |C*****************************************************************
000744 |      IMPLICIT REAL*8 (A-H),(O-Z)
000745 |C
000746 |      C = 0.
000747 |      IF ( RT .GT. 1.0 )     GO TO 11
000748 |      IF ( RT .GE. 0.5 ) C=(RT-1.5+(1/RT)*(1/RT)/2.)/3.
000749 |      IF ( RT .LT.0.5 ) C=1.-RT*RT*2./3. - RT
000750 |      C = C * DIF*RC
000751 |   11 CONTINUE
000752 |      RETURN
000753 |      END
000754 |C
000755 |C*****************************************************************
000756 |      SUBROUTINE AVESDV(N1,N2,X,XAV,EXV,EX1)
000757 |C*****************************************************************
000758 |      IMPLICIT REAL*8 (A-H),(O-Z)
000759 |C
000760 |C       THIS PROGRAM FINDS THE MEAN [ XAV], STANDARD DEVIATION [EX1],
000761 |C       AND THE STANDARD ERROR [EXV] OF THE DATA CONTAINED IN THE ARRAY
000762 |C       X BETWEEN THE TWO INDICES N1 AND N2.
000763 |C
000764 |      DIMENSION X(1024)
000765 |C
000766 |C       CHECK THE ORDER OF THE INDICES. IF REVERSED PRINT MESSAGE
000767 |C       AND EXIT.
000768 |C
000769 |      IF(N2 .GE. N1) GO TO 1
000770 |      WRITE(OUT,601) N1,N2
000771 |      XAV = 0.
000772 |      EXV = 0.
000773 |      EX1 = 0.
000774 |      RETURN
000775 |C
000776 |C       NORMALIZE VARIABLES TO ZERO.
000777 |C
000778 |  1   SX=0.
000779 |      RESQ=0.
000780 |C       CALCULATE THE MEAN VALUE.
000781 |      DO  2  I=N1,N2
000782 |    2 SX=SX+X(I)
000783 |      XN=N2-N1+1
000784 |      XAV=SX/XN
000785 |C
000786 |C       CALCULATE STANDARD DEVIATION AND ERROR.
000787 |      DO  3  I=N1,N2
000788 |    3 RESQ=RESQ+(X(I)-XAV)*(X(I)-XAV)
000789 |      F=XN-1.
000790 |      IF ( F .EQ. 0. ) F=1.
000791 |      EX1=DSQRT( RESQ / F )
000792 |      EXV=DSQRT( RESQ / ( XN * F))
000793 |C       CALCULATIONS COMPLETED. RETURN TO CALLING PROGRAM.
000794 |  601 FORMAT('0','INCORRECT LIMITS',2I10)
000795 |      RETURN
000796 |      END
000797 |C*****************************************************************
000798 |      SUBROUTINE MATCH(OUT,SA,A,NPS,CS,N1,N2,RI,SH,ES,RAV,CHIAV)
000799 |C*****************************************************************
000800 |      IMPLICIT REAL*8 (A-H),(O-Z)
000801 |      INTEGER OUT
000802 |      DOUBLE PRECISION B(3),SOLN(3),ALPHA(2,2),AM(3,3),AI(3,3),
000803 |     *Y(81),C(3),AB(3),YMIN,DOF,P(2),SIGP(2),SOLD,CHIOLD,CHISQR,
000804 |     *R,R2,T,TR,STR2,S,FN,FS,DD1,DD2,XM,EXM,SI(2),
000805 |     *DM1,DM2,SIL(2),BL,A12L
000806 |      DIMENSION SA(4,1024),A(4,1024),ASM(4,1024),
000807 |     *M(81),CS(3),SH(3),ES(3)
000808 |      NP=2
000809 |      NM=5
000810 |      CHIAV=0.
000811 |      RAV=0.
000812 |      DOF=DFLOAT(N2-N1+1-NP)
000813 |      DO 101 NN=1,3
000814 |      IQ=NN+1
```

```
000815 |      P(2)=RI
000816 |      SP1=CS(NN)
000817 |      M(2)=NINT(SP1)
000818 |      E=SP1-DFLOAT(M(2))
000819 |      IF(E.LT.0.)GO TO 330
000820 |      IF(E.LT.0.5)GO TO 331
000821 |      M(2)=M(2)+1
000822 |      GO TO 331
000823 |  330 IF(DABS(E).LT.0.5)GO TO 331
000824 |      M(2)=M(2)-1
000825 |  331 P(1)=DFLOAT(M(2))
000826 |      SOLD=P(1)
000827 |      CHIOLD=0.D0
000828 |      JFLAG=0
000829 |      KFLAG=0
000830 |      N=1
000831 |      DO 1 N=1,NM
000832 |      LFLAG=0
000833 |C*************************************************************************
000834 |C M.S:THIS PART PREPARES THE DATA REQUIRED FOR THE INITIAL SEARCH FOR CHISQ
000835 |C     THE INTIAL SEARCH IS AN ITERATIVE PROCEDURE IN SUCH WAY THAT :
000836 |C           CHISQ (CHA-4) > CHISQ (CHA) < CHISQ (CHA+4)
000837 |C     THIS REPRESENTS THE INITIAL GUESS FOR CHISQ (CHA)
000838 |C*************************************************************************
000839 |  199 INC=-4
000840 |      DO 300 I=1,3
000841 |      M(I)=M(2)+INC
000842 |      Y(I)=0.D0
000843 |      AB(I)=0.D0
000844 |  300 INC=INC+4
000845 |      DM1=DFLOAT(M(1))
000846 |      DM2=DFLOAT(M(2))
000847 |      DO 7 I=1,NP
000848 |      B(I)=0.D0
000849 |      DO 7 J=I,NP
000850 |    7 ALPHA(I,J)=0.D0
000851 |      R=P(2)
000852 |      R2=R*R
000853 |      IF((JFLAG+KFLAG).EQ.2) GO TO 700
000854 |      IF(N.EQ.NM) GO TO 700
000855 |      DO 2 I=N1,N2
000856 |      T=A(1,I)
000857 |      TR=T*R
000858 |      STR2=SA(1,I)*R2
000859 |      DO 21 K=1,3
000860 |      IPM=I+M(K)
000861 |      S=STR2+SA(IQ,IPM)
000862 |      FN=TR-A(IQ,IPM)
000863 |      FS=FN/S
000864 |      Y(K)=Y(K)+FN*FS
000865 |      AB(K)=AB(K)+FS*T
000866 |      IF(K-2) 21,23,21
000867 |   23 ALPHA(2,2)=ALPHA(2,2)+T*T/S
000868 |   21 CONTINUE
000869 |    2 CONTINUE
000870 |      YMIN=Y(2)
000871 |      MMIN=M(2)
000872 |      DO 50 I=1,3,2
000873 |      YMIN=DMIN1(YMIN,Y(I))
000874 |      IF(YMIN.EQ.Y(I)) MMIN=M(I)
000875 |   50 CONTINUE
000876 |      IF(MMIN.EQ.M(2)) GO TO 51
000877 |      IF(YMIN.EQ.Y(2)) GO TO 51
000878 |      M(2)=MMIN
000879 |      IF(LFLAG.EQ.1) GO TO 1
000880 |      LFLAG=1
000881 |      IF(IABS(M(2)).GT.80) GO TO 3
000882 |      GO TO 199
000883 |C*************************************************************
000884 |C     END OF THE INITIAL SEARCH
000885 |C*************************************************************
000886 |   51 DD1=(Y(2)-Y(1))/4.D0
000887 |      DD2=(Y(3)-Y(2))/4.D0
000888 |      C(3)=(DD2-DD1)/8.D0
```

```
000889       IF(C(3).EQ.0.D0) GO TO 666
000890       C(2)=DD1-(DM1+DM2)*C(3)
000891       C(1)=Y(1)-DM1*(DD1-DM2*C(3))
000892       XM=-C(2)/(2.D0*C(3))
000893       CHISQR=(C(1)+(C(2)+C(3)*XM)*XM)/DOF
000894       GO TO 777
000895     666 CHISQR=Y(2)/DOF
000896       XM=DM2
000897       GO TO 777
000898  C*********************************************************************
000899  C M.S:THIS PART PREPARES THE DATA REQUIRED FOR THE FINAL SEARCH FOR CHISQ
000900  C     THE FINAL SEARCH IS BY DEFAULT AN 11 POINTS PARABOLIC FITTING,
000901  C     THOUGH IT MAY BE SET TO ANY ODD NUMBER BY THE USER
000902  C     ASM : COUNTS WHICH ARE SUBTRACTED FROM THE BASE LINE AND THEN
000903  C           SMOOTHED OVER 9 POINTS SMOOTHING CODE (SUBROUTINE NINESM)
000904  C*********************************************************************
000905     700 KU=(NPS+1)/2
000906       M(KU)=M(2)
000907       INC=-(NPS-1)/2
000908       DO 701 I=1,NPS
000909       M(I)=M(KU)+INC
000910       Y(I)=0.D0
000911     701 INC=INC+1
000912       DO 702 I=N1,N2
000913       T=A(1,I)
000914       TR=T*R
000915       STR2=SA(1,I)*R2
000916       II=1
000917       DO 721 K=1,NPS
000918       IPM=I+M(K)
000919       S=STR2+SA(IQ,IPM)
000920       FN=TR-A(IQ,IPM)
000921       FS=FN/S
000922       Y(K)=Y(K)+FN*FS
000923       KM6=IABS(K-KU)
000924       IF(KM6)724,722,724
000925     724 IF(KM6-4)721,722,721
000926     722 AB(II)=AB(II)+FS*T
000927       II=II+1
000928       IF(KM6)721,723,721
000929     723 ALPHA(2,2)=ALPHA(2,2)+T*T/S
000930     721 CONTINUE
000931     702 CONTINUE
000932  C  M.S:INVESTIGATION ABOUT THE PARABOLA FITTING
000933  C
000934  C      DO 333 L=1,11
000935  C      WRITE(*,*)' NQ = ',NN,' CHA = ',M(L),' Y = ',Y(L)
000936  C 333 CONTINUE
000937  C
000938       CALL QFIT(OUT,M,Y,NPS,KU,C,DOF,XM,EXM,CHISQR,0)
000939  C
000940  C     WRITE(*,*)' NQ = ',NN,' CHISQR = ',CHISQR
000941  C*********************************************************************
000942  C     END OF THE FINAL SEARCH
000943  C*********************************************************************
000944     777 B(1)=-.5D0*C(2)-C(3)*DM2
000945       ALPHA(1,1)=C(3)
000946       B(2)=-AB(2)
000947       ALPHA(1,2)=.125 D0*(AB(3)-AB(1))
000948       DO 60 I=1,NP
000949       SI(I)=DSQRT(DABS(ALPHA(I,I)))
000950       SIL(I) = DLOG10(SI(I))
000951       BL = DLOG10(DABS(B(I)))
000952       IF ((BL-SIL(I)) .LE. -70.D0 ) B(I)=0.D0
000953       B(I)=B(I)/SI(I)
000954       AM(I,I)=1.D0
000955      60 CONTINUE
000956       A12L = DLOG10(DABS(ALPHA(1,2)))
000957       IF ( (A12L-SIL(1)-SIL(2)) .LE. -70.D0 ) ALPHA(1,2)=0.D0
000958       AM(1,2) = ALPHA(1,2)/(SI(1)*SI(2))
000959       AM(2,1) = AM(1,2)
000960       IF((JFLAG+KFLAG).EQ.2) GO TO 99
```

```
000961       IF(N.EQ.NM) GO TO 99
000962       KFLAG=0
000963       IF(DABS(CHIOLD-CHISQR).LE.2.D-2) KFLAG=1
000964       CHIOLD=CHISQR
000965       CALL INVERT(AM,B,AI,SOLN,NP,0)
000966       P(1)=DM2+SOLN(1)/SI(1)
000967       JFLAG=0
000968       IF(DABS(P(1)-SOLD).LE.1.D-2) JFLAG=1
000969       SOLD=P(1)
000970       DO 84 J=2,NP
000971    84 P(J)=P(J)+SOLN(J)/SI(J)
000972       SP1=SNGL(P(1))
000973       M(2)=NINT(SP1)
000974       E=SP1-DFLOAT(M(2))
000975       IF(E.LT.0.) GO TO 30
000976       IF(E.LT.0.5) GO TO 31
000977       M(2)=M(2)+1
000978       GO TO 31
000979    30 IF(DABS(E).LT.0.5) GO TO 31
000980       M(2)=M(2)-1
000981    31 CONTINUE
000982       IF(IABS(M(2)).GT.80) GO TO 3
000983     1 CONTINUE
000984    99 CALL INVERT(AM,B,AI,SOLN,NP,2)
000985       DO 85 J=1,NP
000986       P(J)=P(J)+SOLN(J)/SI(J)
000987    85 SIGP(J)=DSQRT(DABS(AI(J,J)/ALPHA(J,J)))
000988       P(1)=DM2+SOLN(1)/SI(1)
000989       GO TO 98
000990     3 WRITE (OUT,600) M(2)
000991   600 FORMAT('-','ILLEGAL SHIFT',I15)
000992       GO TO 999
000993    98 CONTINUE
000994       SH(NN)=P(1)
000995       ES(NN)=SIGP(1)
000996       DIFF=CS(NN)-P(1)
000997       IF(P(2).GT.1.D0) GO TO 103
000998       P(2)=1.D0/P(2)
000999       SIGP(2)=SIGP(2)*P(2)**2
001000   103 WRITE(OUT,100)IQ,(P(I),SIGP(I),I=1,NP),N,DIFF,CHISQR
001001   100 FORMAT(' ',' S',I1,'1=',F10.4,' +-',F7.4,'  R=',
001002      *F8.4,' +-',F8.4,I3,2F10.4)
001003       RAV=RAV+P(2)
001004       CHIAV=CHIAV+CHISQR
001005   101 CONTINUE
001006       RAV=RAV/3.
001007       CHIAV=CHIAV/3.
001008   999 RETURN
001009       END
001010 C*************************************************************
001011       SUBROUTINE QFIT (OUT,M,Y,N,KU,C,DOF,XM,EXM,CHISQR,MODE )
001012 C*************************************************************
001013       IMPLICIT REAL*8 (A-H),(O-Z)
001014       INTEGER OUT
001015       DOUBLE PRECISION Y(81),AM(3,3),AI(3,3),B(3),C(3),
001016      *XSQ,X,SA(3),DOF,XM,CHISQR,EXM
001017       DIMENSION M(81),L(3,3)
001018       DO 1 I=1,3
001019       B(I)=0.D0
001020       DO 1 J=I,3
001021     1 L(I,J)=0
001022       DO 2 I=1,N
001023       M2=M(I)*M(I)
001024       L(1,2)=L(1,2)+M(I)
001025       L(1,3)=L(1,3)+M2
001026       L(2,3)=L(2,3)+M2*M(I)
001027       L(3,3)=L(3,3)+M2*M2
001028       B(1)=B(1)+Y(I)
001029       B(2)=B(2)+Y(I)*M(I)
001030     2 B(3)=B(3)+Y(I)*M2
001031       L(1,1)=N
001032       L(2,2)=L(1,3)
001033       DO 4 I=1,3
001034       SA(I)=DSQRT(DFLOAT(L(I,I)))
```

```
001035 |       B(I)=B(I)/SA(I)
001036 |     4 AM(I,I)=1.D0
001037 |       DO 5 I=1,2
001038 |       K=I+1
001039 |       DO 5 J=K,3
001040 |       AM(I,J)=DFLOAT(L(I,J))/(SA(I)*SA(J))
001041 |     5 AM(J,I)=AM(I,J)
001042 |       CALL INVERT(AM,B,AI,C,3,0)
001043 |       DO 7 I=1,3
001044 |     7 C(I)=C(I)/SA(I)
001045 |       IF(C(3).EQ.0.D0) GO TO 666
001046 |       XM=-C(2)/(2.D0*C(3))
001047 |       IF(C(3).GT.0.D0) GO TO 6
001048 |       C(3)=DABS(C(3))
001049 |       WRITE(OUT,601)
001050 |   601 FORMAT('0 C(3) NEGATIVE')
001051 |     6 EXM=DSQRT(1.D0/C(3))
001052 |       CHISQR=(C(1)+(C(2)+C(3)*XM)*XM)/DOF
001053 |       GO TO 665
001054 |   666 CHISQR=Y(KU)/DOF
001055 |       XM=DFLOAT(M(KU))
001056 |   665 CONTINUE
001057 |       IF(MODE)31,99,31
001058 |    31 XSQ=0.D0
001059 |       DO 3 I=1,N
001060 |       X=DFLOAT(M(I))
001061 |     3 XSQ=XSQ+(Y(I)-C(1)-(C(2)+C(3)*X)*X)**2
001062 |       XSQ=XSQ/DFLOAT(N-3)
001063 |       DO 10 I=1,N
001064 |    10 Y(I)=Y(I)/DOF
001065 |       WRITE(OUT,950)(M(I),Y(I),I=1,11),XSQ
001066 |   950 FORMAT(' ',11(I4,F7.3),F7.1)
001067 |       WRITE(OUT,951)(C(I),I=1,3)
001068 |   951 FORMAT(' ',3D11.4)
001069 |    99 RETURN
001070 |       END
001071 |C*****************************************************************
001072 |       SUBROUTINE INVERT(A,B,AINV,X,N,MODE)
001073 |C*****************************************************************
001074 |       IMPLICIT REAL*8 (A-H),(O-Z)
001075 |       DOUBLE PRECISION A(3,3),B(3),AINV(3,3),X(3),Z,AMAX,SUM
001076 |       INTEGER R(3),C(3),ROW,COL
001077 |       DO 2 I=1,N
001078 |       R(I)=I
001079 |     2 C(I)=I
001080 |       M=N-1
001081 |       DO 4 I=1,M
001082 |       AMAX=DABS(A(R(I),C(I)))
001083 |       ROW=I
001084 |       COL=I
001085 |       DO 5 L=I,N
001086 |       DO 6 J=I,N
001087 |       IF(DABS(A(R(L),C(J))).LE.AMAX) GO TO 6
001088 |       AMAX=DABS(A(R(L),C(J)))
001089 |       ROW=L
001090 |       COL=J
001091 |     6 CONTINUE
001092 |     5 CONTINUE
001093 |       IF(ROW.EQ.I) GO TO 25
001094 |       NR=R(ROW)
001095 |       R(ROW)=R(I)
001096 |       R(I)=NR
001097 |    25 IF(COL.EQ.I) GO TO 26
001098 |       NC=C(COL)
001099 |       C(COL)=C(I)
001100 |       C(I)=NC
001101 |    26 II=I+1
001102 |       DO 7 J=II,N
001103 |       Z=A(R(J),C(I))/A(R(I),C(I))
001104 |       A(R(J),C(I))=Z
001105 |       DO 8 K=II,N
001106 |     8 A(R(J),C(K))=A(R(J),C(K))-Z*A(R(I),C(K))
001107 |     7 B(R(J))=B(R(J))-Z*B(R(I))
001108 |     4 CONTINUE
```

```
001109       IF(MODE.EQ.1) GO TO 98
001110       X(C(N))=B(R(N))/A(R(N),C(N))
001111       DO 9 J=1,M
001112       SUM=0.D0
001113       DO 30 L=1,J
001114    30 SUM=SUM+A(R(N-J),C(N-J+L))*X(C(N-J+L))
001115     9 X(C(N-J))=(B(R(N-J))-SUM)/A(R(N-J),C(N-J))
001116       IF(MODE.EQ.0) GO TO 99
001117    98 CONTINUE
001118       DO 11 J=1,N
001119       DO 12 K=1,J
001120    12 B(R(K))=0.D0
001121       B(R(J))=1.D0
001122       IF(J.EQ.N) GO TO 17
001123       JJ=J+1
001124       DO 14 K=JJ,M
001125    14 B(R(K))=-A(R(K),C(J))
001126       IF(JJ.EQ.N) GO TO 17
001127       DO 15 K=JJ,M
001128       KK=K+1
001129       DO 16 L=KK,N
001130    16 B(R(L))=B(R(L))-B(R(K))*A(R(L),C(K))
001131    15 CONTINUE
001132    17 AINV(C(N),R(J))=B(R(N))/A(R(N),C(N))
001133       I=N-1
001134       DO 18 K=1,I
001135       SUM=0.D0
001136       DO 31 L=1,K
001137    31 SUM=SUM+A(R(N-K),C(N-K+L))*AINV(C(N-K+L),R(J))
001138    18 AINV(C(N-K),R(J))=(B(R(N-K))-SUM)/A(R(N-K),C(N-K))
001139    11 CONTINUE
001140    99 RETURN
001141       END
001142 C*****************************************************
001143       SUBROUTINE STRIP(OUT,IBL,VCH,IA,IB,IC,ID,NQ,NIQ)
001144 C*****************************************************
001145       IMPLICIT REAL*8 (A-H),(O-Z)
001146 C*************************************************
001147 C                                                *
001148 C N.B: QUADRATIC BASELINE DEFEATED.               *
001149 C       CONSTANT BASELINE SUBTRACTED.            *
001150 C                                                *
001151 C*************************************************
001152       INTEGER OUT
001153       DIMENSION VCH(1024),A(3,3),E(3),F(3),WB(1024)
001154 C     THIS  ROUTINE FITS A QUADRATIC TO THE BSLN IN THE LIMITS IA,IB,IC
001155 C     AND ID.THE BSLN IS THEN SUBTRACTED FROM VCH.
001156
001157 C  M.S:IOFSET IS THE ORIGIN FOR THE BASE LINES ON EITHER PEAK SIDES
001158
001159       IOFSET=(IB+IC)/2
001160       IE=0
001161       CHISQ=0
001162       NF=0
001163       A(1,1)=0.
001164       A(1,2)=0.
001165       A(1,3)=0.
001166       A(2,3)=0.
001167       A(3,3)=0.
001168       E(1)=0.
001169       E(2)=0.
001170       E(3)=0.
001171       ISTRT = IA
001172       ISTP = IB
001173 C     MATRIX ELEMENTS FOR THE QUAD, FIT ARE EVALUATED HERE.
001174   11  CONTINUE
001175 C
001176       DO  1  I=ISTRT,ISTP
001177       X=DFLOAT(I-IOFSET)
001178 C     X=DFLOAT(I)
001179       A(1,1)=A(1,1)+X**4
001180       A(1,2)=A(1,2)+X**3
001181       A(1,3)=A(1,3)+X**2
001182       A(2,3)=A(2,3)+X
001183       A(3,3)=A(3,3)+1.
```

```
001184 C
001185       E(1)=E(1)+VCH(I)*X**2
001186 C
001187       E(2)=E(2)+VCH(I)*X
001188 C
001189    1  E(3)=E(3)+VCH(I)
001190       IE=IE+1
001191       ISTRT = IC
001192       ISTP = ID
001193       IF(IE .LT. 2) GO TO 11
001194       A(3,1)=A(1,3)
001195       A(2,2)=A(1,3)
001196       A(2,1)=A(1,2)
001197       A(3,2)=A(2,3)
001198 C     SOLVE NORMAL EQNS.
001199       D=A(1,1)*(A(2,2)*A(3,3)-A(3,2)*A(2,3))-A(1,2)*(A(2,1)*A(3,3)-
001200      @A(3,1)*A(2,3))+A(1,3)*(A(2,1)*A(3,2)-A(3,1)*A(2,2))
001201       D1=E(1)*(A(2,2)*A(3,3)-A(3,2)*A(2,3))-A(1,2)*(E(2)*A(3,3)-
001202      @E(3)*A(2,3))+A(1,3)*(E(2)*A(3,2)-E(3)*A(2,2))
001203       D2=A(1,1)*(E(2)*A(3,3)-E(3)*A(2,3))-E(1)*(A(2,1)*A(3,3)-
001204      @A(3,1)*A(2,3))+A(1,3)*(A(2,1)*E(3)-A(3,1)*E(2))
001205       D3=A(1,1)*(A(2,2)*E(3)-A(3,2)*E(2))-A(1,2)*(A(2,1)*E(3)-
001206      @A(3,1)*E(2))+E(1)*(A(2,1)*A(3,2)-A(3,1)*A(2,2))
001207       E(1)=D1/D
001208       E(2)=D2/D
001209       E(3)=D3/D
001210       AVBSL=E(3)/A(3,3)
001211       E(3)=D3/D
001212 C     SUBTRACT BSLN FROM VCH.
001213       ISTRT = IA
001214       DO 4 I=ISTRT,ISTP
001215       IF(I.GT.IB.AND.I.LT.IC) GO TO 4
001216       NF = NF + 1
001217       IF(VCH(I).NE.0) GO TO 5
001218       CHISQ=CHISQ+(((VCH(I)-E(1)*X**2-E(2)*X-E(3))**2)/1.0)
001219       GO TO 4
001220    5  CHISQ=CHISQ+(((VCH(I)-E(1)*X**2-E(2)*X-E(3))**2)/VCH(I))
001221    4  CONTINUE
001222       NFREE = NF - 3
001223       CHISQR=CHISQ/NFREE
001224       DO  2  I=ISTRT,ISTP
001225       X=DFLOAT(I-IOFSET)
001226 C     X=DFLOAT(I)
001227       IF (IBL.NE.0) GO TO 12
001228       VCH(I)=VCH(I)-AVBSL
001229       GO TO 2
001230   12  VCH(I)=VCH(I)-(E(1)*X**2+E(2)*X+E(3))
001231    2  CONTINUE
001232 C***********************************************
001233 C                                              *
001234 C N.B: QUAD BSLINE DEFEATED.                   *
001235 C                                              *
001236 C***********************************************
001237       IF (IBL.NE.0) GO TO 199
001238       GO TO 198
001239  199  WRITE(OUT,202) E(1),E(2),E(3)
001240  202  FORMAT(' ','BSL QUAD. FIT: A=',E11.4,' B=',E11.4,' C=',E11.4)
001241       GO TO 197
001242  198    WRITE(OUT,100) AVBSL
001243  100  FORMAT(' ','CONSTANT BASELINE SUBTRACTED, AVBSL=',E11.4)
001244  197    WRITE(OUT,200) CHISQR
001245  200  FORMAT(' CHISQR= ',E11.4)
001246
001247       RETURN
001248       END
```

```
001249 C*************************************************************************
001250       SUBROUTINE STATS ( X,Y,N1,N2,XBAR,XMOM,TVAR,SGMA,ALPHA3,ALPHA4 )
001251 C*************************************************************************
001252       IMPLICIT REAL*8 (A-H),(O-Z)
001253 C                                SUBROUTINES CALLED         NONE
001254 C               ROUTINE CALCULATES THE MEAN AND FIRST FOUR MOMENTS OF A
001255 C               VARIABLE X , WHEN THE FREQUENCY DISTRIBUTION OF X IS
001256 C               GIVEN BY Y .
001257 C               FOR DEALING WITH PEAKS , Y(I) GIVE THE PEAK HEIGHT.
001258 C               IF A SIMPLE MEAN OF A SET X IS WANTED, EACH Y(I) = 1
001259 C                              INPUT
001260 C               X = THE VARIABLE
001261 C               Y = THE FREQUENCY DISTRIBUTION OF X
001262 C               N1 , N2  ARE THE FIRST AND LAST INDICES OF THE ARRAYS
001263 C                              OUTPUT
001264 C               XBAR = AVERAGE VALUE OF X
001265 C               XMOM(I) ARE THE FIRST FOUR MOMENTS OF THE DISTRIBUTION
001266 C               TVAR IS THE TOTAL VARIANCE
001267 C               SGMA = STANDARD DEVIATION OF THE MEAN
001268 C               ALPHA3 IS A MEASURE OF SKEWNESS
001269 C               ALPHA4 IS A MEASURE OF PEAKEDNESS
001270       DIMENSION X(1024),Y(1024),
001271      1          XMOM(4)
001272       DOUBLE PRECISION SUMXY,SUMY,XBAR
001273 C          MEAN
001274       SUMY = 0.
001275       SUMXY = 0.
001276       DO 1 I=N1,N2
001277       SUMY = SUMY + Y(I)
001278     1 SUMXY = SUMXY + X(I) * Y(I)
001279       XBAR = SUMXY / SUMY
001280 C          MOMENTS
001281 C          XMOM(1) SHOULD BE ZERO
001282 C          TVAR IS THE TOTAL VARIANCE
001283 C          XMOM(2) = TVAR / N-1  IS THE VARIANCE OF X
001284       DO 3 K=1,4
001285       SUMDY = 0.
001286       DO 2 I=N1,N2
001287     2 SUMDY = SUMDY + (( X(I)-XBAR )**K) * Y(I)
001288     3 XMOM(K) = SUMDY / (SUMY-1)
001289       TVAR = XMOM(2) * ( SUMY - 1 )
001290 C          IF THE STANDARD DEVIATION OF A SINGLE DETERMINATION IS
001291 C          REQUIRED , TAXE DSQRT ( XMOM(2) )
001292       SGMA = DSQRT ( XMOM(2) /SUMY )
001293       ALPHA3 = XMOM(3) / ( XMOM(2) )**1.5
001294 C          IF ALPHA 4 < 3.0 , THE DISTRIBUTION IS LESS PEAKED THAN GAUSSIAN
001295 C          IF ALPHA 4 > 3.0 , THE DISTRIBUTION IS MORE PEAKED THAN GAUSSIAN
001296       ALPHA4 = XMOM(4) / ( XMOM(2)**2 )
001297       RETURN
001298       END
001299 C*************************************************************************
001300       SUBROUTINE WTFIT3 ( N,X,EX,Y,EY,A,B,EA,EB,IWR,LNPRNT,MXIT,XSQ )
001301 C*************************************************************************
001302       IMPLICIT REAL*8 (A-H),(O-Z)
001303       DIMENSION X(N) ,EX(N),Y(N),EY(N) ,
001304      2          U(100),V(100),W(100)
001305 C          ROUTINE FITS A STRAIGHT LINE TO THE SET OF PAIRS OF POINTS
001306 C          Y(I) , X(I) WHEN THERE IS ERROR IN BOTH COORDINATES .
001307 C
001308 C                                  Y(I) = A + B * X(I)
001309 C
001310 C          B      THE SLOPE OF THE FITTED LINE .
001311 C          VB     THE VARIANCE OF B .
001312 C          A      THE INTERCEPT OF THE FITTED LINE .
001313 C          VA     THE VARIANCE OF A .
001314 C
001315 C           MODIFIED FROM J.H. WILLIAMSON   C.J.P. V46 P1845 , 1968
001316 C
001317       NF = N-2
001318       DO 10 I=1,N
001319       U(I) = EX(I)*EX(I)
001320    10 V(I) = EY(I)*EY(I)
001321       A = 0.
001322       B = 0.
```

```
001323       IT = 0
001324    11 IT = IT + 1
001325       IF ( IT .GT. MXIT )     GO TO 15
001326       AO = A
001327       BO = B
001328       SW = 0.
001329       SWX = 0.
001330       SWY = 0.
001331       DO 12 I=1,N
001332       W(I) = 1. / ( V(I) + B*B*U(I) )
001333       SW = SW + W(I)
001334       SWX = SWX + W(I)*X(I)
001335    12 SWY = SWY + W(I)*Y(I)
001336       XBAR = SWX / SW
001337       YBAR = SWY / SW
001338       SL = 0.
001339       SWZ = 0.
001340       SWZX = 0.
001341       SWZY = 0.
001342       SWZZ = 0.
001343       SWXY = 0.
001344       SWXP = 0.
001345       DO 13 I=1,N
001346       XP = X(I) - XBAR
001347       YP = Y(I) - YBAR
001348       WZ = W(I) * W(I) *( V(I)*XP + B*U(I)*YP )
001349       SL = SL + W(I)*W(I) * ( XP*XP*V(I) + YP*YP*U(I) )
001350       SWXY = SWXY + W(I) * XP * YP
001351       SWZ = SWZ + WZ
001352       SWZX = SWZX + WZ * XP
001353       SWZY = SWZY + WZ * YP
001354       SWXP = SWXP + W(I)*XP
001355    13 SWZZ = SWZZ + WZ*WZ/W(I)
001356       B = SWZY / SWZX
001357       A = YBAR - B * XBAR
001358       ZBAR = SWZ / SW
001359       Q = SWXY/B + 4.*( SWZZ-SWZ*ZBAR-SWZX + ZBAR*SWXP )
001360       VB = SL / (Q*Q)
001361       XZ = XBAR + 2.*ZBAR
001362       VA = ( VB*XZ + 2.*ZBAR/Q )*XZ + 1./SW
001363       IF ( DABS(B-BO) .GT. .001*DSQRT(VB) )     GO TO 11
001364       IF ( DABS(A-AO) .GT. .001*DSQRT(VA) )    GO TO 11
001365       XSQ = 0.
001366       DO 14 I=1,N
001367       F = A + B*X(I)
001368       ERR = Y(I) - F
001369    14 XSQ = XSQ + ERR*ERR*W(I)
001370    15 CONTINUE
001371       EA = DSQRT( VA )
001372       EB = DSQRT( VB )
001373       IF(IWR .EQ. 1) WRITE(LNPRNT,101) A,EA,B,EB,XBAR,YBAR,XSQ,NF,IT
001374   101 FORMAT ('0', 4X,2(F12.4,' +- ',F9.4),2F12.4,F12.2,2I8 )
001375       RETURN
001376       END
001377 C*********************************************************************
001378       SUBROUTINE CUT3 ( VCH,BSL,PC,N1,N2,N1NW,N2NW,NCPS,IM,CL,KK )
001379 C*********************************************************************
001380       IMPLICIT REAL*8 (A-H),(O-Z)
001381 C
001382 C       THIS PROGRAM SEARCHES FOR THE MAXIMUM VALUE IN THE ARRAY VCH
001383 C       BETWEEN THE INDICES N1 AND N2. THE INDEX WHERE THE MAXIMUM VALUE
001384 C       OCCURS IS RETURNED IN IM.
001385 C
001386       DIMENSION VCH(1024)
001387       N1 = N1 - 2
001388       N2 = N2 + 2
001389       N = N2 - N1
001390       VM = VCH(N1)
001391 C          FIND MAXIMUM VALUE AND ITS LOCATION
001392       DO 11 I=N1,N2
001393       IF ( VCH(I) .GE. VM )      VM = VCH(I)
001394       IF ( VCH(I) .GE. VM )      IM = I
001395    11 CONTINUE
001396 C         SMOOTH THE PEAK AT THE MAXIMUM
001397 C             7 POINT PARABOLIC SMOOTHING
```

```
001398        VM = ( VCH(IM-3) + VCH(IM+3) + (VCH(IM-2)+VCH(IM+2))*6. +
001399       2  (VCH(IM-1)+VCH(IM+1))*9.+ VCH(IM)*10. ) / 42.
001400  C
001401  C          SET LEVEL ABOVE BASELINE FOR PEAK LIMITS.
001402  C
001403        CL = BSL + (VM-BSL)*.01*PC
001404        IC = 0
001405  C          SEARCH FOR START OF PEAK.
001406        DO 12 I=N1,N2
001407        IF ( VCH(I) .LT. CL )    GO TO 10
001408        IC = IC + 1
001409        IF ( IC .LT. NCPS )      GO TO 12
001410        N1NW = I -(NCPS-1)
001411        GO TO 15
001412     10 IC = 0
001413     12 CONTINUE
001414     15 CONTINUE
001415        JC = 0
001416  C          SEARCH FOR END OF PEAK.
001417        DO 13 J=1,N
001418        I = N2 + 1 - J
001419        IF ( VCH(I) .LT. CL )    GO TO 16
001420        JC = JC + 1
001421        IF ( JC .LT. NCPS )      GO TO 13
001422        N2NW = I + (NCPS-1)
001423        GO TO 14
001424     16 JC = 0
001425     13 CONTINUE
001426     14 CONTINUE
001427        N1 = N1 + 2
001428        N2 = N2 - 2
001429        RETURN
001430        END
001431  C*********************************************************************
001432        SUBROUTINE WTDAVG ( D,E,N,IWR,LNPRNT,WM,S )
001433  C*********************************************************************
001434        IMPLICIT REAL*8 (A-H),(O-Z)
001435        DIMENSION D(1),E(1)
001436  C          ROUTINE CALCULATES THE WEIGHTED AVERAGE OF N DETERMINATIONS D
001437  C                  WHERE THE WEIGHTING IS INVERSELY AS THE VARIANCE .
001438  C          IF N=1 I.E. ONLY ONE DETERMINATION , IT EXITS UNCHANGED .
001439        WM = D(1)
001440         S = E(1)
001441        IF ( N .EQ. 1 )      GO TO 13
001442        SMW = 0.
001443        SMD = 0.
001444  C          SMW   THE SUM OF THE WEIGHTS . WEIGHT OF THE MEAN = SMW .
001445        DO 11 I=1,N
001446        SMW = SMW + 1. / ( E(I)*E(I) )
001447     11 SMD = SMD + D(I) / ( E(I)*E(I) )
001448  C          THE VARIANCE OF THE MEAN = 1. / SMW .
001449  C          S1    SIGMA INTERNAL
001450        S1 = DSQRT ( 1./SMW )
001451  C          WM    THE WEIGHTED MEAN
001452        WM = SMD / SMW
001453        SME = 0.
001454        DO 12 I=1,N
001455     12 SME = SME + ( D(I)-WM )*( D(I)-WM ) / ( E(I)*E(I) )
001456  C          S2    SIGMA EXTERNAL
001457        S2 = DSQRT ( SME / ( (N-1)*SMW ) )
001458        IF ( IWR .EQ. 1 )   WRITE ( LNPRNT,101 ) WM,S1,S2
001459    101 FORMAT ('0     WEIGHTED MEAN =' F13.3,2F11.3 )
001460  C          S     THE OUTPUT STANDARD OF WM ....THE LARGER OF S1,S2 .
001461        S = DMAX1 ( S1,S2 )
001462     13 CONTINUE
001463        RETURN
001464        END
001465  C*********************************************************************
001466        SUBROUTINE NINESM ( N1,N2,V,SMV )
001467  C*********************************************************************
001468        IMPLICIT REAL*8 (A-H),(O-Z)
001469  C          ROUTINE CONVOLUTES DATA SET 'V' WITH SPECIFIED INTEGERS
001470  C          INPUT  ---  DATA SET 'V' ,   NUMBER OF DATA POINTS 'N'
001471  C          OUTPUT  ---  SMOOTHED DATA SET 'SMV'
```

```
001472 |      DIMENSION  V(1),SMV(1)
001473 |      M1 = N1 + 4
001474 |      M2 = N2 - 4
001475 |      DO 1 I=N1,M1
001476 |    1 SMV(I) = V(I)
001477 |      DO 2 I=M1,M2
001478 |      VS=59.*V(I) + 54.*(V(I-1)+V(I+1)) + 39.*(V(I-2)+V(I+2)) +
001479 |     @  14.*(V(I-3)+V(I+3)) - 21.*(V(I-4)+V(I+4))
001480 |    2 SMV(I) = VS/231.
001481 |      DO 3 I=M2,N2
001482 |    3 SMV(I) = V(I)
001483 |      RETURN
001484 |      END
001485 |C*******************************************************
001486 |      SUBROUTINE SRCHTP (N)
001487 |C*******************************************************
001488 |      IMPLICIT REAL*8 (A-H),(O-Z)
001489 |      NE=1
001490 |   70 READ ( 9,END=74,ERR=1 ) NT
001491 |      GO TO 73
001492 |    1 GO TO 70
001493 |   73 IF(NT-N+1)75,71,72
001494 |   74 BACKSPACE 9
001495 |      BACKSPACE 9
001496 |      NE=2
001497 |      GO TO 70
001498 |   72 NB=NT-N+2
001499 |      DO 81 J1=1,NB
001500 |   81 BACKSPACE 9
001501 |      GO TO 70
001502 |   75 IF(NE.EQ.1) GO TO 70
001503 |      WRITE(OUT,91)N,NT
001504 |   91 FORMAT('1  SRCHTP LOOKED FOR REC'I6,' ,MAX REC IS NO.'I6)
001505 |   71 RETURN
001506 |      END
001507 |C*************************************************************
001508 |      SUBROUTINE GETDAT ( NRECN )
001509 |C*************************************************************
001510 |      IMPLICIT REAL*8 (A-H),(O-Z)
001511 |C       PROGRAM MASTER
001512 |        BYTE ANS
001513 |        INTEGER IDATA(4096), ILIN, MARKS(4,2)
001514 |        LOGICAL QUIT /.FALSE./
001515 |        COMMON / DATA_A / IDATA, ILIN, QUIT, ID
001516 |        COMMON / DATA_B / MARKS
001517 |C
001518 |C
001519 |        WRITE(6,600)
001520 |C
001521 |C               GET DATA
001522 |C
001523 |  5     WRITE(*,*) 'Data will be taken from a file.'
001524 |C       WRITE(6,610)
001525 |C       READ(5,500),ANS
001526 |C       hardwire an F for file.
001527 |        ANS = '106'O
001528 |        ANS = ANS .AND. '137'O
001529 |C
001530 |        IF (ANS .EQ. 'T') THEN
001531 |C  <==>    CALL GETAPE
001532 |        ELSE IF (ANS .EQ. 'F') THEN
001533 |           CALL GETFIL (NRECN)
001534 |        ELSE IF (ANS .EQ. 'I') THEN
001535 |           CALL GETINT
001536 |        ELSE
001537 |           TYPE *,'Incorrect response, try again.'
001538 |           GO TO 5
001539 |        END IF
001540 |C
001541 |C               DISPLAY DATA
001542 |C
001543 |        WRITE(6,620)
001544 |        READ(5,500),ANS
001545 |        ANS = ANS .AND. '137'O
001546 |        IF (ANS .EQ. 'N') GO TO 6
```

```
001547 |        CALL DISP
001548 |C
001549 |C               WRITE DATA TO OUTPUT FILE
001550 |C
001551 |C       WRITE(6,660)
001552 |C       READ(5,500) ANS
001553 |C       ANS = ANS .AND. '137'O
001554 |C       IF (ANS .NE. 'Y') GO TO 6
001555 |C       CALL PUTDAT
001556 |        GOTO 6
001557 |C
001558 |C       WRITE(6,650)
001559 |C       READ(5,500) ANS
001560 |C       ANS = ANS .AND. '137'O
001561 |C       IF (ANS .NE. 'Y') GO TO 5
001562 |C
001563 |C               ANALYZE DATA
001564 |C
001565 |C       CLOSE(4)
001566 |C       WRITE(6,640)
001567 |C       READ(5,500) ANS
001568 |C       ANS = ANS .AND. '137'O
001569 |C
001570 |C       IF (ANS .EQ. 'N') GO TO 6
001571 |C        CALL RESANAL
001572 |C       END IF
001573 |C
001574 |  6     CONTINUE
001575 |        RETURN
001576 |  10    STOP
001577 |C
001578 |500     FORMAT(A1)
001579 |600     FORMAT(' ','WELCOME')
001580 |610     FORMAT(' ','Where do you want to take the data from,',
001581 |     *         ' tape, file or interface?',/,' ','ENTER [T/F/I]:  ',$)
001582 |620     FORMAT(' ','Do you want the data displayed?[Y|<CR>/N] ',$)
001583 |630     FORMAT('+',A1,$)
001584 |640     FORMAT(' ','Do you want to analyze the data now?[Y|<CR>/N] ',$)
001585 |650     FORMAT(' ','Is that all the data?[Y/N|<CR>] ',$)
001586 |660     FORMAT(' ','Do you want this data stored? ',$)
001587 |        END
001588 |C*****************************************************************
001589 |        SUBROUTINE GETFIL(NRECN)
001590 |C*****************************************************************
001591 |      IMPLICIT REAL*8 (A-H),(O-Z)
001592 |        LOGICAL QUIT
001593 |        INTEGER IDATA(4096),ICH(4096), ITRANS(8), ID(4)
001594 |        CHARACTER*64 DATA(512),BLANK
001595 |        CHARACTER*12 FILNAM
001596 |        CHARACTER*1 ANS
001597 |        COMMON / DATA_A / IDATA, ILIN, QUIT, ID
001598 |
001599 |C               READ IN DATA FROM AN OLD FILE
001600 |  32    IQUAD = 4
001601 |
001602 |        ILIN=IQUAD*128
001603 |
001604 |        OPEN(UNIT=3,FILE='PP.D',STATUS='OLD',READONLY,ACCESS='SEQUENTIAL'
001605 |     *  ,ERR=35)
001606 |
001607 |  46    READ(3,310,END=42,ERR=40) ID(1),ID(2),ID(3),ID(4)
001608 |        READ(3,300,END=42,ERR=40) (IDATA(I), I=1,ILIN*8)
001609 |
001610 |C
001611 |C       CHECK FOR CORRECT RECORD NUMBER.
001612 |
001613 |C  76   WRITE(*,146), ID                ! for debugging. Too tedious for real
001614 |  146   FORMAT(' ',4(3X,I10))
001615 |C       WRITE(*,*) (I,IDATA(I),I=1,ILIN*8) ! more debugging stuff.
001616 |        IF(NRECN .EQ. ID(1)) THEN
001617 |          WRITE(*,147) NRECN,(ID(I),I=1,4)
001618 |  147   FORMAT(' Record found:',5(1X,I10))
001619 |          CALL AUTOMARKSCALE
001620 |          GO TO 45
001621 |
```

```
001622          ELSE
001623            GO TO 46
001624          END IF
001625    35    WRITE(6,650), FILNAM
001626          READ(5,500), ANS
001627          IF (ANS .EQ. 'C'.OR.ANS.EQ.'c') GO TO 32
001628          QUIT=.TRUE.
001629          GO TO 45
001630    40    WRITE(6,660), ILIN
001631          READ(5,500), ANS
001632          IF (ANS .EQ. 'Q'.OR.ANS.EQ.'q') QUIT=.TRUE.
001633          GO TO 45
001634    42    WRITE(6,670), ILIN
001635
001636    45    CLOSE(3)          ! somebody had commented this out! (before jan90)
001637          RETURN            ! this closure is important.
001638
001639 300      FORMAT(1024A4)
001640 310      FORMAT(4A4)
001641 500      FORMAT(A)
001642 520      FORMAT(I)
001643 550      FORMAT(A12)
001644 630      FORMAT(' ','How many quarters to be read? '$)
001645 650      FORMAT(' ','Error opening file ',A12,' Continue or Quit ',
001646      *   '(C/Q)? ',$)
001647 660      FORMAT(' ','Error reading line ',I3,'.  Continue or Quit ',
001648      *   '(C/Q)? ',$)
001649 670      FORMAT(' ','End of file encountered at line ',I3)
001650 680      FORMAT(' ','Name of file containing data: ',$)
001651 C
001652          END
001653 C*********************************************************************
001654          SUBROUTINE GETINT
001655 C*********************************************************************
001656        IMPLICIT REAL*8 (A-H),(O-Z)
001657          INTEGER IDATA(4096), ITRANS(8)
001658          CHARACTER*64 DATA(512),BLANK
001659          COMMON / DATA_A / IDATA, ILIN
001660 C
001661 5        OPEN(UNIT=1,FILE='_TTB3:',STATUS='OLD',readonly,ACCESS='SEQUENTIAL'
001662      *   ,RECORDSIZE=64,BLOCKSIZE=68)
001663 C
001664 C                 DETERMINE NUMBER OF QUARTERS
001665 C
001666 10       WRITE(6,630)
001667          READ(5,520)UADIQAD
001668          GO TO (15,15,15,15),IQAD
001669          GO TO 10
001670 C
001671 15       ILIN=IQAD*128-1
001672          WRITE(6,*) 'Push READOUT on MCA.'
001673 C
001674 C                 READ OUT FIRST (BLANK) LINE
001675 C
001676          READ(1,110) BLANK
001677 C
001678 C                 READ DATA
001679 C
001680          DO 20 I=1,ILIN
001681             READ(1,110,END=25) DATA(I)
001682 20       CONTINUE
001683 C
001684 25       CLOSE(1)
001685 C
001686          WRITE(6,*) 'Read complete. Filling MCA.DAT.'
001687 C
001688          OPEN(UNIT=2,FILE='MCA.DAT',STATUS='NEW')
001689 C
001690 C                 CONVERT CHARACTER DATA TO INTEGER DATA
001691 C
001692          DO 30 I=1,ILIN
001693             DECODE (64,100,DATA(I)) ITRANS
001694                DO 30 J=1,8
001695                IDATA((I-1)*8+J) = ITRANS(J)
001696 30       CONTINUE
```

```
001697 C
001698 C               STORE INTEGER DATA IN MCA.DAT
001699 C
001700         WRITE(2,200) (IDATA(I), I=1,ILIN*8)
001701 C
001702         CLOSE(2)
001703 C
001704         RETURN
001705 C
001706 100     FORMAT(8(1x,I7))
001707 110     FORMAT(A64)
001708 200     FORMAT(' ',8(1X,I7))
001709 520     FORMAT(I)
001710 630     FORMAT(' ','How many quarters to be read? '$)
001711 C
001712         END
001713 C*************************************************************
001714         SUBROUTINE DISP
001715       IMPLICIT REAL*8 (A-H),(O-Z)
001716         BYTE ANS, STP
001717         BYTE BEEP
001718         INTEGER IDATA(4096),MARKS(4,2),ISC(2)
001719         COMMON / DATA_A / IDATA, ILIN
001720         COMMON / DATA_B / MARKS
001721         COMMON / DATA_C / ISC
001722         COMMON / DATA_D / IPART
001723         COMMON / DATA_E / IX,IY,IA,IB
001724         BEEP=7
001725         IPART=3
001726 C
001727         NPTS=ILIN*8
001728 C
001729 C                PLOTTING BEGINS HERE
001730 C
001731   99    WRITE(*,*) 'Scale factor for quadrant 1 is:   ',ISC(1)
001732         WRITE(*,*) 'Scale factor for quadrants 2-3 is:',ISC(2)
001733         WRITE(*,*) 'Hit return to continue:'
001734         READ(*,500) ANS
001735 C
001736         CALL SETUP
001737 C
001738         CALL PLOT
001739 C
001740         WRITE(6,699) BEEP
001741         WRITE(6,200), ILIN*8
001742 C
001743 C                RE-SCALE DATA
001744 C
001745 100     WRITE(6,680)
001746 680     FORMAT(' Would you like to re-scale some of the data?',
001747      *'[Y/N|<CR>] ',$)
001748         READ(5,500),ANS
001749         ANS = ANS .AND. '137'O
001750 C
001751         IF (ANS .EQ. 'Y'.OR.ANS.EQ.'y') THEN
001752            CALL RESCALE
001753            CALL PLOT
001754            WRITE(6,699) BEEP
001755         END IF
001756 C
001757 C       END OF PLOTTING POINTS.
001758 C
001759 C                CROSS-HAIRS
001760 C
001761         IA = 4
001762         IB = 4
001763 C       The eight marks were read at the start or given as defaults.
001764 C       Clear text off screen.
001765 75      CALL GETEXT
001766         CALL XHAIRS
001767         TYPE*, MARKS(1,1)
001768 C
001769
001770 80      WRITE(6,*) 'Continue (to replot or xhairs) or Stop (dump out of this'
001771         WRITE(6,630)
```

```
001772 |630     FORMAT(' spectrum and on to the next one)[C/S|<CR>]? ',$)
001773 |        READ(5,500), ANS
001774 |        ANS = ANS.AND.'137'O
001775 |C
001776 |        IF(ANS .EQ. 'C'.OR.ANS.EQ.'c') THEN
001777 |           WRITE (6,640)
001778 |640     FORMAT(' ','Replot data or X-hairs [R/X|<CR>]? ',$)
001779 |           READ(5,500), ANS
001780 |           ANS = ANS.AND.'137'O
001781 |           IF (ANS .EQ. 'R'.OR.ANS.EQ.'r')THEN
001782 |             GO TO 100
001783 |           END IF
001784 |           CALL POS(0,700)
001785 |           GO TO 75
001786 |        END IF
001787 |C
001788 |C CLEAN UP AND SHUT DOWN GRAPHICS.
001789 |C
001790 |95      CALL GERASE
001791 |        CALL GVT100
001792 |C
001793 |        CALL SORT
001794 |C
001795 |        DO 97 I=1,2
001796 |           DO 97 J=1,4
001797 |97         WRITE(6,670),J,I,MARKS(J,I)
001798 |        RETURN
001799 |C
001800 |200     FORMAT('    THERE WERE ',I4,' POINTS READ.')
001801 |500     FORMAT( A )
001802 |520     FORMAT( I )
001803 |670     FORMAT(' ','MARKS(',I1,',',I1,') = ',I4)
001804 |699     FORMAT('+',A1,$)
001805 |        END
001806 |C
001807 |*************************************************************************
001808 |*************************************************************************
001809 |C
001810 |        SUBROUTINE SETUP
001811 |      IMPLICIT REAL*8 (A-H),(O-Z)
001812 |C
001813 |        INTEGER X(4)/0,1023,0,1023/
001814 |        INTEGER Y(4)/29,29,30,30/
001815 |        INTEGER XTIK(2), YTIK(2)/20,40/
001816 |C               INITIALIZE GRAPHICS
001817 |C
001818 |        CALL GVT640
001819 |        CALL GERASE
001820 |C
001821 |C               DRAW BASELINE
001822 |C
001823 |        CALL POS(0,0)
001824 |        WRITE(6,660)
001825 |        CALL GDRAW1(0,X,Y,4)
001826 |        DO 50 I=1,6
001827 |           XTIK(1) = (I-1)*200
001828 |           XTIK(2) = XTIK(1)
001829 |           CALL POS(XTIK(1),YTIK(1))
001830 |           CALL LINE(XTIK(1),YTIK(1),XTIK(2),YTIK(2))
001831 |C          CALL GPLOT1(TEXT(I),150,150,4)
001832 |  50    CONTINUE
001833 |        RETURN
001834 |C
001835 |660     FORMAT(' ','0',13X,'200',13X,'400',12X,'600',
001836 |     *         13X,'800',12X,'1000')
001837 |        END
001838 |C
001839 |*************************************************************************
001840 |*************************************************************************
001841 |C
001842 |        SUBROUTINE PLOT
001843 |      IMPLICIT REAL*8 (A-H),(O-Z)
001844 |C
001845 |        INTEGER IDATA(4096),ISC(2)
001846 |        INTEGER MATRIX_OF_POINTS(2,4096)
001847 |        INTEGER OLD
```

```
001848          COMMON / DATA_A / IDATA, ILIN
001849          COMMON / DATA_C / ISC
001850          COMMON / DATA_D / IPART
001851          IQUAD = (ILIN+1)/128
001852  C
001853          IF (IPART .EQ. 1) THEN
001854             IA = 1
001855             IB = 1
001856          ELSE IF (IPART .EQ. 2) THEN
001857             IA = 2
001858             IB = IQUAD
001859          ELSE
001860             IA = 1
001861             IB = IQUAD
001862          END IF
001863  C
001864  C                START PLOTING POINTS.
001865  C
001866    60    DO 70 J=IA,IB
001867  C
001868  C                CHOSE SCALING FACTOR
001869  C
001870             IF (J .EQ. 1) THEN
001871                K=1
001872             ELSE
001873                K=2
001874             END IF
001875  C
001876             IF (J .LT. IQUAD) THEN
001877                NPTS=1024
001878             ELSE
001879                NPTS=1016
001880             END IF
001881  C
001882  C*****************************************************************
001883  C
001884             DO 70 I=0,NPTS-1
001885  C
001886  C                 CREATE MATRIX_OF_POINTS
001887  C
001888                   INDEX1 = I+1+(J-1)*1024
001889
001890
001891                   IF(ISC(K).GT.0) THEN
001892                      MATRIX_OF_POINTS(2,INDEX1)
001893       *                 = IDATA(INDEX1)*ISC(K)+780-J*180
001894                   ELSE
001895                      MATRIX_OF_POINTS(2,INDEX1)
001896       *                 = IDATA(INDEX1)/IABS(ISC(K))+780-J*180
001897                   END IF
001898
001899                   MATRIX_OF_POINTS(1,I+1+(J-1)*1024) = I
001900  C
001901  C                    OFFSET DATA IF THE NUMBER IS TOO LARGE.
001902  C
001903                   IF(MATRIX_OF_POINTS(2,INDEX1).GT.(780-(J-1)*180)) THEN
001904                      MOP=MATRIX_OF_POINTS(2,INDEX1)
001905                      MOP=MOD(MOP,180)+(780-J*180)
001906                      MATRIX_OF_POINTS(2,INDEX1)=MOP
001907                   END IF
001908
001909    70    CONTINUE
001910          NUMPOINTS = (IQUAD-1)*1024+1016
001911                CALL GRF_PLOT_POINTS(NUMPOINTS,MATRIX_OF_POINTS)
001912  C*****************************************************************
001913          RETURN
001914          END
001915  C
001916  ***********************************************************************
001917  ***********************************************************************
001918  C
001919          SUBROUTINE RESCALE
001920        IMPLICIT REAL*8 (A-H),(O-Z)
```

```
001921 C
001922         BYTE ANS
001923         INTEGER ISC(2)
001924         COMMON / DATA_C / ISC
001925         COMMON / DATA_D / IPART
001926 C
001927         WRITE(6,*) '+ve scale factor multplies spectrum, -ve scale factor'
001928         WRITE(*,*) 'divides spectrum (by abs mag of scale factor).'
001929         WRITE(*,*) 'First factor applies to quadrant 0, second to quads 1-3.'
001930 10      WRITE(*,*) 'Current scale factors are:',ISC(1),ISC(2)
001931         IPART = 3
001932         WRITE(*,*) 'Enter new scale factors (integers only, and not 0!):'
001933         READ(*,*,ERR=10) ISC(1),ISC(2)
001934         IF(ISC(1).EQ.0) ISC(1)=1
001935         IF(ISC(2).EQ.0) ISC(2)=1
001936
001937         WRITE(6,20)
001938 20      FORMAT(' ','Ready to re-plot?[Y|<CR>, or N to rescale] ',$)
001939         READ(5,500),ANS
001940         ANS=ANS.AND.'137'O
001941 C
001942         IF (ANS .EQ. 'N'.OR.ANS.EQ.'n') THEN
001943            CALL GETEXT
001944            WRITE(*,*) 'Then we''ll change the scale factors again.'
001945            GO TO 10
001946         END IF
001947
001948         CALL GERASE
001949         CALL GVT100
001950         CALL SETUP
001951         RETURN
001952
001953 500     FORMAT( A )
001954         END
001955 C
001956 ********************************************************************************
001957 ********************************************************************************
001958 C
001959         SUBROUTINE ERASE
001960       IMPLICIT REAL*8 (A-H),(O-Z)
001961 C
001962         BYTE CHAR,ESC,SLSH,ONE,D,ZERO,BEEP
001963         COMMON / DATA_D / IPART
001964         ESC=27
001965         SLSH=47
001966         ONE=49
001967         D=100
001968         ZERO=48
001969 C
001970         CALL GETEXT
001971         CALL GVT640
001972         CALL PUTCHR(ESC,5)
001973         CALL PUTCHR(SLSH,5)
001974         CALL PUTCHR(ONE,5)
001975         CALL PUTCHR(D,5)
001976 C
001977         IF (IPART .EQ. 1) THEN
001978            IA=600
001979            IB=779
001980            ISTART=1
001981            IQUAD=1
001982         ELSE
001983            IA=60
001984            IB=599
001985            ISTART=2
001986            IQUAD=(ILIN+1)/128
001987         END IF
001988 C
001989         DO 71 I=IA,IB
001990            CALL POS(1,I)
001991            CALL LINE(0,I,1023,I)
001992   71    CONTINUE
```

```
001993 C
001994         CALL PUTCHR(ESC,5)
001995         CALL PUTCHR(SLSH,5)
001996         CALL PUTCHR(ZERO,5)
001997         CALL PUTCHR(D,5)
001998 C
001999         RETURN
002000 C
002001         END
002002 C
002003 ************************************************************************
002004 ************************************************************************
002005
002006         SUBROUTINE XHAIRS
002007       IMPLICIT REAL*8 (A-H),(O-Z)
002008
002009         BYTE C
002010         INTEGER MARKS(4,2)
002011         CHARACTER LOADX(3)
002012         COMMON / DATA_B / MARKS
002013         COMMON / DATA_E / IX,IY
002014         LOADX(1) = CHAR(27)
002015         LOADX(2) = '/'
002016         LOADX(3) = 'f'
002017
002018         WRITE(*,*) 'X:exit M:mark D:delete 1-4: goto upper mark 5-8: ',
002019      *'goto lower mark'
002020         WRITE(*,*)
002021         CALL SHOWMARKS(MARKS)
002022         CALL GVT640
002023
002024 10      CALL GCURS1(C,IX,IY)
002025         CALL GVT100
002026         CALL GETEXT
002027         WRITE(*,*) 'X|<CR>:exit M:mark D:delete 1-4: goto upper mark ',
002028      *'5-8: goto lower mark'
002029         WRITE(*,*)
002030         WRITE(6,600) C, IX, IY
002031
002032         IF((C.EQ.'X').OR.(C.EQ.'x').OR.C.EQ.13)THEN
002033           GOTO 60          ! dump out.
002034         ELSE IF((C.EQ.'M').OR.(C.EQ.'m'))THEN
002035           CALL MARK
002036           CALL GVT640
002037         ELSE IF((C.EQ.'D').OR.(C.EQ.'d'))THEN
002038           CALL DELETE
002039           CALL GVT640
002040         ELSE IF(C.EQ.'1')THEN
002041           CALL GVT640
002042           CALL POS(MARKS(1,1),610)
002043           WRITE(6,700) LOADX
002044         ELSE IF(C.EQ.'2')THEN
002045           CALL GVT640
002046           CALL POS(MARKS(2,1),610)
002047           WRITE(6,700) LOADX
002048         ELSE IF(C.EQ.'3')THEN
002049           CALL GVT640
002050           CALL POS(MARKS(3,1),610)
002051           WRITE(6,700) LOADX
002052         ELSE IF(C.EQ.'4')THEN
002053           CALL GVT640
002054           CALL POS(MARKS(4,1),610)
002055           WRITE(6,700) LOADX
002056         ELSE IF(C.EQ.'5')THEN
002057           CALL GVT640
002058           CALL POS(MARKS(1,2),590)
002059           WRITE(6,700) LOADX
002060         ELSE IF(C.EQ.'6')THEN
002061           CALL GVT640
002062           CALL POS(MARKS(2,2),590)
002063           WRITE(6,700) LOADX
002064         ELSE IF(C.EQ.'7')THEN
002065           CALL GVT640
```

```
002066            CALL POS(MARKS(3,2),590)
002067            WRITE(6,700) LOADX
002068          ELSE IF(C.EQ.'8')THEN
002069            CALL GVT640
002070            CALL POS(MARKS(4,2),590)
002071            WRITE(6,700) LOADX
002072          ELSE
002073            CALL GVT640
002074          END IF
002075
002076          GO TO 10
002077
002078    60    RETURN
002079
002080  600     FORMAT('+','--',A4,2I)
002081  700     FORMAT('+',3A1,$)
002082          END
002083
002084  ********************************************************************************
002085          SUBROUTINE SHOWMARKS(MARKS)
002086        IMPLICIT REAL*8 (A-H),(O-Z)
002087          INTEGER MARKS(4,2)
002088          CALL GVT640
002089          DO 20 J=1,2
002090          DO 10 K=1,4
002091            CALL TXT(MARKS(K,J)-5,(770-180*J),'^')
002092  10      CONTINUE
002093  20      CONTINUE
002094          CALL GVT100
002095          RETURN
002096          END
002097  ********************************************************************************
002098  C
002099          SUBROUTINE MARK
002100        IMPLICIT REAL*8 (A-H),(O-Z)
002101  C
002102          INTEGER MARKS(4,2)
002103          COMMON / DATA_B / MARKS
002104          COMMON / DATA_E / IX,IY,IA,IB
002105  C
002106          IF (IY .GE. 600) THEN
002107             IA=IA+1
002108             MARKS(IA,1) = IX
002109             CALL GVT640
002110             CALL TXT(IX-5,590,'^')
002111             CALL GVT100
002112          ELSE
002113             IB=IB+1
002114             MARKS(IB,2) = IX
002115             CALL GVT640
002116             CALL TXT(IX-5,410,'^')
002117             CALL GVT100
002118          END IF
002119  C
002120          RETURN
002121          END
002122  C
002123  ********************************************************************************
002124  ********************************************************************************
002125  C
002126          SUBROUTINE DELETE
002127        IMPLICIT REAL*8 (A-H),(O-Z)
002128  C
002129          BYTE ESC,SLSH,ONE,ZERO,D
002130          INTEGER MARKS(4,2),DIFF(4)
002131          INTEGER OLD
002132          COMMON / DATA_B / MARKS
002133          COMMON / DATA_E / IX,IY,IA,IB
002134          ESC=27
002135          SLSH=47
002136          ONE=49
002137          ZERO=48
```

```
002138          D=100
002139 C
002140          IF (IY .GE. 600) THEN
002141             J = 590
002142 C
002143             DO 20 I=1,4
002144                MDUM = MARKS(I,1)-IX
002145                DIFF(I)=ABS(MDUM)
002146 20          CONTINUE
002147 C
002148             K=1
002149 C
002150             DO 30 I=2,4
002151             IF (DIFF(I).LT.DIFF(K)) THEN
002152                IF (MARKS(I,1).NE.0) K=I
002153             END IF
002154   30        CONTINUE
002155 C
002156             OLD = MARKS(K,1)-5
002157             MARKS(K,1) = MARKS(4,1)
002158             MARKS(4,1) = 0
002159             IA = IA-1
002160          ELSE
002161             J = 410
002162 C
002163             DO 40 I=1,4
002164   40           DIFF(I)=ABS(MARKS(I,2)-IX)
002165 C
002166             K=1
002167 C
002168             DO 50 I=2,4
002169             IF (DIFF(I).LT.DIFF(K)) THEN
002170                IF(MARKS(I,2).NE.0) K=I
002171             END IF
002172   50        CONTINUE
002173 C
002174             OLD = MARKS(K,2)-5
002175             MARKS(K,2) = MARKS(4,2)
002176             MARKS(4,2) = 0
002177             IB = IB-1
002178          END IF
002179 C
002180          CALL GVT640
002181          CALL PUTCHR(ESC,5)
002182          CALL PUTCHR(SLSH,5)
002183          CALL PUTCHR(ONE,5)
002184          CALL PUTCHR(D,5)
002185          CALL TXT(OLD,J,'^')
002186          CALL PUTCHR(ESC,5)
002187          CALL PUTCHR(SLSH,5)
002188          CALL PUTCHR(ZERO,5)
002189          CALL PUTCHR(D,5)
002190          CALL GVT100
002191 C
002192          RETURN
002193          END
002194 C
002195 ************************************************************************
002196 ************************************************************************
002197 C
002198          SUBROUTINE SORT
002199        IMPLICIT REAL*8 (A-H),(O-Z)
002200 C
002201          INTEGER MARKS(4,2)
002202          INTEGER BOTTOM, EXCH, CURRNT, TEMP
002203          COMMON / DATA_B / MARKS
002204 C
002205          DO I=1,2
002206 C
002207          BOTTOM = 4
002208 C
```

```
002209          DO WHILE (BOTTOM .GT. 1)
002210             EXCH=0
002211             CURRNT=1
002212  C
002213             DO WHILE (CURRNT .LT. BOTTOM)
002214  C
002215                IF (MARKS(CURRNT,I) .GT. MARKS(CURRNT+1,I)) THEN
002216                   TEMP = MARKS(CURRNT,I)
002217                   MARKS(CURRNT,I) = MARKS(CURRNT+1,I)
002218                   MARKS(CURRNT+1,I) = TEMP
002219                   EXCH = CURRNT
002220                END IF
002221  C
002222                CURRNT = CURRNT+1
002223             END DO
002224  C
002225             BOTTOM = EXCH
002226          END DO
002227  C
002228          END DO
002229  C
002230          RETURN
002231  C
002232          END
002233
002234  C*************************************************************************
002235          SUBROUTINE AUTOMARKSCALE
002236  C*************************************************************************
002237  C       Calculate scale factor for peaks.
002238  C       If MARKS(1,1)=0, put in marks automatically.
002239  C       20jan90
002240  C       25jan90 - change from 11 point SMOOTHED to 21 point.
002241  C                 !PT labels lines that are point number dependant.
002242  C*************************************************************************
002243          IMPLICIT REAL*8 (A-H),(O-Z)
002244          INTEGER IDATA(4096),MARKS(4,2),ISC(2),MOX(2),OFFSET(4)
002245          INTEGER MON(2,4),MYMORKS(4,4)
002246          REAL*8 SMOOTHED(1002,4),R(2),S,VMIN(2,4),FACTOR(4),FSET          !PT
002247          COMMON /DATA_A/ IDATA
002248          COMMON /DATA_B/ MARKS,FSET
002249          COMMON /DATA_C/ ISC
002250
002251  C       Find MOX(1) and MOX(2) for first two quadrants.
002252          MOX(1) = 0
002253          MOX(2) = 0
002254          DO 100 J=256,768        ! look at middle half of spectrum.
002255            IF(IDATA(J).GT.MOX(1)) MOX(1)=IDATA(J)
002256            IF(IDATA(J+1024).GT.MOX(2)) MOX(2)=IDATA(J+1024)
002257  100     CONTINUE
002258          DO 200 J=1,2
002259            R(J) = DFLOAT(MOX(J))/180.
002260            IF(R(J).GT.1)THEN
002261              ISC(J) = -INT(R(J)+1)
002262            ELSE IF(R(J).EQ.1)THEN
002263              ISC(J) = 1
002264            ELSE IF(R(J).LT.1.AND.R(J).GT.0)THEN
002265              ISC(J) = INT(1./R(J))
002266            ELSE IF(R(J).LE.0)THEN
002267              ISC(J) = 1
002268            END IF
002269  200     CONTINUE
002270
002271  C       Make smoothed array for marking, if there are no existing marks.
002272  C       Uses 11 point smoothing, which fixes some of the following numbers.
002273  C                                                  10,11,506,507,1012
002274  C       Use 21 point smoothing with numbers        20,21,501,502,1002
002275          OFFSET(1) = 1
002276          OFFSET(2) = 1025
002277          OFFSET(3) = 2047
002278          OFFSET(4) = 3073
```

```
002279
002280          IF(MARKS(1,1).EQ.0)THEN          !**********************BIG IF
002281
002282          DO 500 K=1,4                                                    !PT
002283          DO 400 J=1,1002
002284            S = 0.                                                        !PT
002285            DO 300 L=0,20
002286              S = S + DFLOAT(IDATA(J+OFFSET(K)+L))
002287  300       CONTINUE                                                      !PT
002288            SMOOTHED(J,K) = S/21.
002289  400     CONTINUE
002290  500     CONTINUE
002291
002292  C       Now find the left and right side minimums for each spectrum.
002293  C       Left side search from 1 to 501, minimum in MON(1,K).
002294          DO 700 K=1,4
002295            VMIN(1,K) = SMOOTHED(1,K)
002296            MON(1,K) = 1                                                  !PT
002297            DO 600 J=1,501
002298              IF(SMOOTHED(J,K).LT.VMIN(1,K))THEN
002299                VMIN(1,K) = SMOOTHED(J,K)
002300                MON(1,K) = J
002301              END IF
002302  600       CONTINUE
002303  700     CONTINUE
002304
002305  C       Right side search from 1002 to 502.
002306          DO 900 K=1,4                                                    !PT
002307            VMIN(2,K) = SMOOTHED(1002,K)                                  !PT
002308            MON(2,K) = 1002                                               !PT
002309            DO 800 J=1002,502,-1
002310              IF(SMOOTHED(J,K).LT.VMIN(2,K))THEN
002311                VMIN(2,K) = SMOOTHED(J,K)
002312                MON(2,K) = J
002313              END IF
002314  800       CONTINUE
002315  900     CONTINUE
002316
002317  C       VMIN as minimum works inconsistently for finding marks. Try
002318  C       VMIN = MAX around MON+OFFSET+11+-10
002319          DO 930 L=1,2
002320          DO 920 K=1,4
002321            VMIN(L,K) = 0.                                                !PT
002322            DO 910 J=-10,10
002323              IF(IDATA(OFFSET(K)+MON(L,K)+11).GT.VMIN(L,K))THEN           !PT
002324                VMIN(L,K) = IDATA(OFFSET(K)+MON(L,K)+11)
002325              END IF
002326  910       CONTINUE
002327            IF(VMIN(L,K).LE.0) VMIN(L,K)=1
002328  920     CONTINUE
002329  930     CONTINUE
002330
002331
002332  C       For each quadrant, search out good mark positions, left and right
002333  C       from each minimum. Criterion is where smoothed equals FACTOR*MON.
002334          FACTOR(1) = FSET
002335          FACTOR(2) = FSET
002336          FACTOR(3) = FSET
002337          FACTOR(4) = FSET
002338          DO 1400 K=1,4
002339
002340  C       Left side, going left.
002341          MYMORKS(1,K) = MON(1,K)
002342          DO 1000 J=MON(1,K),1,-1
002343            IF(SMOOTHED(J,K).LE.FACTOR(K)*VMIN(1,K)) MYMORKS(1,K)=J
002344  1000    CONTINUE
002345
002346  C       Left side, going right.
002347          MYMORKS(2,K) = MON(1,K)+1                                       !PT
002348          DO 1100 J=MON(1,K)+1,501
002349            IF(SMOOTHED(J,K).LE.FACTOR(K)*VMIN(1,K)) MYMORKS(2,K)=J
002350  1100    CONTINUE
002351
```

```
002352 C       Right side, going left.
002353         MYMORKS(3,K) = MON(2,K)-1
002354         DO 1200 J=MON(2,K)-1,502,-1                                    !PT
002355           IF(SMOOTHED(J,K).LE.FACTOR(K)*VMIN(2,K)) MYMORKS(3,K)=J
002356 1200    CONTINUE
002357
002358 C       Right side, going right.
002359         MYMORKS(4,K) = MON(2,K)
002360         DO 1300 J=MON(2,K),1002                                        !PT
002361           IF(SMOOTHED(J,K).LE.FACTOR(K)*VMIN(2,K)) MYMORKS(4,K)=J
002362 1300    CONTINUE
002363
002364 1400    CONTINUE
002365
002366 C       Now translate MYMORKS to MARKS.
002367 C       Top quadrant is easy.
002368         DO 1500 K=1,4
002369           MARKS(K,1) = MYMORKS(K,1) + 11                               !PT
002370 1500    CONTINUE
002371
002372 C       Must find best values from among the other three quadrants.
002373         MARKS(1,2) = MAX(MYMORKS(1,2),MYMORKS(1,3),MYMORKS(1,4)) + 11  !PT
002374         MARKS(2,2) = MIN(MYMORKS(2,2),MYMORKS(2,3),MYMORKS(2,4)) + 11  !PT
002375         MARKS(3,2) = MAX(MYMORKS(3,2),MYMORKS(3,3),MYMORKS(3,4)) + 11  !PT
002376         MARKS(4,2) = MIN(MYMORKS(4,2),MYMORKS(4,3),MYMORKS(4,4)) + 11  !PT
002377
002378 C       Check for no good region of baseline at all.
002379         IF(MARKS(2,2).LE.MARKS(1,2)) MARKS(2,2)=MARKS(1,2)+1
002380         IF(MARKS(3,2).GE.MARKS(4,2)) MARKS(3,2)=MARKS(4,2)-1
002381
002382 C       Now marks are set. End big if and return.
002383         END IF                  !************************END BIG IF
002384
002385         RETURN
002386         END
002387
```

A-2 NOTES FOR THE COMPUTER PROGRAM

The input data to the computer program (p.119) are refereed to the following :

Line	Variable	Description
112	NDUBS	number of doublets
115	NRUNS	number of runs to be analysed for a doublet
115	NCP	number of contaminant peaks
115	DIFC	difference (in μu) between main peak and contaminant peak
115	RC	ratio of contaminant peak to main peak
118	NRECS	number of records in a run (usually 8)
118	IZRANL	= 0 for normal run = 1 for zero shift analysis
118	IADD	the unchanged part of ΔV_e
118	VEE	potential V_e applied to the electrostatic analyzer (in Bishop units)
118	EMLT	mass of light member of doublet (in mass units)
118	EMHV	mass of heavy member of doublet (in mass units)
118	PPM	proportional error in ppm
118	EPPM	standard deviation in proportional error
118	ISADD	the unchanged part of the split voltages δV_1 and δV_3
145	NRECN	sequential record number on tape
145	IT	type of match (NAF, NSF, etc.)

Line	Variable	Description
145	CAL	calibration of the signal averager
145	BDV	offset for ΔV_e (to be added to IADD)
145	SDV01	offset for split voltage δV_1 in quadrant 1 (to be added to ISADD)
145	SDV03	offset for split voltage δV_3 in quadrant 3 (to be added to ISADD)
145	MARKS	baseline marks